Photo-detection

Principles, Performance and Limitations

Nicoleta Dinu (LAL Orsay)
Thierry Gys (CERN)
Christian Joram (CERN)

This lecture was originally prepared for the EDIT 2011 School together with
Samo Korpar (Univ. of Maribor and JSI Ljubljana)
Yuri Musienko (Fermilab/INR)
Veronique Puill (LAL, Orsay)
Dieter Renker (TU Munich)

OUTLINE

- Basics
- Requirements on photo-detectors
- Photosensitive materials
- ‘Family tree’ of photo-detectors
- Detector types
- Applications

Basics

1. Photoelectric effect
2. Solids, liquids, gaseous materials
3. Internal vs. external photo-effect, electron affinity
4. Photo-detection as a multi-step process
5. The human eye as a photo-detector

Basics of photon detection

Purpose: Convert light into detectable electronic signal

(we are not covering photographic emulsions!)

Principle:

- Use photoelectric effect to 'convert' photons (γ) to photoelectrons (pe)
- Details depend on the type of the photosensitive material (see below).
- Photon detection involves often materials like K, Na, Rb, Cs (alkali metals). They have the smallest electronegativity → highest tendency to release electrons.
- Most photo-detectors make use of solid or gaseous photosensitive materials.
- Photo-effect can in principle also be observed from liquids.

A. Einstein.
Annalen der Physik **17** (1905) 132–148.

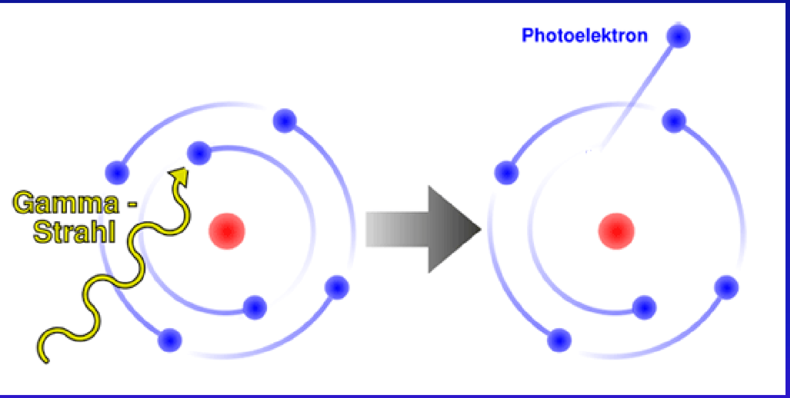

Basics of photon detection

Solid materials (usually semiconductors)

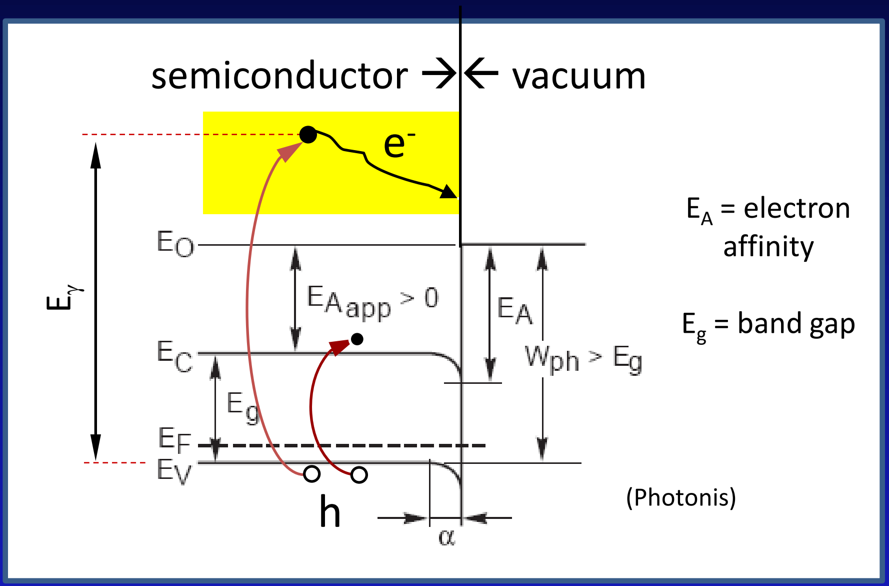

Multi-step process:

1. absorbed γ's impart energy to electrons (e) in the material; If $E_\gamma > E_g$, electrons are lifted to conductance band.
   → In a Si-photodiode, these electrons can create a photocurrent. → Photon detected by Internal Photoeffect.

However, if the detection method requires extraction of the electron, 2 more steps must be accomplished:

2. energized e's diffuse through the material, losing part of their energy (~random walk) due to electron-phonon scattering. ΔE ~ 0.05 eV per collision. Free path between 2 collisions λ_f ~ 2.5 - 5 nm → escape depth λ_e ~ some tens of nm.
3. only e's reaching the surface with sufficient excess energy escape from it
   → External Photoeffect

$$E_\gamma = h\nu > W_{ph} = E_G + E_A$$

Basics of photon detection

Opaque photocathode

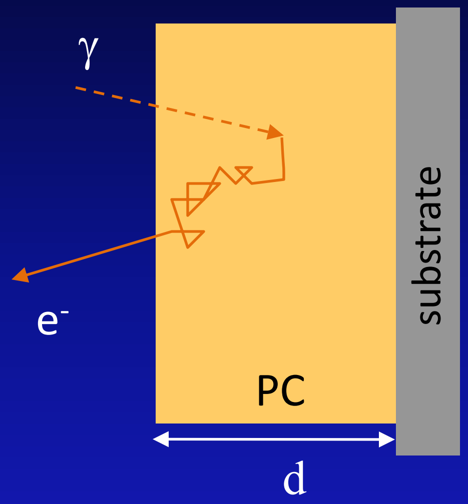

Light absorption in photocathode

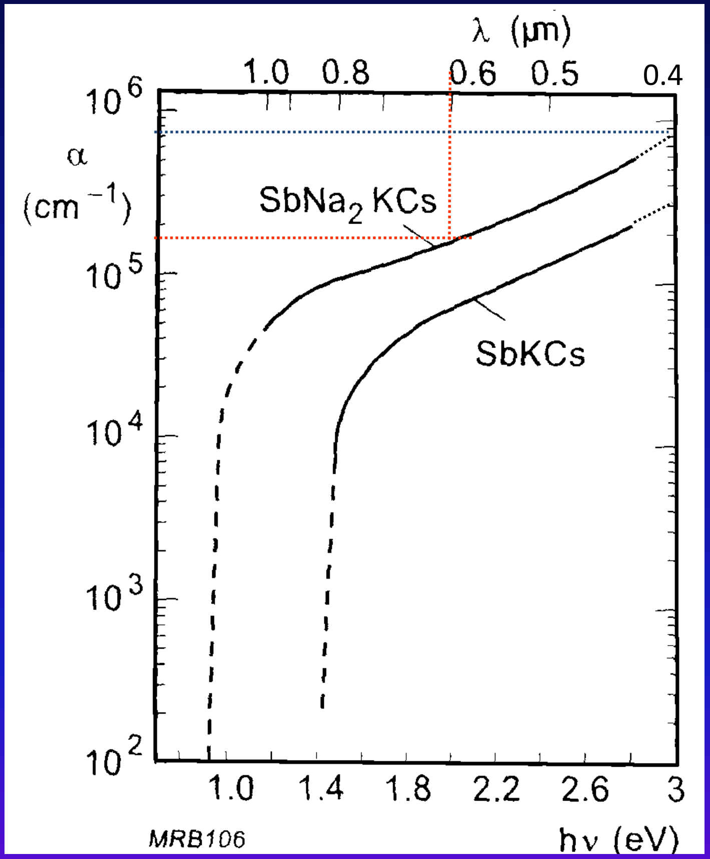

$$N = N_0 \cdot \exp(-\alpha d)$$

$$\lambda_A = 1/\alpha$$

Red light ($\lambda \approx 600$ nm)
$\alpha \approx 1.5 \cdot 10^5$ cm^{-1}
$\lambda_A \approx 60$ nm

Blue light ($\lambda \approx 400$ nm)
$\alpha \approx 7 \cdot 10^5$ cm^{-1}
$\lambda_A \approx 15$ nm

Blue light is stronger absorbed than red light !

Semitransparent photocathode

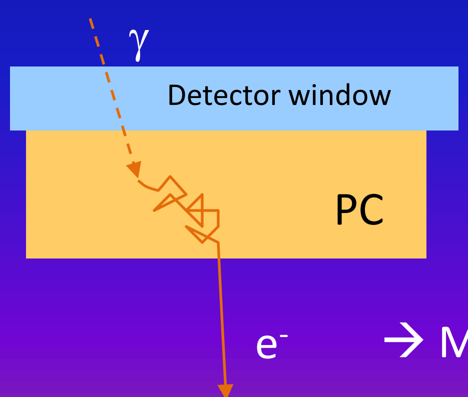

→ Make semitransparent photocathode just as thick as necessary!

The human eye as photosensor

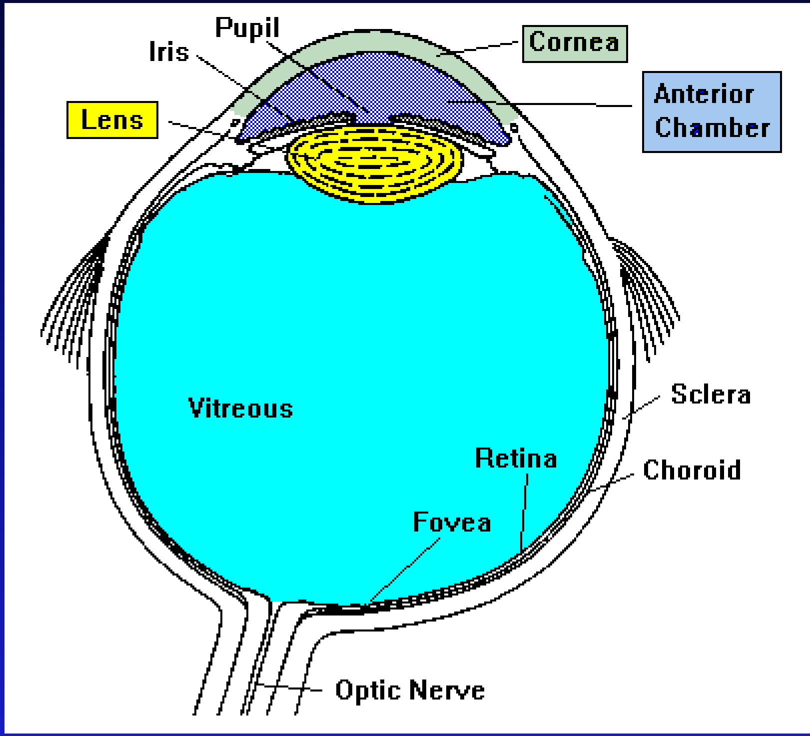

The first proto-eyes evolved among animals 540 million years ago.

Light passes through the cornea, pupil and lens before hitting the retina. The iris controls the size of the pupil and therefore, the amount of light that enters the eye. Also, the color of your eyes is determined by the iris.

The vitreous is a clear gel that provides constant pressure to maintain the shape of the eye.
The retina is the area of the eye that contains the receptors (rods for low light contrast and cones for colours) that respond to light. The receptors respond to light by generating electrical impulses that travel out of the eye through the optic nerve to the brain.

The optic nerve contains 1.2 million nerve fibers. This number is low compared to the roughly 100 million photoreceptors in the retina.

Rods
~100·10⁶ cells

Cones
~5·10⁶ cells

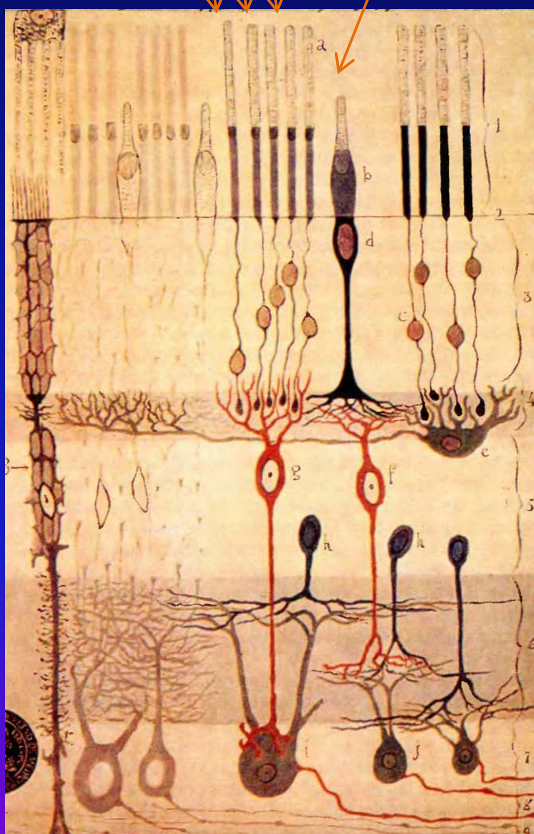

Rods & cones. Spectral sensitivity

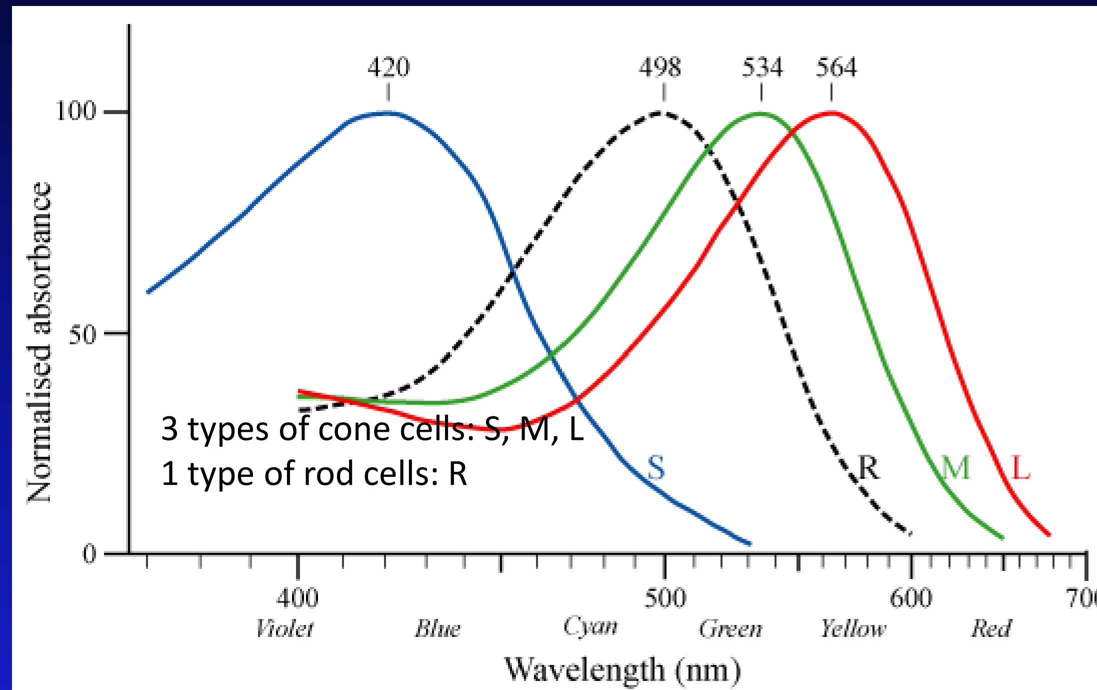

The human eye can detect light pulse of 10-40 photons. Taking into account that absorption of light in retina is ~10-20% and transparency of vitreous is ~50% →~2-8 photons give detectable signal.

Visual photo-transduction is a VERY COMPLEX process by which light is converted into electrical signals in the rod and cone cells of the retina of the eye.

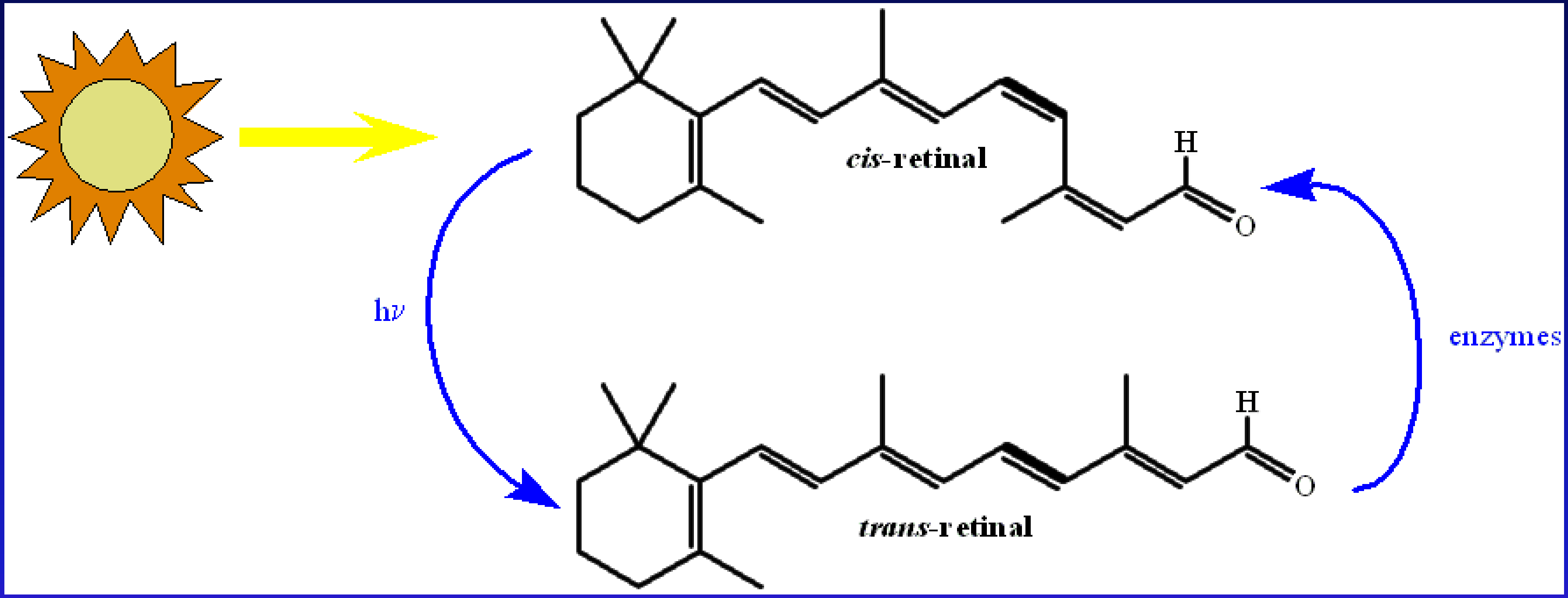

See e.g. http://en.wikipedia.org/wiki/Phototransduction

After having built it many billion times, the eye can be considered as a very successful and reliable photo-detector.

It provides…

- Good spatial resolution. <1 mm, with certain accessories even <0.01 mm
- Very large dynamic range (1:10^6)
  + automatic threshold adaptation
- Energy (wavelength) discrimination → colours
- Long lifetime. Performance degradation in second half of lifecycle can be easily mitigated.

Weak points

- Modest sensitivity: 500 to 900 photons must arrive at the eye every second for our brain to register a conscious signal
- Modest speed. Data taking rate ~ 10Hz (incl. processing)
- Trigger capability is very poor. "Look now" → Time jitter ~1 s.

→ There is room for improvement

2 Requirements on photo-detectors

1. Sensitivity
2. Linearity
3. Signal fluctuations
4. Time response
5. Rate capability / aging
6. Dark count rate
7. Operation in magnetic fields
8. Radiation tolerance

2.1. Sensitivity

Probability that the incident photon (N_γ) generates a photoelectron (N_{pe})

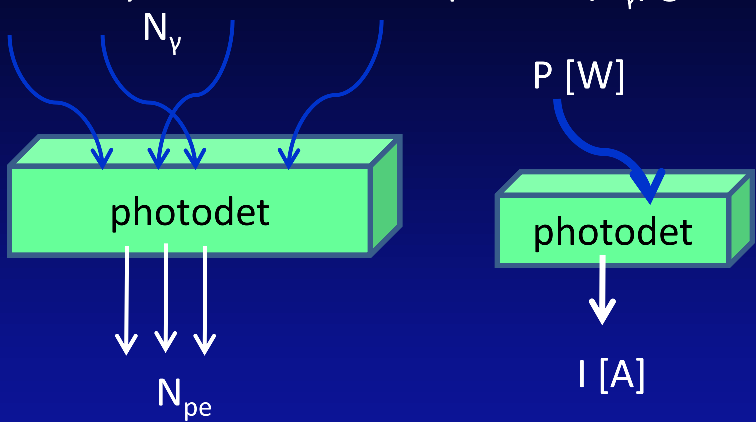

Quantum efficiency

$$QE[\%] = \frac{N_{pe}}{N_\gamma}$$

Radiant sensitivity

$$S[mA/W] \approx \frac{QE[\%] \cdot \lambda[nm] \cdot e}{hc} = \frac{QE[\%] \cdot \lambda[nm]}{124}$$

Photo detection efficiency : combined probability to produce a photoelectron and to detect it

$PDE[\%] = \mathcal{E}_{geom} \cdot QE \cdot P_{trig}$ for a SiPM ($\mathcal{E}_{geom}$: geometrical factor, P_{trig}: triggering probability)

$PDE[\%] = QE \cdot CE \cdot P_{mult}$ for a PMT (CE: collection efficiency, P_{mult}: multiplication probability)

High sensitivity required in:

UV- blue : water Cherenkov telescope, Imaging Atmospheric Cherenkov Telescopes (HESS II, CTA)
Blue-green : HEP calorimeters (CMS, ILC HCAL)

2.2 Linearity

Requirement: Photocurrent response of the photo-detector is linear with incident radiation over a wide range. Any variation in responsivity with incident radiation represents a variation in the linearity of the detector

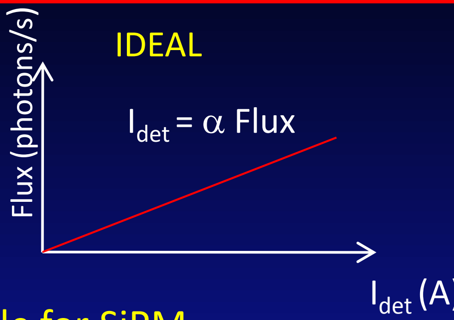

Example for PMT : non linearity curves

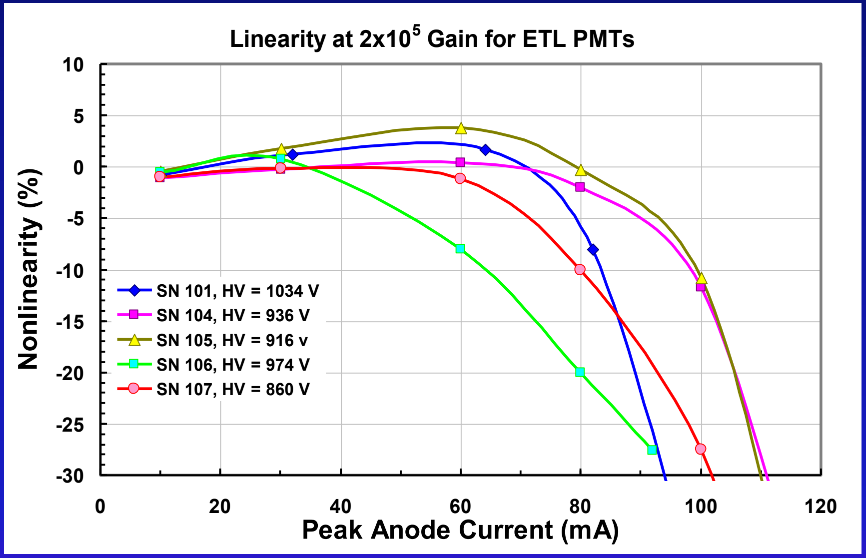

at UCLA PMT Test Facility

Example for SiPM

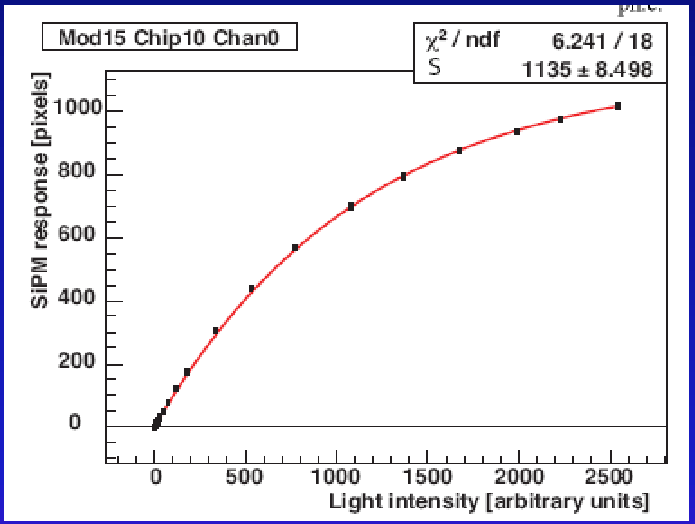

arXiv:0902.2848v1 [physics.ins-det] 17 Feb 2009

	PMT	HPD	MCP-PMT	APD	SiPM
Dynamic range (p.e.)	10^6	10^7	10^7	10^7	10^3

Example of dynamic range required : HCAL of ILC

Min: 20 photons/mm² (μ for calibration)

Max: 5.10^3 photons/mm² (high-energy jet)

(C. Cheshkov et al., NIM A440(2000)38)

2.3 Signal fluctuations

PMT

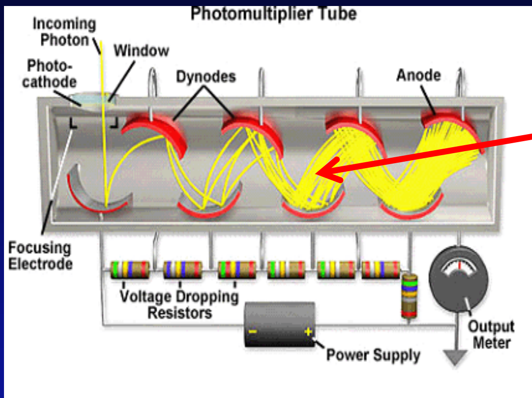

Photo-detectors with internal gain

statistical fluctuation of the avalanche multiplication widen the response of a photo-detector to a given photon signal beyond what would be expected from simple photoelectron statistics (Poissonian distribution)

APD

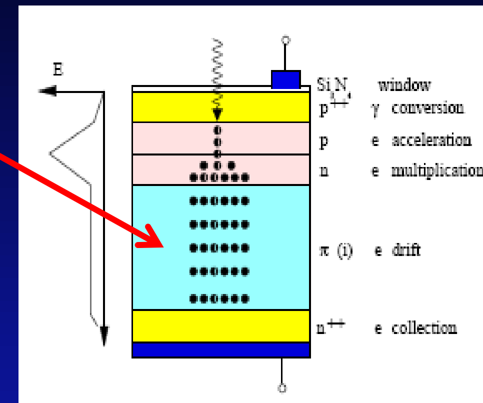

➡ fluctuations characterized by the **excess noise factor ENF**

$$ENF = \frac{\sigma_{out}^2}{\sigma_{in}^2}$$

general definition (gain = 1)

$$ENF = 1 + \frac{\sigma_M^2}{M^2}$$

M = gain

$$\frac{\sigma}{E} = \sqrt{\frac{ENF}{N_{pe}}}$$

quality of energy measurement

Approximate values for photodetectors

detector	ENF
PMT	1 - 1,5
APD	2 @ gain=50
HPD	~1
SiPM	1 - 1,5
MCP-PMT	~1

- impacts the photon counting capability for low light measurements
- deteriorates the stochastic term in the energy resolution of a calorimeter

2.4 Time response

★ light travels 300µm in 1 ps

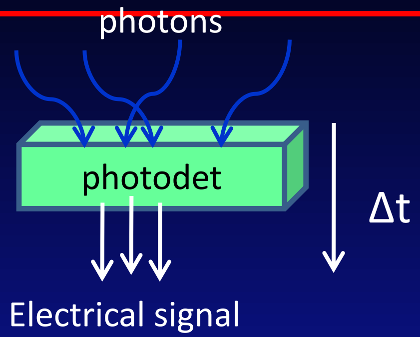

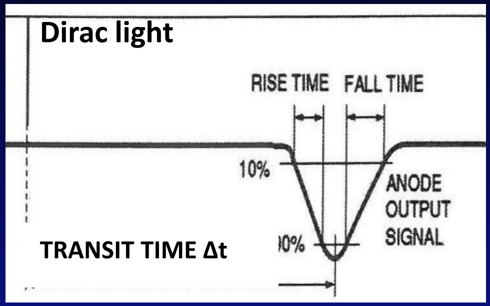

- Rise time, fall time (or decay time)
- Duration
- Transit time (Δt): time between the arrival of the photon and the electrical signal
- Transit time spread (TTS): transit time variation between different events ➡ timing resolution

⚠ to the readout electronics used !

Example of signal shapes

standard PMT

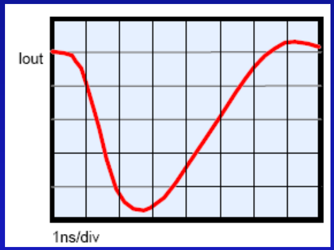

MCP- PMT

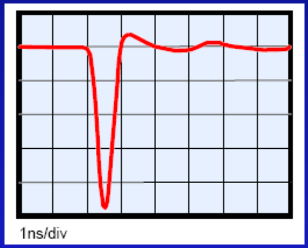

SiPM

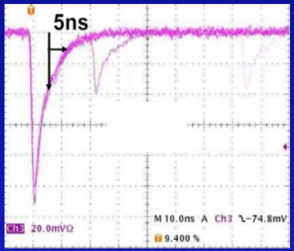

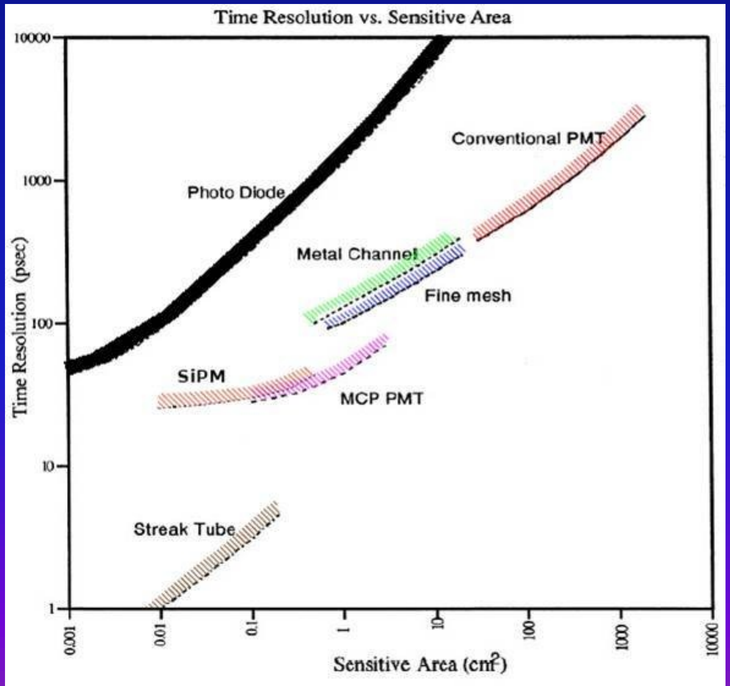

modified from K.Arisaka NIMA 422 (2000)

Good time resolution required in :

Particle identification in SuperB : 30 ps for the π/K separation (arXiv:1007.4241v1 [physics.ins-det] 24 Jul 2010)

Diffractive physics at the LHC (search for the Higgs Boson at low mass) : 15 ps (B. Cox, F. Loebinger, A. Pilkington, JHEP 0710 (2007) 090)

2.5 Rate capability/aging

Rate capability: inversely proportional to the time needed, after the arrival of one photon, to get ready to receive the next

Requirements in calorimeters:
100 kHz → few MHz

SiPM

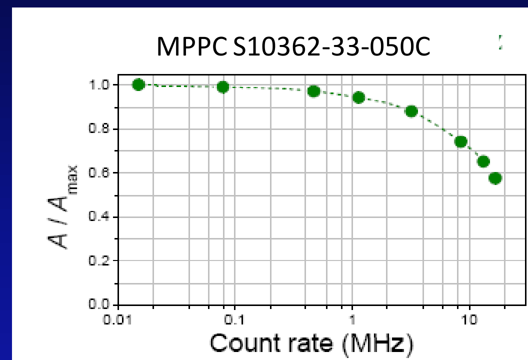

A. Stoykov, µSR at PSI

MCP-PMT

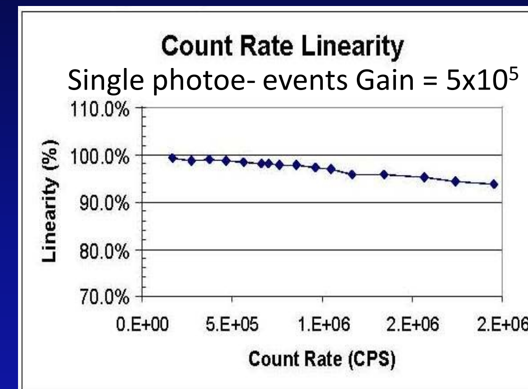

Aging (long-term operation at high counting rates): how is the photo-detector behavior changed when operated at high counting rate during several years ?

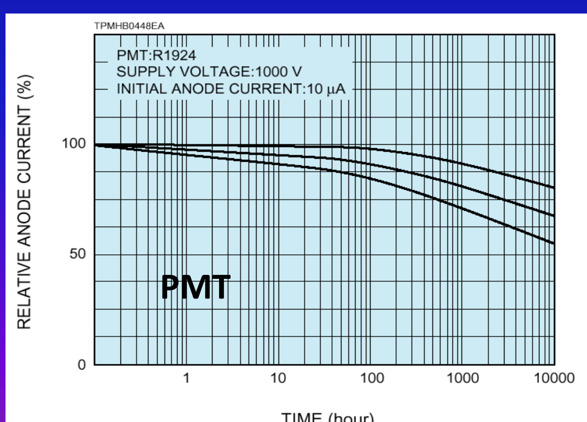

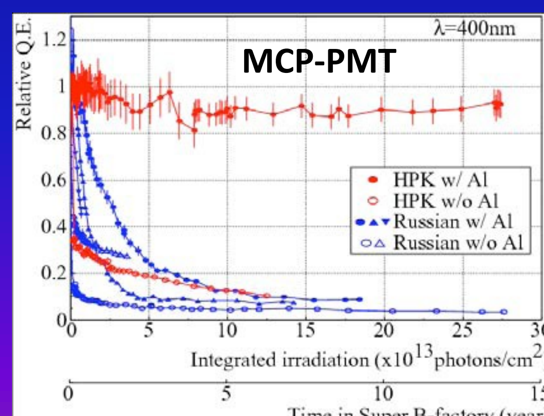

I.Adachi, et al., **Nagoya University, SuperB workshop at SLAC**

Parameter affected (generally in a negative way):

- gain
- quantum efficiency
- dark current

2.6 Dark count rate (DCR)

Dark noise: the electrical signal when there is no photon

DCR of different photocathodes

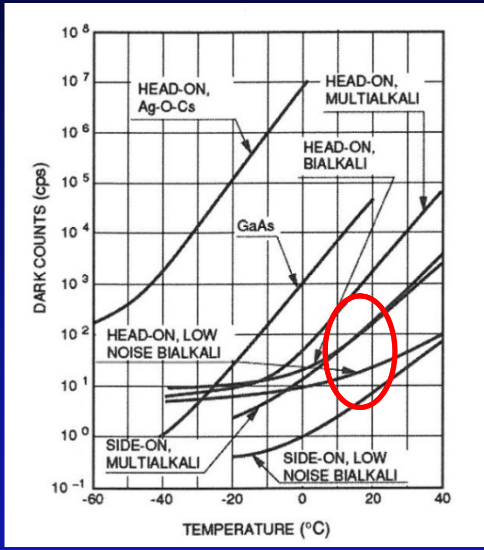

DCR of a PMT

- depends on the cathode type, the cathode area, and the temperature.
- few kHz (threshold = 1 pe)
- is highest for cathodes with high sensitivity at long wavelengths.
- increases considerably if exposed to daylight

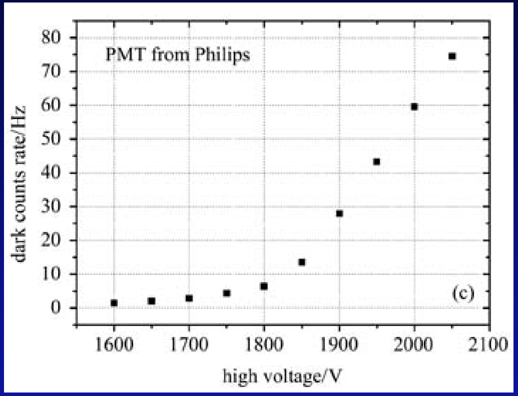

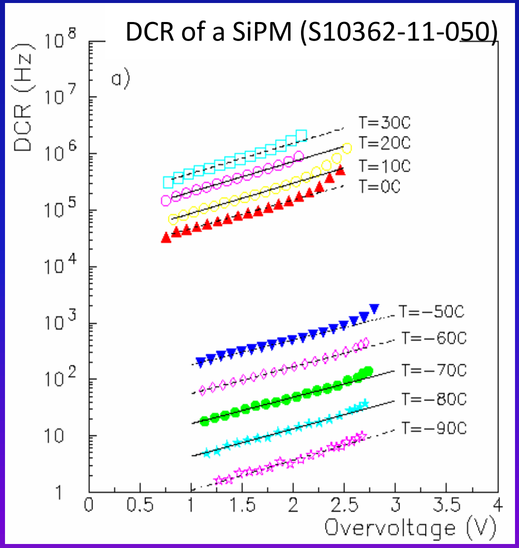

N. Dinu, IEEE NSS 2010

DCR of a SiPM

- depends on the pixel size, the bias voltage, the temperature
- quite high (0.3–2MHz/mm² at room temp, threshold = 1 p.e)

DCR depends a lot on the threshold → not a big issue when we want to detect hundreds or thousands of photons.

The most efficient way to keep the DCR low is cooling.

2.7 Operation in magnetic fields

★ Earth's magnetic field = 30-60 µT

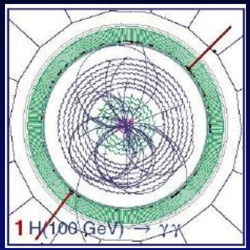

curves the trajectory of charges particles → separate the particles → easier analysis

curves the trajectory of charges particles → reduce the detector size → reduce the detector price

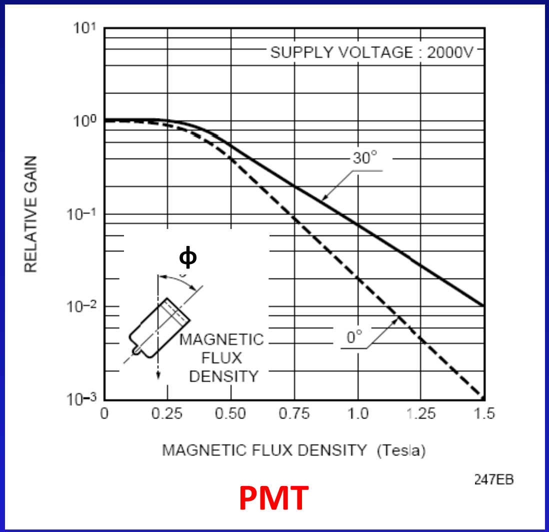

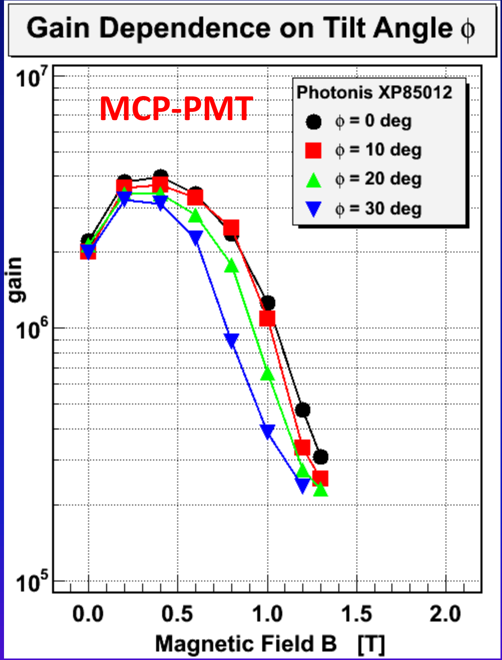

Albert Lehmann RICH 2010

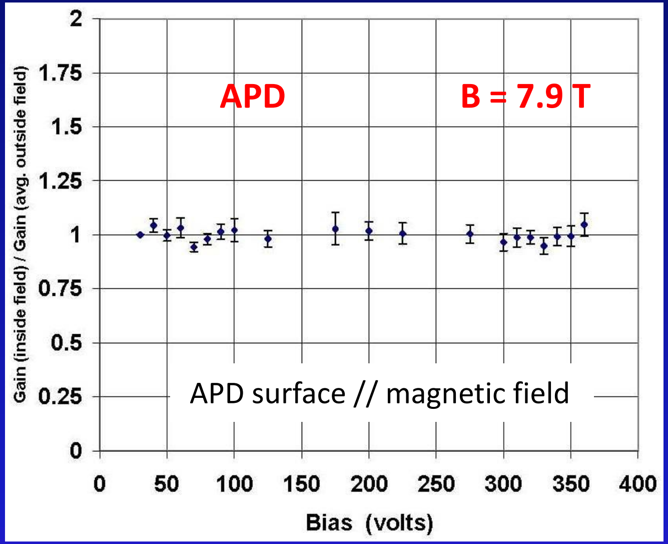

NJ. Marler, IM. A449 (2000) 311-313

PMT very sensitive to magnetic field → shielding required (µ metal)

APD, SiPM no sensitive to magnetic field

Requirements : detection in magnetic fields up to 2T (PANDA, SuperB factory) or more (4 T in CMS ECAL, ILC HCAL)

2.8 Radiation tolerance

Electromagnetic calorimeter: very hostile environment for photo-detectors
Damages caused by:

- ionizing radiation: energy deposited by particles in the detector material (the unit of absorbed dose is Gray (Gy) ==> 1 Gy = 1 J/kg = 100 rad) and by photons from electromagnetic showers
- neutrons created in hadronic shower, also in the forward shielding of the detectors and in beam collimators

<u>degradation of the dark current, gain, quantum efficiency ….</u>

Dark current of PMT

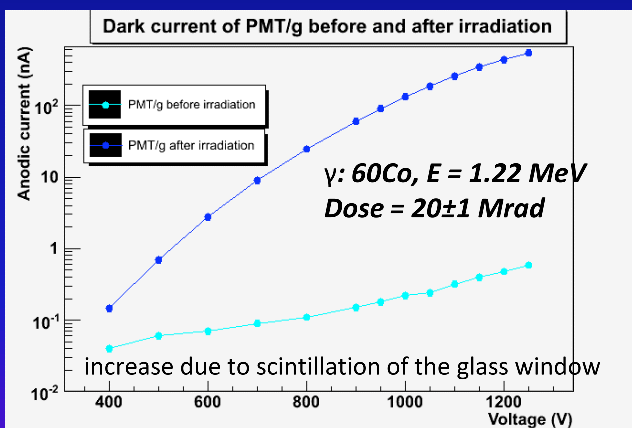

A. Sbrizzi LUCID in ATLAS

SiPM amplitude proton irradiation

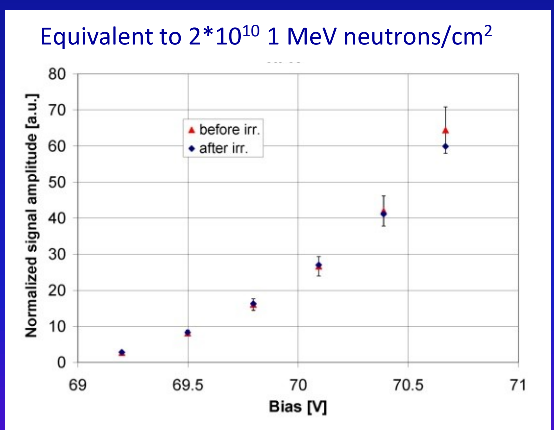

DCR of SiPM neutron irradiation

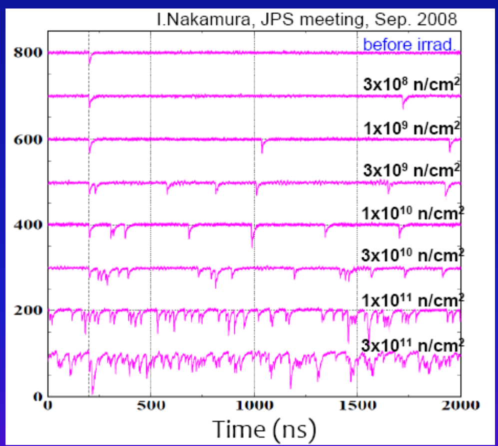

Y. Musienko, AMPDs for Frontier Detector Systems

At LHC, the ionizing dose is ~ 2 x10^6 Gy / r_T^2 / year (r_T = transverse distance to the beam)

Example in LHC for the CMS ECAL (10 years) 2.10^{13} n/cm2 + 250 kRad

3 Photosensitive materials

1. Classical photo-cathodes (bialkali, S20), super/ultra bialkali
2. UV sensitive, solar blind (CsTe, CsI)
3. Crystalline cathodes (GaAs etc.)
4. Silicon
5. Exotics: TMAE, TEA
6. Windows/substrates

…quently used photosensitive materials / photo-cathodes

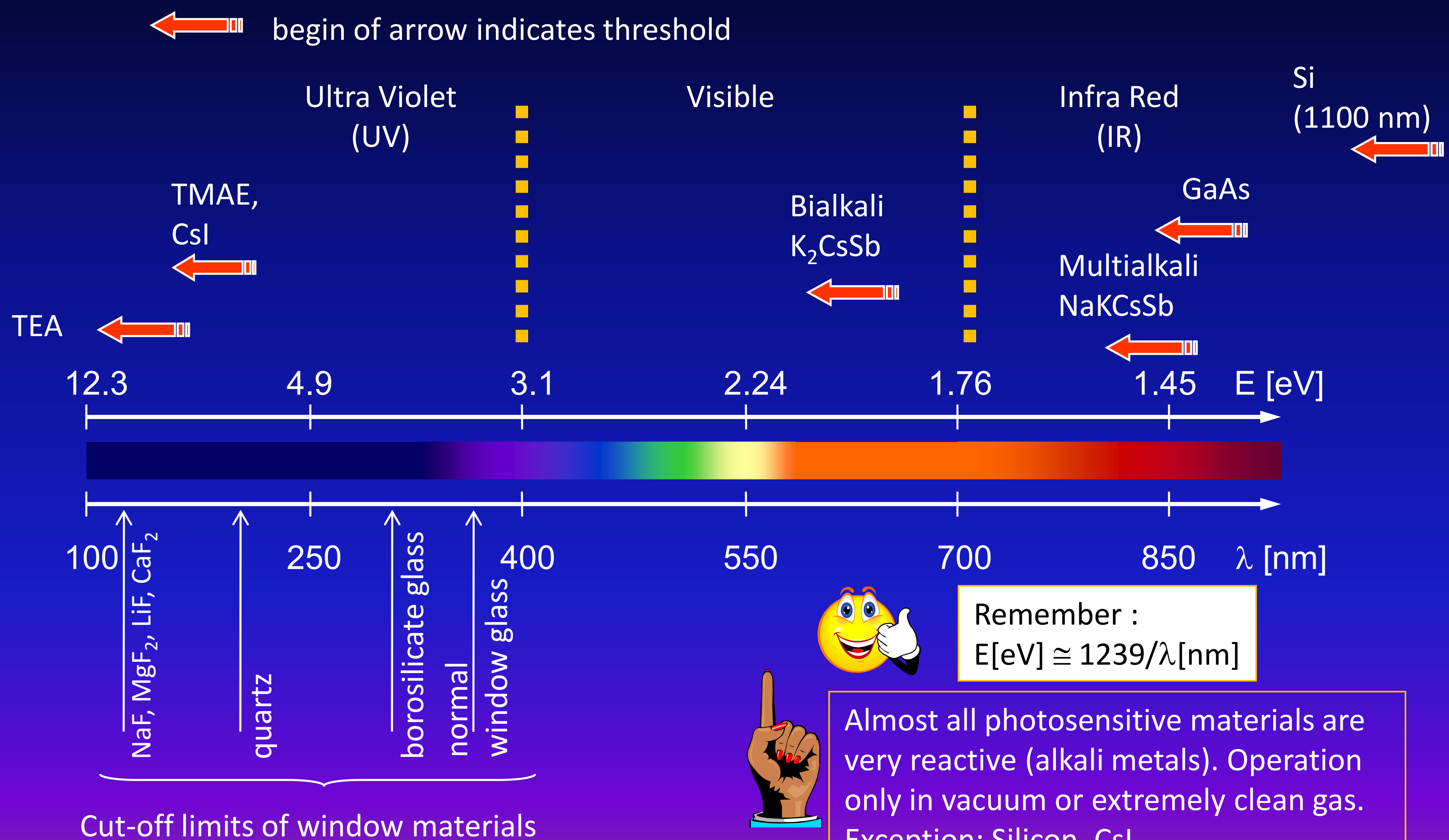

Remember :
$E[eV] \cong 1239/\lambda[nm]$

Almost all photosensitive materials are very reactive (alkali metals). Operation only in vacuum or extremely clean gas. Exception: Silicon, CsI.

xternal) QE of typical semitransparent photo-cathodes

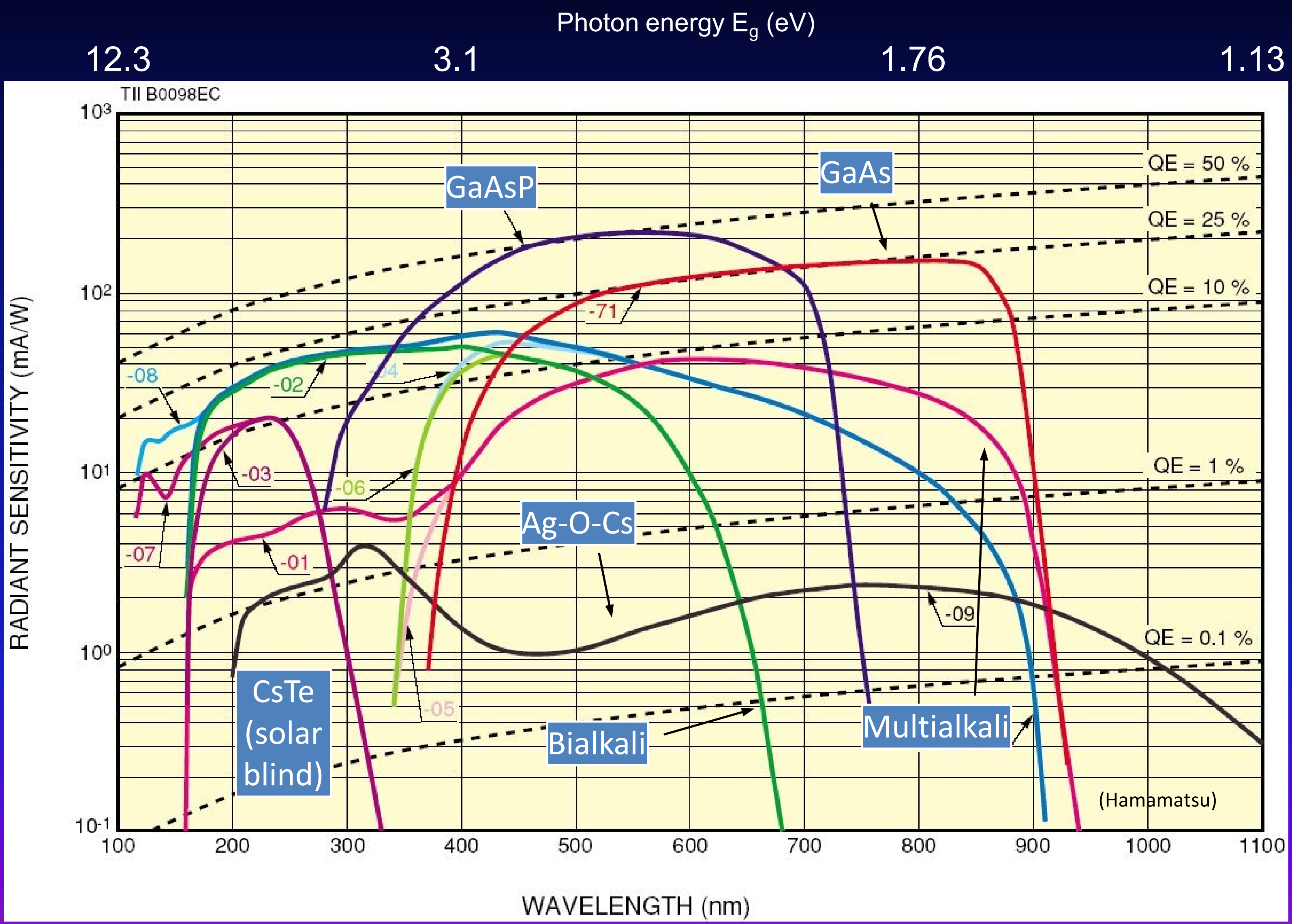

Bialkali: SbKCs, SbRbCs Multialkali: $SbNa_2KCs$ (alkali metals have low work function)

generation of high performance photo-cathodes

QE Comparison of semitransparent bialkali QE

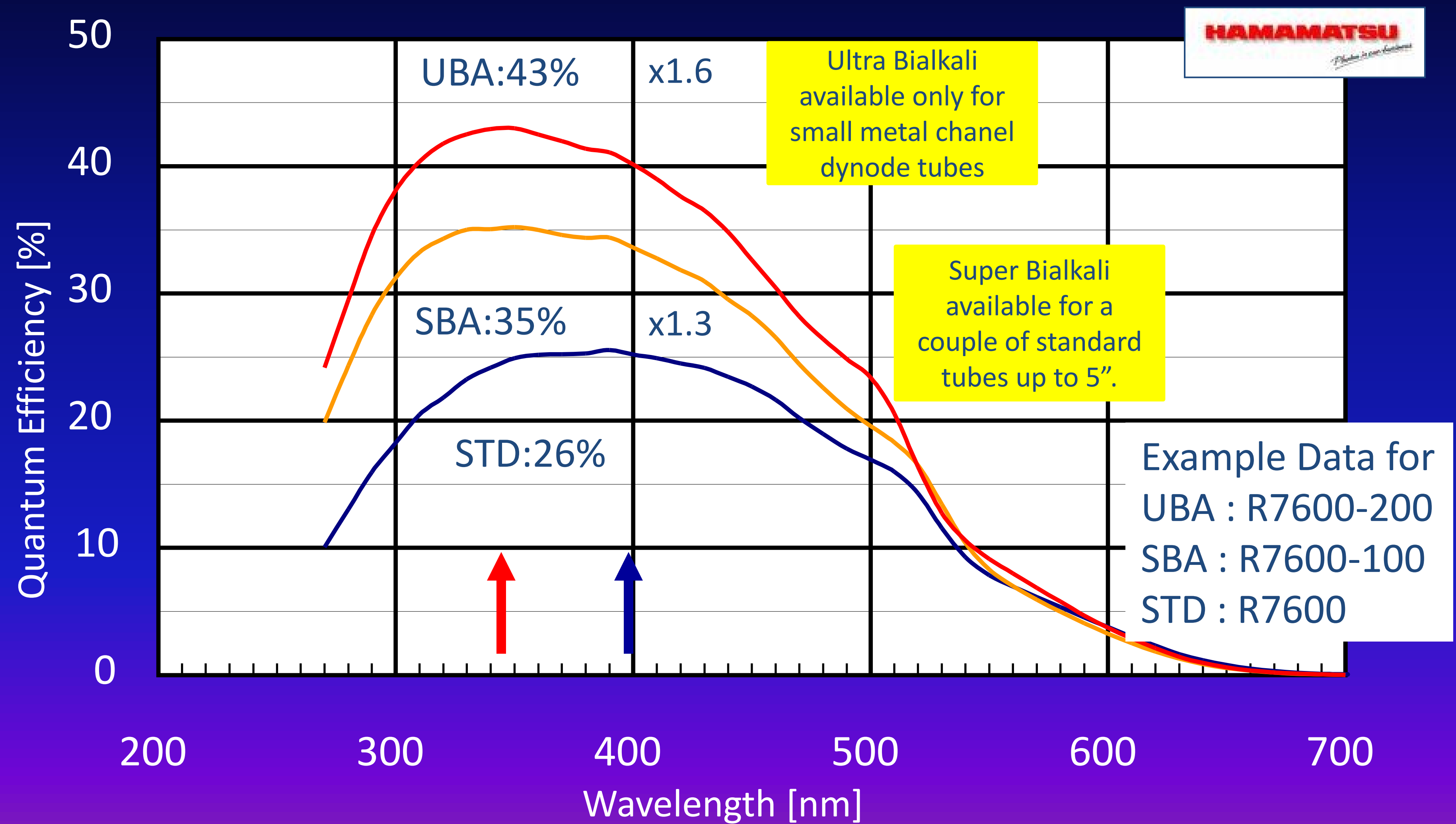

Light absorption in Silicon

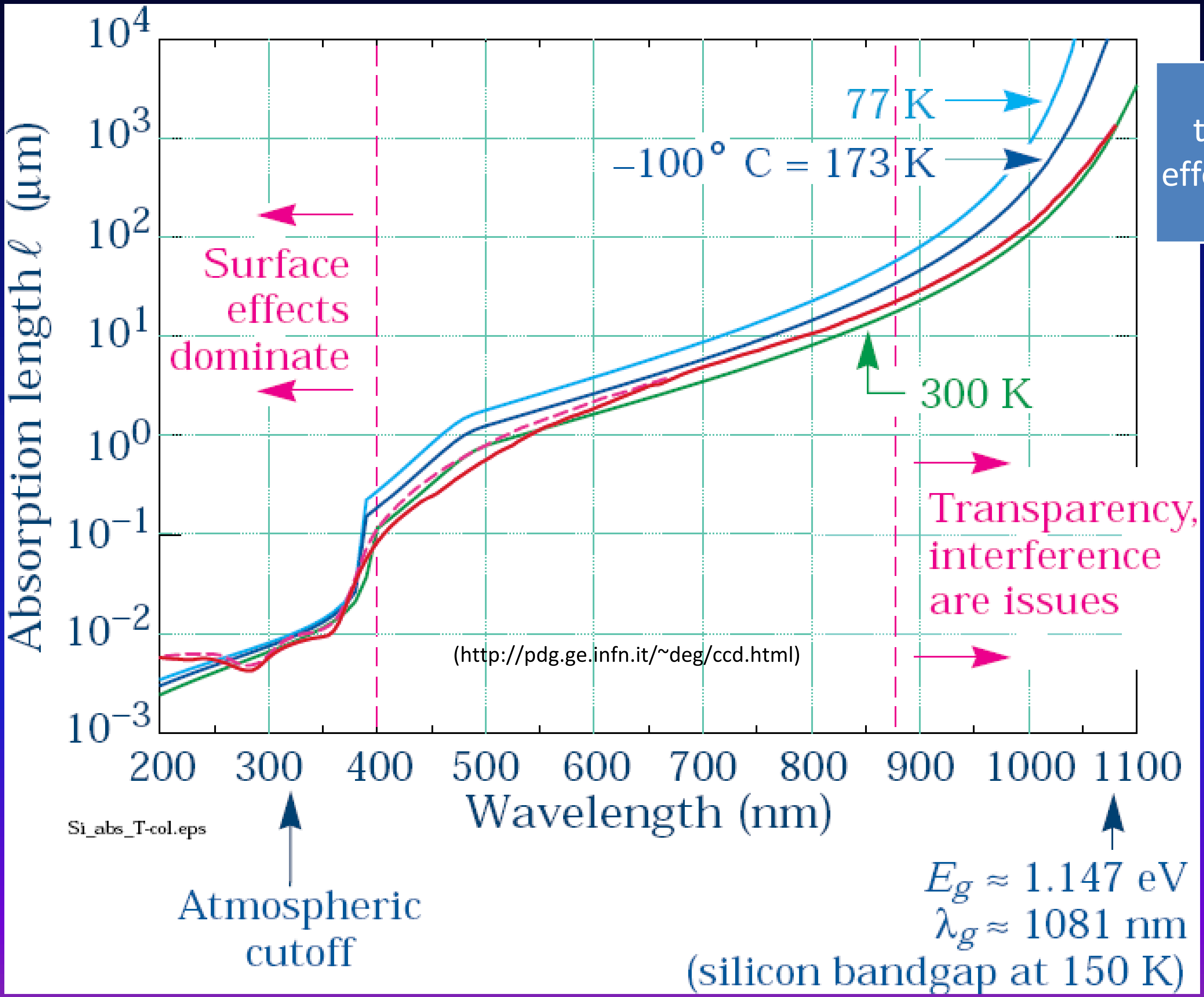

At long λ, temperature effects dominate

'Exotics:' Photosensitive vapours used in LEP/SLC generation of Cherenkov detectors

These detectors were based on MWPCs or TPCs.

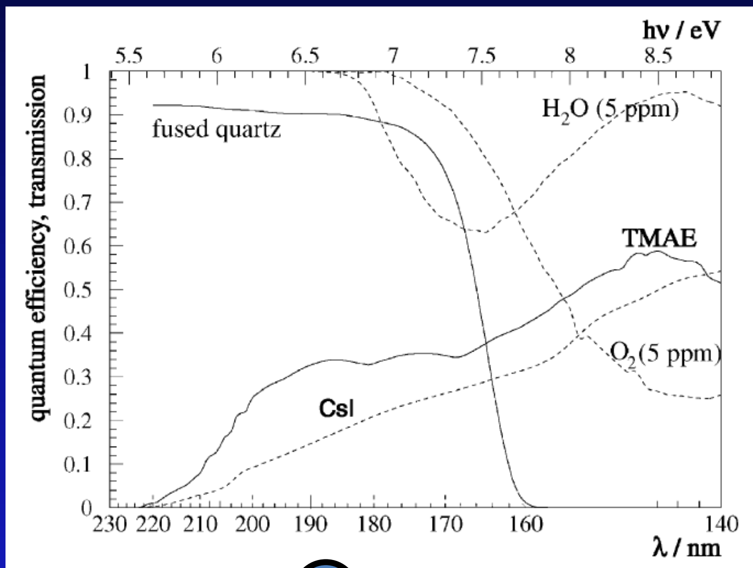

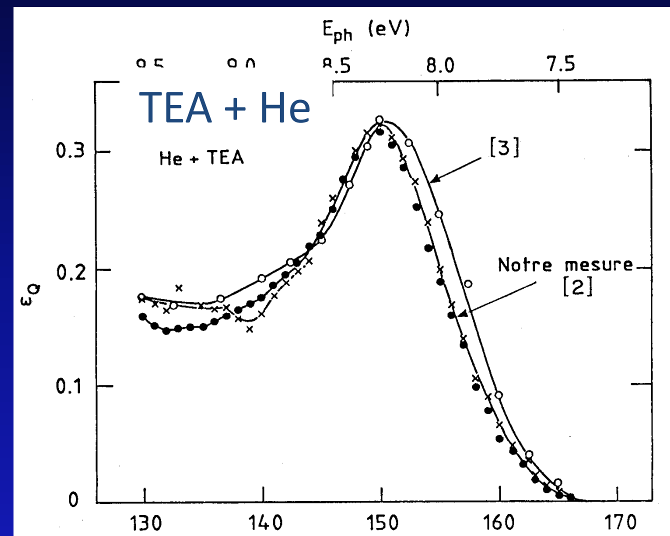

Detection of UV / VUV light only!

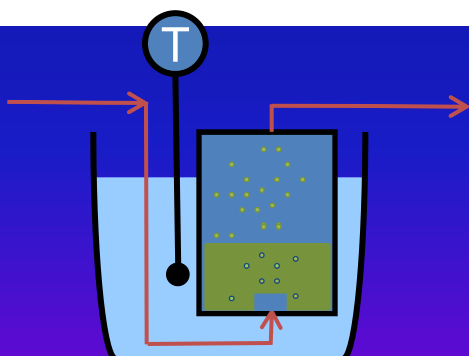

molecule	formula	E_I [eV] (λ_I [nm])	max. ε_Q (E)	λ_{ph} (at 293K)
TEA	$(C_2H_5)_3N$	7.5 (164)	0.33 (8.2)	0.43 mm
TMAE	$C_2[(CH_3)_2N]_4$	5.36 (230)	0.51 (8.3)	26 mm
DMA	$(CH_3)_2NH$	8.3 (148)	0.2 (9.2)	
TMA	$(CH_3)_3N$	7.9 (156)	0.27 (8.6)	

Photosensitive agent was admixed to the counting gas of a MWPC by bubbling the gas through the liquid agent at a given temperature.

Optical transmission of typical window materials

2 types of losses:

- Fresnel reflection at interface air/window and window/photocathode

  $R_{Fresnel} = (n-1)^2 / (n+1)^2$ n = refractive index (wavelength dependent!)
  $n_{glass} \sim 1.5$ $R_{Fresnel} = 0.04$ (per interface)

- Bulk absorption due to impurities or intrinsic cut-off limit. Absorption is proportional to window thickness

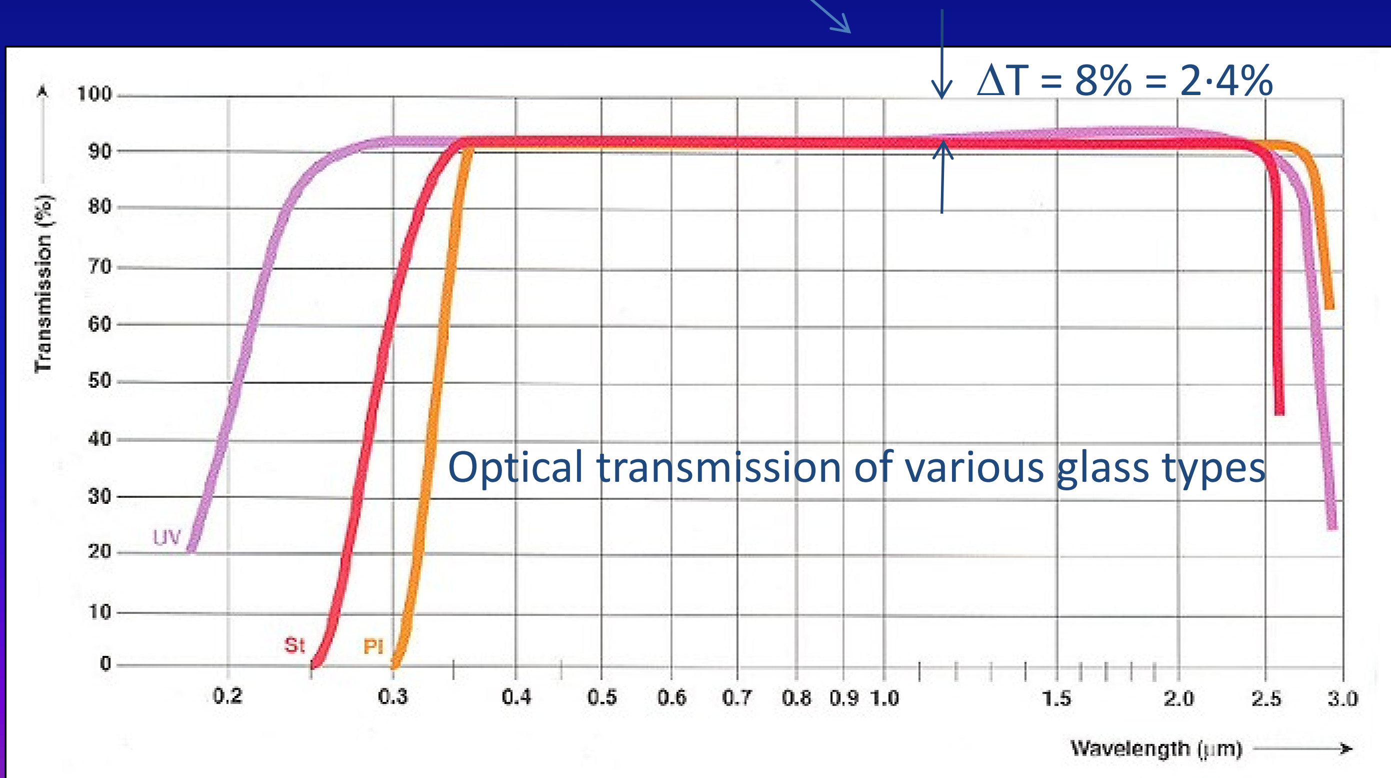

Schott

Windows/substrates

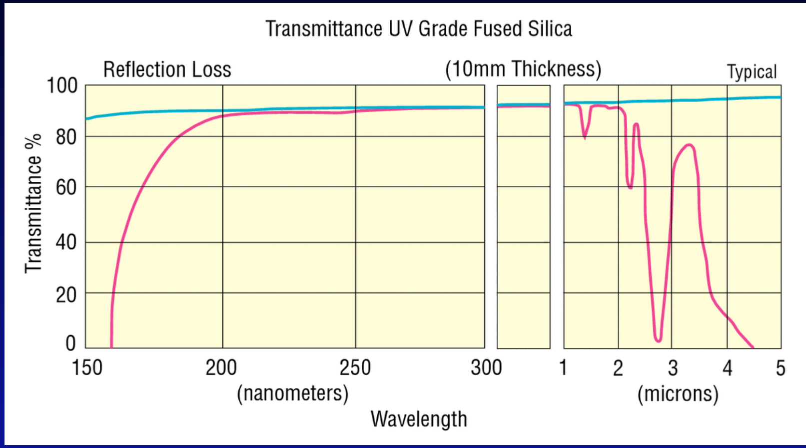

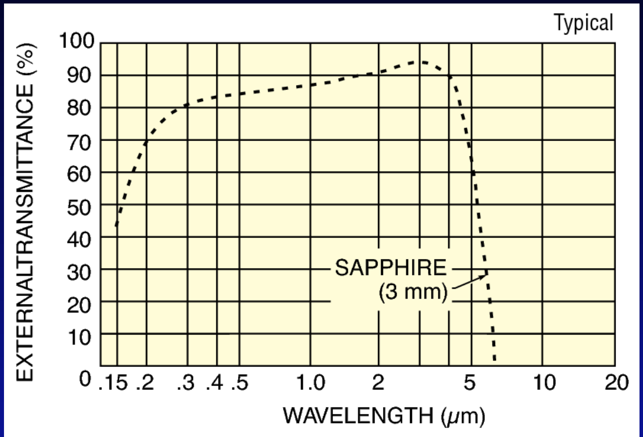

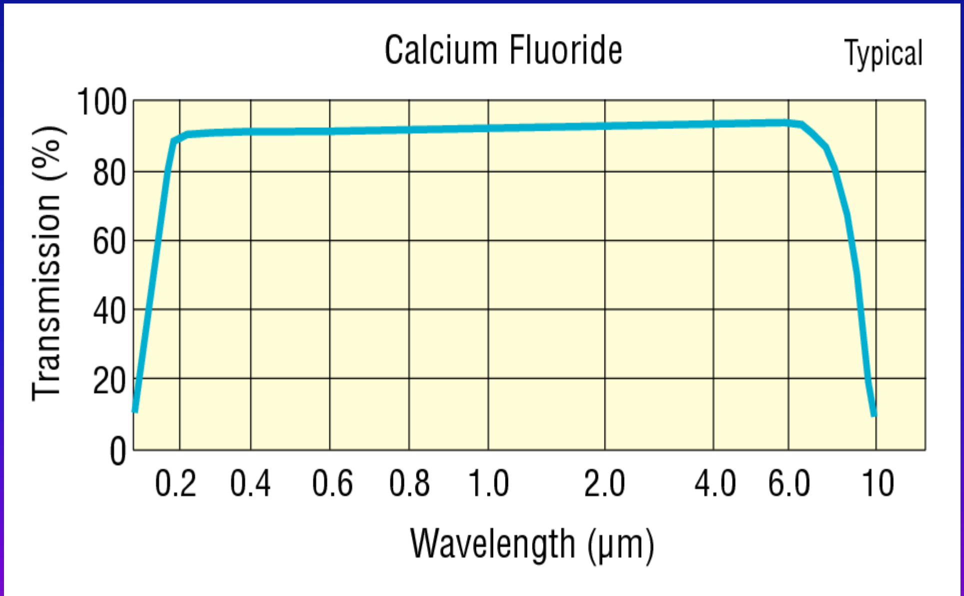

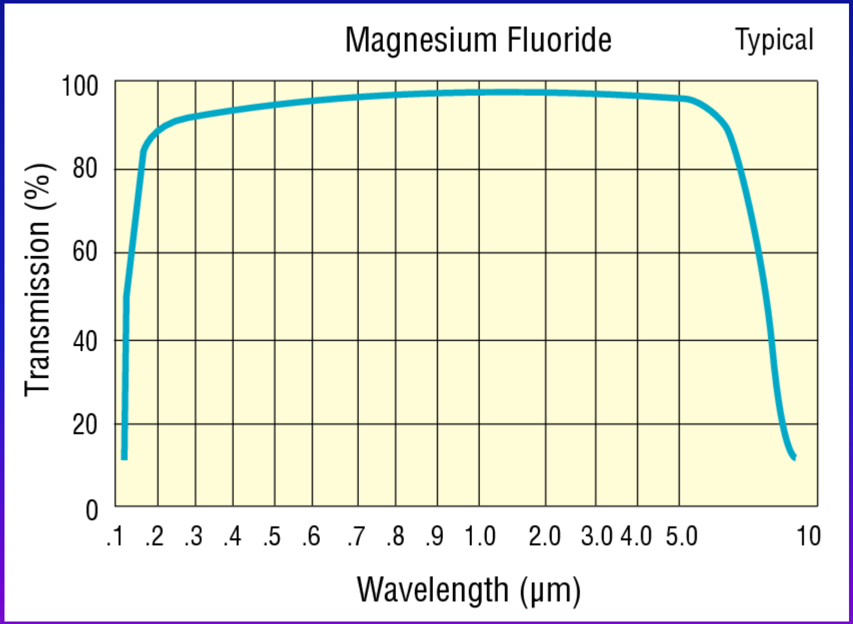

Newport

‘Family tree’ of photo-detectors

Detector types

1. PMT
2. MAPMT
3. MCP-PMT
4. HPD, HAPD
5. Photosensitive gas detectors (MWPC / MPGD)
6. PIN diode (design)
7. APD
8. G-APD / SiPM

Applications

1. Readout of scintillators / fibres with PMT/MAPMT
2. Ultrafast timing for TOF with MCP-PMT
3. Readout of RICH detectors with HPD
4. Readout of RICH detector with gas-based detectors
5. Readout of inorganic crystals with APD
6. Readout of scintillators with G-APD

Family tree of photo-detectors

photo-detectors

Gas
External photoeffect

- TMAE, TEA, CsI + { MWPC, GEM, … }

Vacuum
External photoeffect

Avalanche gain Process

- Dynodes → PMT
- Continuous dynode →Channeltron, MCP
- Multi-Anode devices

Other gain process = Hybrid tubes

Silicon	Luminescent anodes
HPD	SMART/Quasar
HAPD	X-HPD
G-APD-HPD	

Proposed by G. Barbarino et al., NIM A 594 (2008) 326–331
Proof of principle by C. Joram et al., NIM A 621 (2010) 171-176

Solid state
Internal photoeffect

- PIN-diode
- APD
- G-APD (SiPM)
- CMOS
- CCD

Photo-multiplier tubes (PMT's)

Basic principle:

- Photo-emission from photo-cathode
- Secondary emission (SE) from N dynodes:
  - dynode gain g≈3-50 (function of incoming electron energy E);
  - total gain *M*:

$$M = \prod_{i=1}^{N} g_i$$

- Example:
  - 10 dynodes with g=4
  - $M = 4^{10} \approx 10^6$

(Hamamatsu)

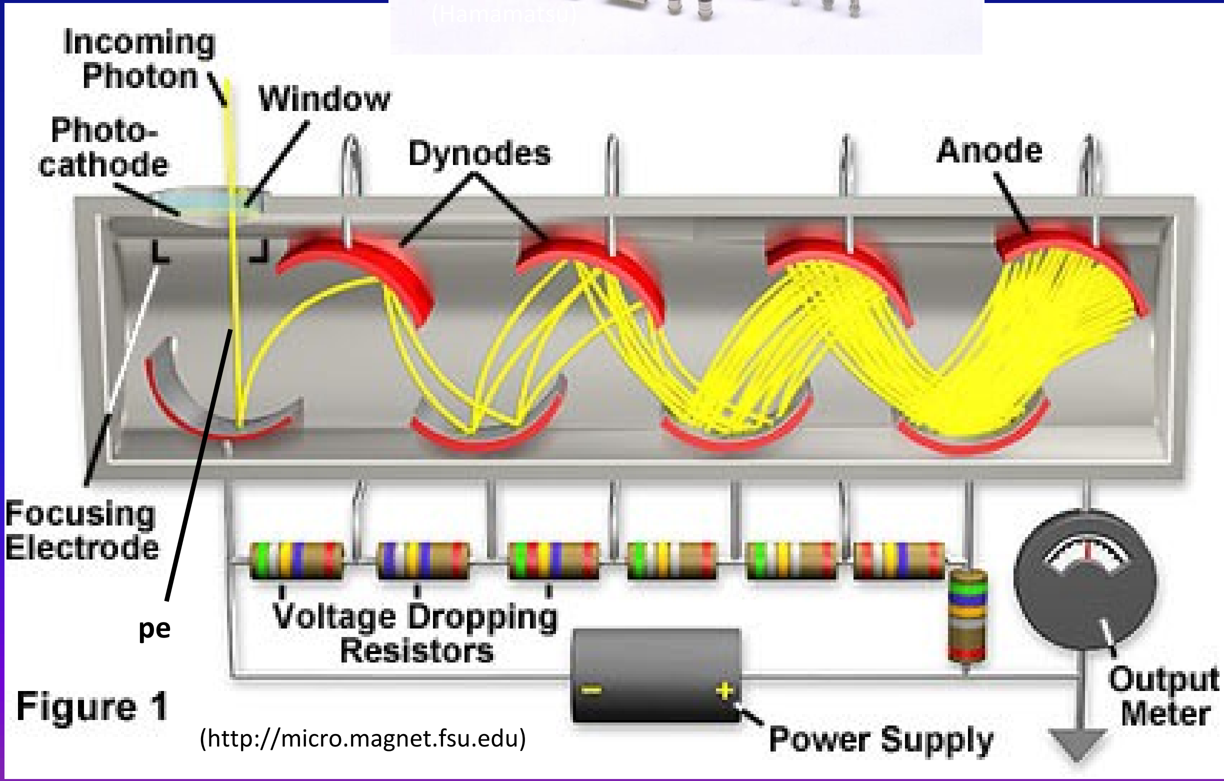

(http://micro.magnet.fsu.edu)

Gain fluctuations of PMT's

- Mainly determined by the fluctuations of the number m(δ) of secondary e's emitted from the dynodes;
- Poisson distribution: $$P_\delta(m) = \frac{\delta^m e^{-\delta}}{m!}$$
- Standard deviation: $$\frac{\sigma_m}{\delta} = \frac{\sqrt{\delta}}{\delta} = \frac{1}{\sqrt{\delta}}$$
- $\Rightarrow$ fluctuations dominated by 1st dynode gain;

GaP(Cs) dynodes $E_A<0$

SE coefficient δ

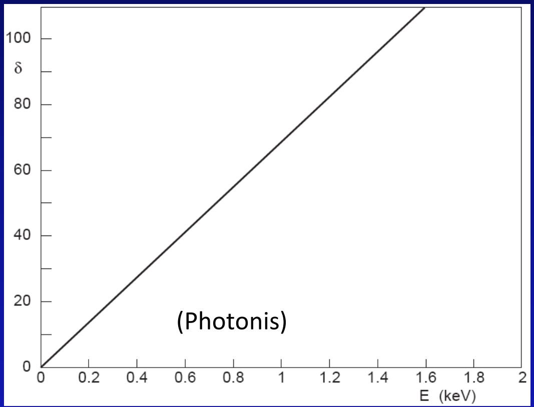

e energy

Counts

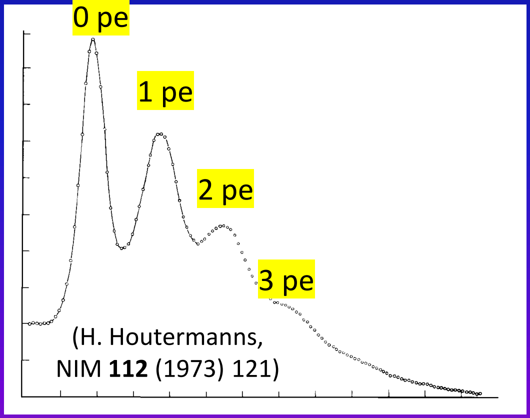

Pulse height

CuBe dynodes $E_A>0$

SE coefficient δ

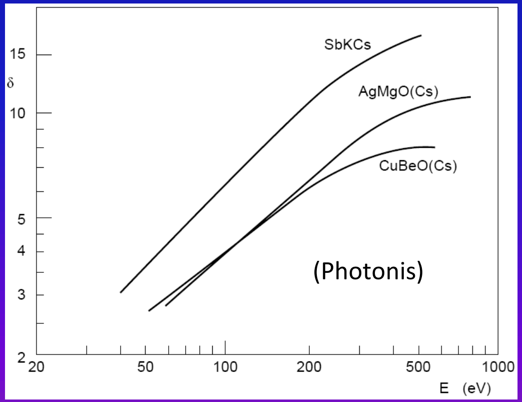

e energy

Counts

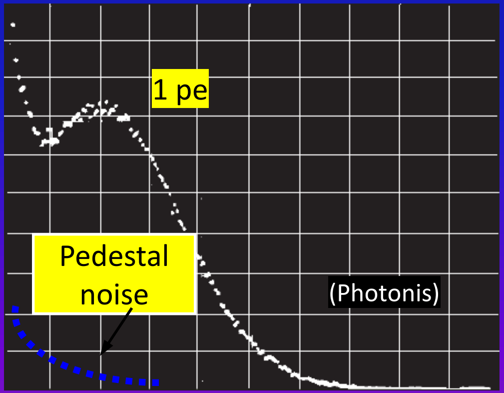

Pulse height

Dynode configurations of PMT's

Traditional

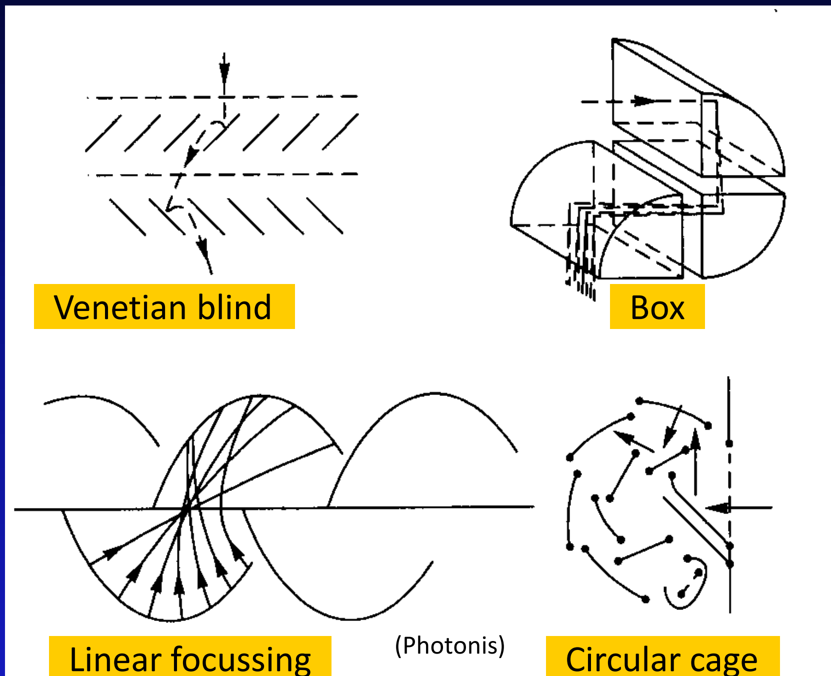

Position-sensitive

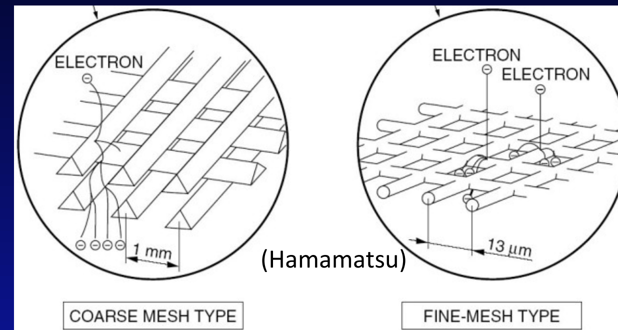

Mesh

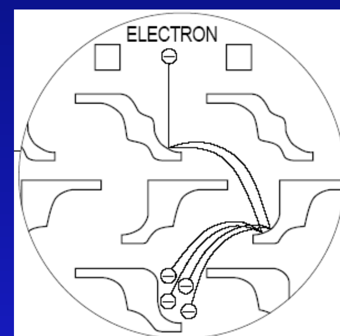

Metal-channel (fine-machining techniques)

(Hamamatsu)

The design of a dynode structure is a compromise between

- collection efficiency (input optics: from cathode to first dynode)
- gain (minimize losses of electrons during passage through structure)
- transit time and transit time spread (minimize length of path and deviations)
- immunity to magnetic field

Modern micro-machining techniques allow fabricating fine dynode structures. Avalanche is confined in a narrow channel. → Multi-anode designs.

Dynode configurations of PMT's

Estimate transit time: $t = \frac{l}{v} = \frac{l}{\sqrt{\frac{2 \cdot eU}{m_e}}} = \frac{0.1\,\text{m}}{\sqrt{\frac{2 \cdot e \cdot 100\text{V}}{0.5\,\text{MeV/c}^2}}} = \frac{0.1\,\text{m}}{0.02\,\text{c}} = 16.7\,\text{ns}$

- Compact construction (short distances between dynodes) keeps the overall transit time small (~10 ns).
- "Fast" PMT's require well-designed input electron optics to limit (e) chromatic and geometric aberrations $\rightarrow$ transit time spread < 100 ps;

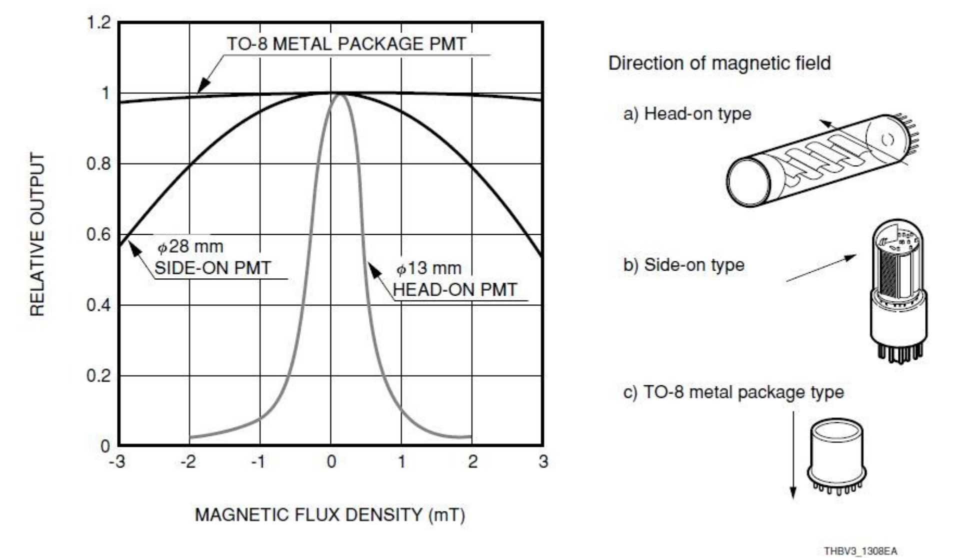

Figure 13-8: Magnetic characteristics of typical photomultiplier tubes

- PMT's are in general very sensitive to magnetic fields, even to earth field (30-60 μT = 0.3-0.6 Gauss).
- Magnetic shielding required.

Multi-anode and flat-panel PMT's

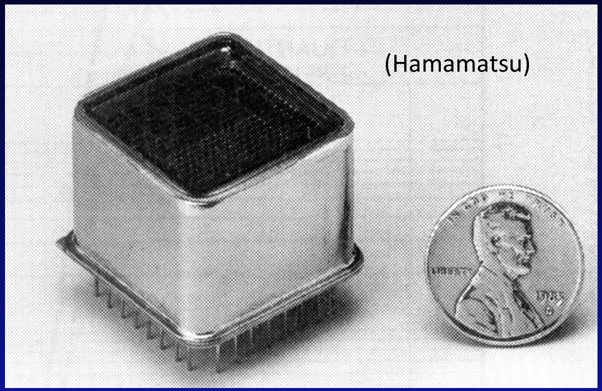

Multi-anode (Hamamatsu H7546)

- Up to 8 × 8 channels (2 × 2 mm^2 each);
- Size: 28 × 28 mm^2;
- Active area 18.1 × 18.1 mm^2 (41%);
- Bialkali PC: QE ≈ 25 - 45% @ λ_{max} = 400 nm;
- Gain ≈ 3 10^5;
- Gain uniformity typ. 1 : 2.5;
- Cross-talk typ. 2%

Cherenkov rings from
3 GeV/c π^- through aerogel

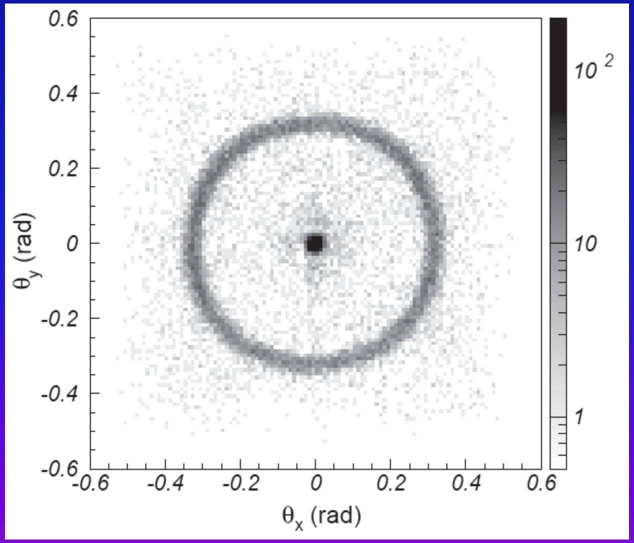

(T. Matsumoto et al., NIMA **521** (2004) 367)

Flat-panel (Hamamatsu H8500):

- 8 x 8 channels (5.8 x 5.8 mm^2 each)
- Excellent surface coverage (89%)

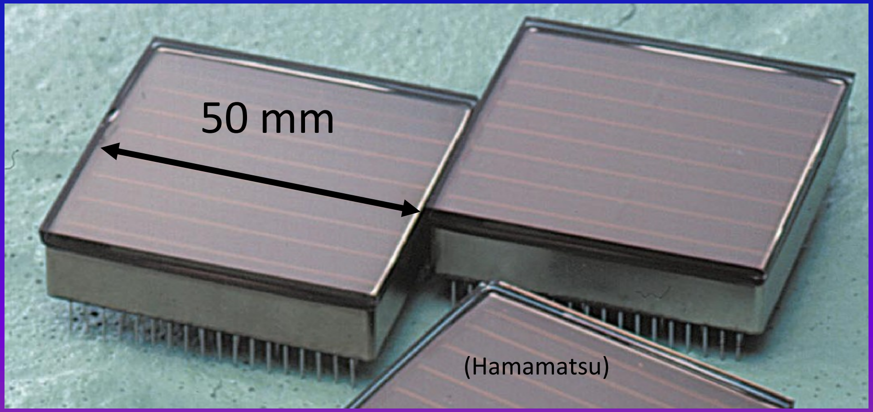

Readout of Scintillating fibres with MAPMTs

Working principle of scintillating plastic fibres :

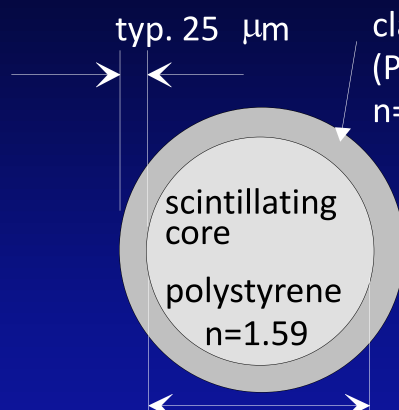

light transport by

total internal reflection

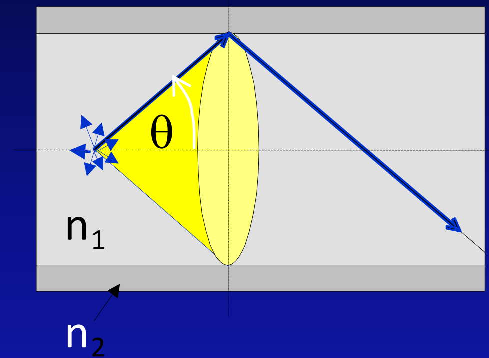

$$\theta \le \arccos\frac{n_2}{n_1} \approx 20.4^\circ$$

$$\frac{d\Omega}{4\pi} = 0.5\,(1-\cos\theta) = 3\%$$ (per side)

Double cladding system

(developed by CERN RD7)

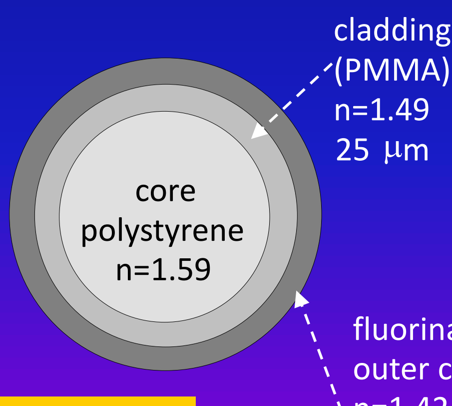

$$\frac{d\Omega}{4\pi} = 0.5\,(1-\cos\theta) \approx 5.3\%$$

Example: ATLAS ALFA – A fibre tracker (for luminosity measurement)

- Technology: Scintillating plastic fibres, square cross-section, 500 μm overall width, single cladded (10 μm). Type: Kuraray SCSF-78.

- Geometry: UV (45°)

10 UV layers, staggered by 70.7 μm

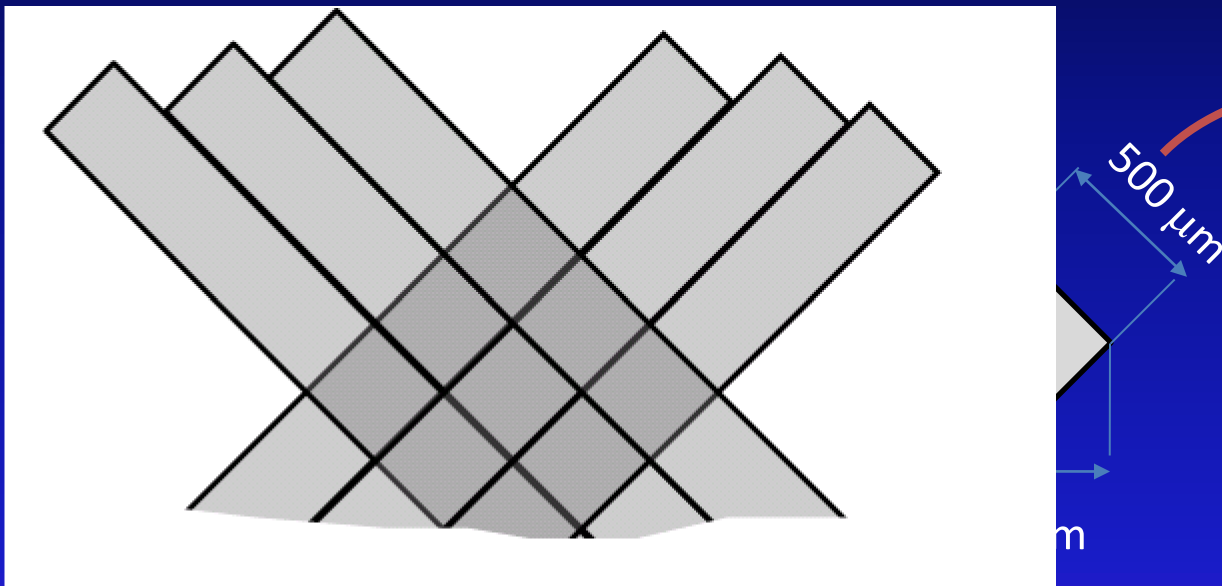

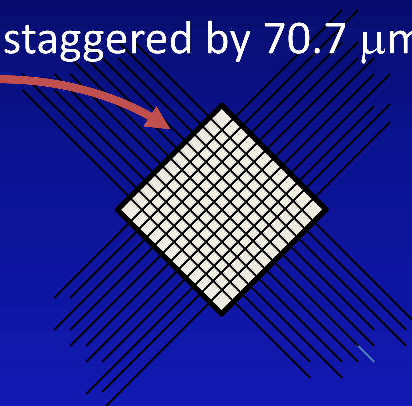

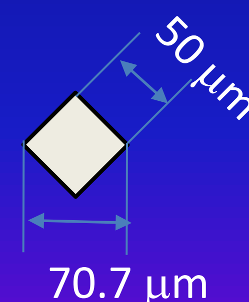

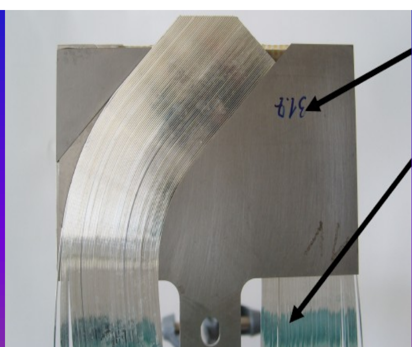

Expect:

$\sigma_x = \sigma_y \sim 707 / \sqrt{24}\ \mu$m

$= 144\ \mu$m

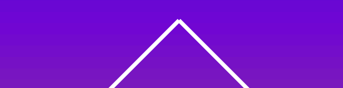

remember: triangular distribution function

ultimately: $\sigma_x = \sigma_y$

$\sim 70.7 / \sqrt{24}\ \mu$m

$= 14.4\ \mu$m

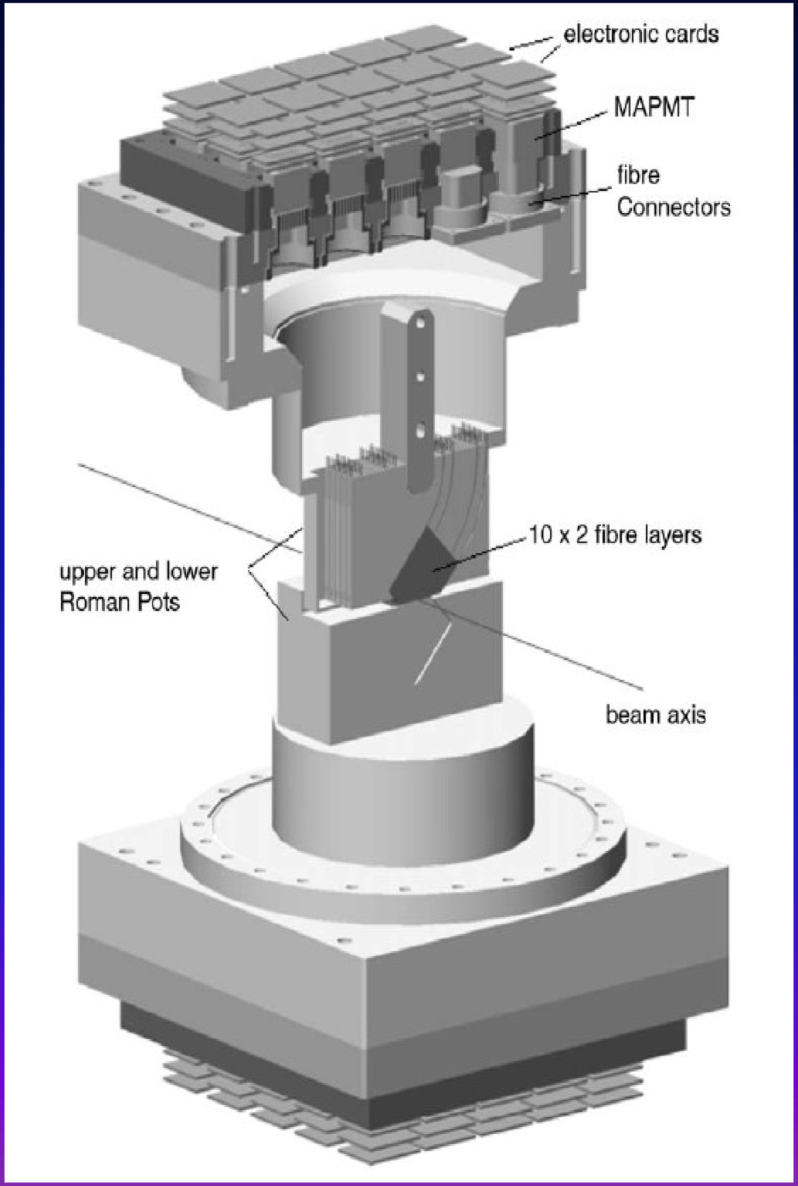

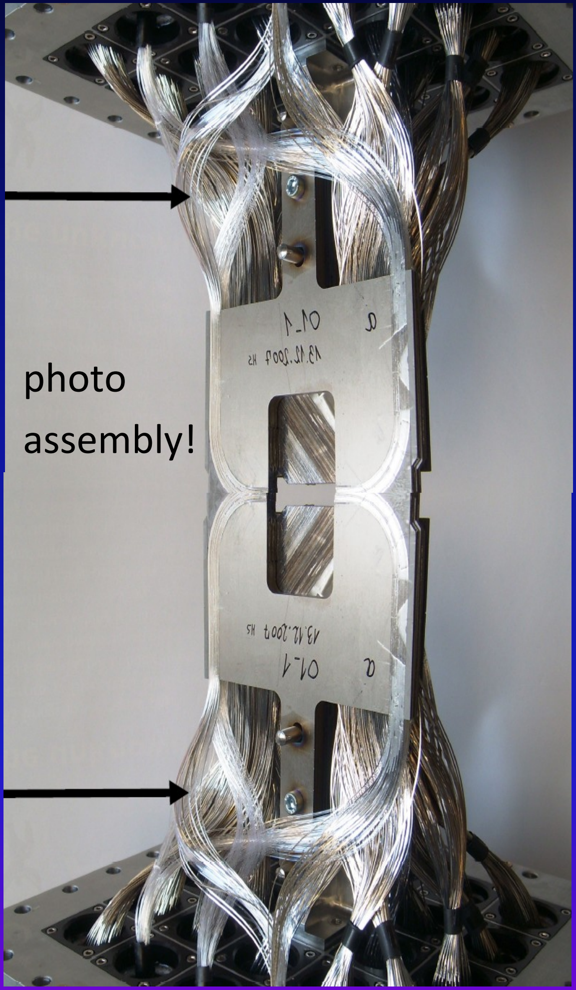

~2 x 1400 fibres

64 Fibres are glued in a 8x8 matrix ‘connector’ . The pitch of 2.2 mm corresponds exactly to the one of the MAPMT.

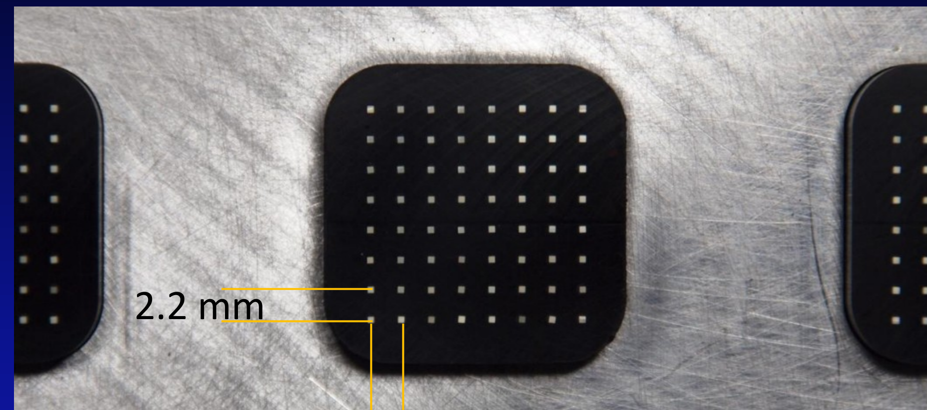

2.2 mm

2.2 mm

2.2 mm

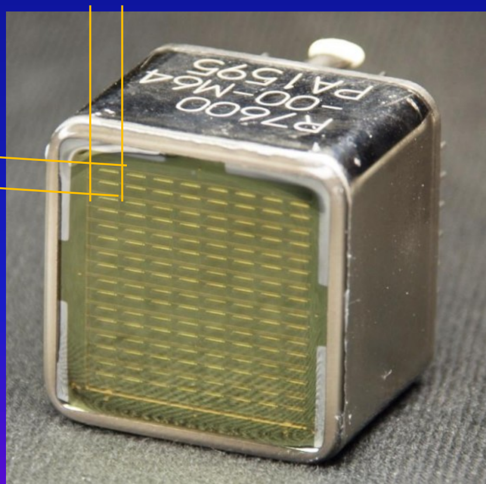

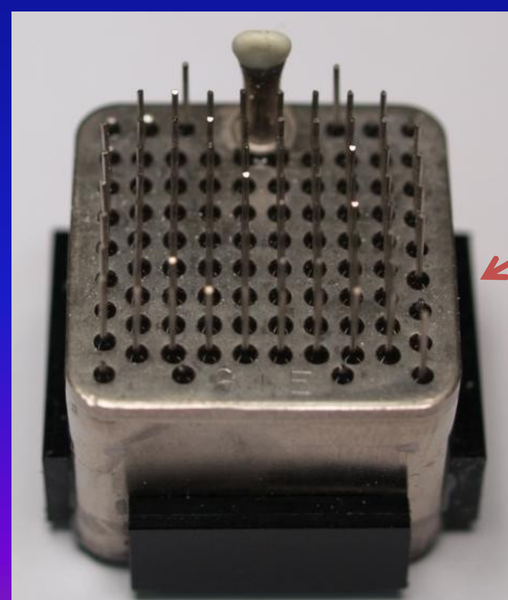

4 shims centre the MAPMT w.r.t. the fibre connector → Maximize light coupling and minimize cross-talk!

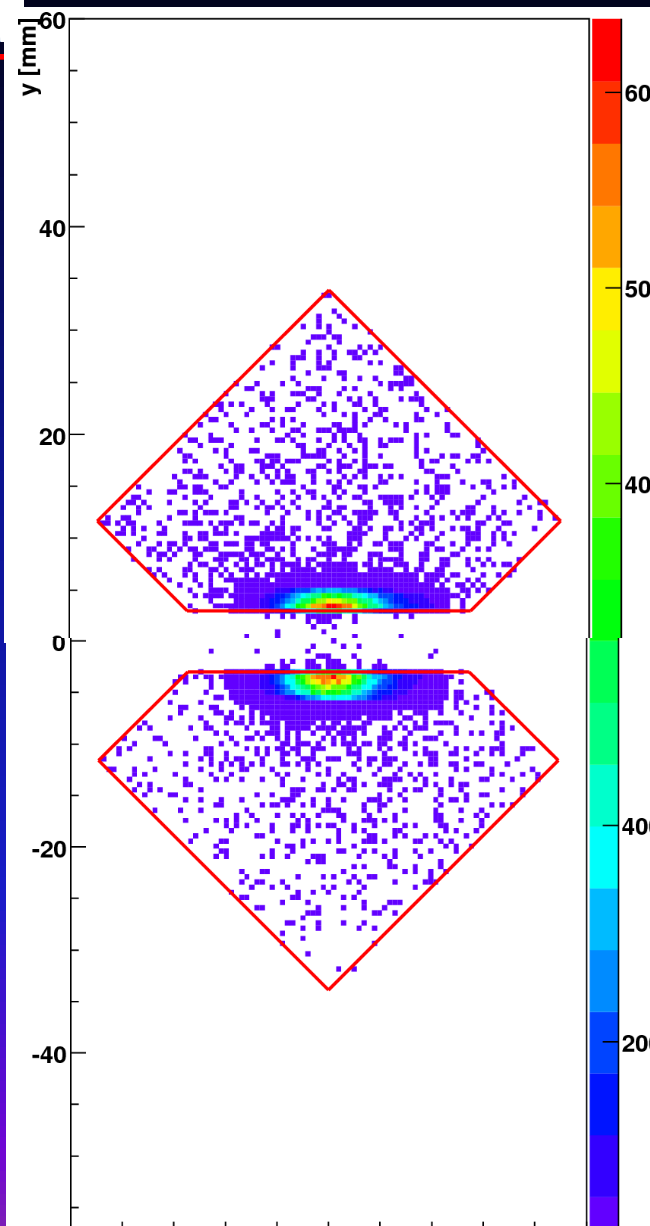

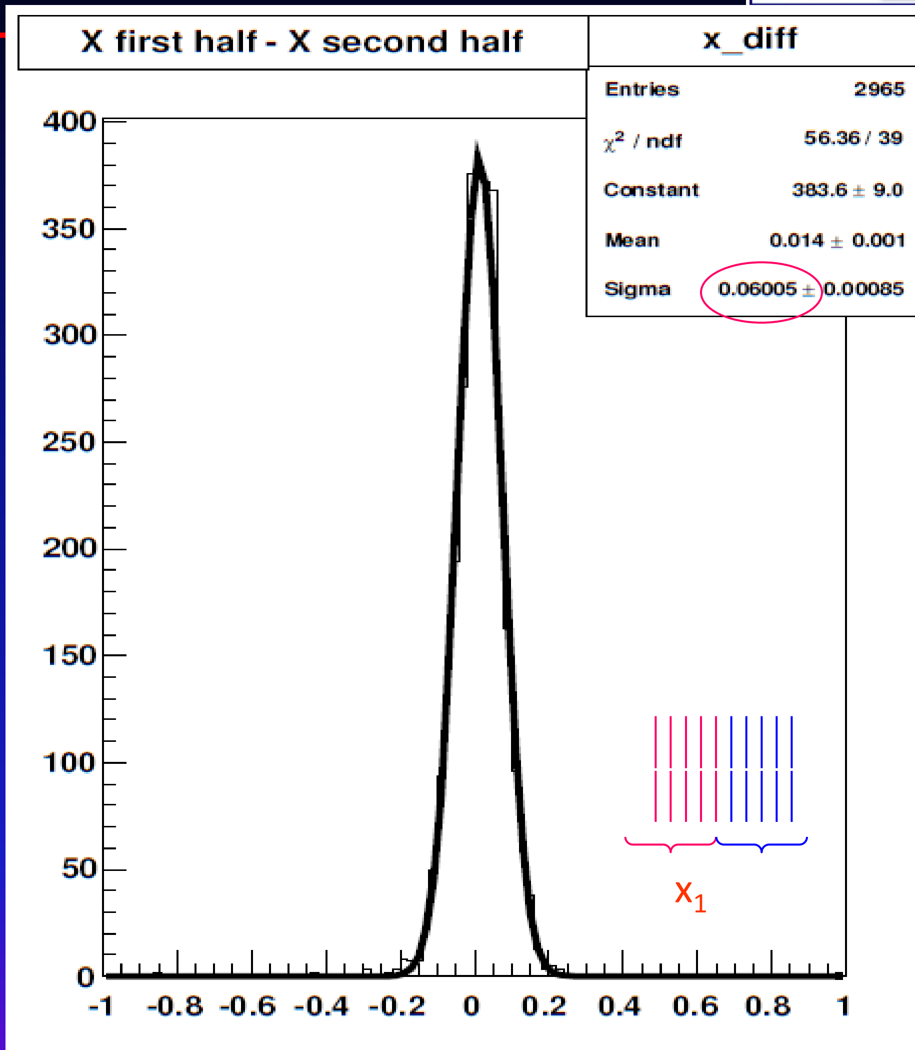

Expect σ_{ALFA} ~ 32 μm

Micro Channel plate PMT (MCP-PMT)

Similar to ordinary PMT – dynode structure is replaced by MCP.

Basic characteristics:

- Gain ~ 10^6 → single photon
- Collection efficiency ~ 60%
- Small thickness, high field → small TTS
- Works in magnetic field
- Segmented anode → position sensitive

MCP is a thin glass plate with an array of holes (<10-100 µm diameter) - continuous dynode structure

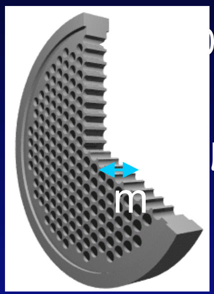

MCP gain depends on L/D ratio – typically 1000
For L/D=40

PHOTONIS

HAMAMATSU

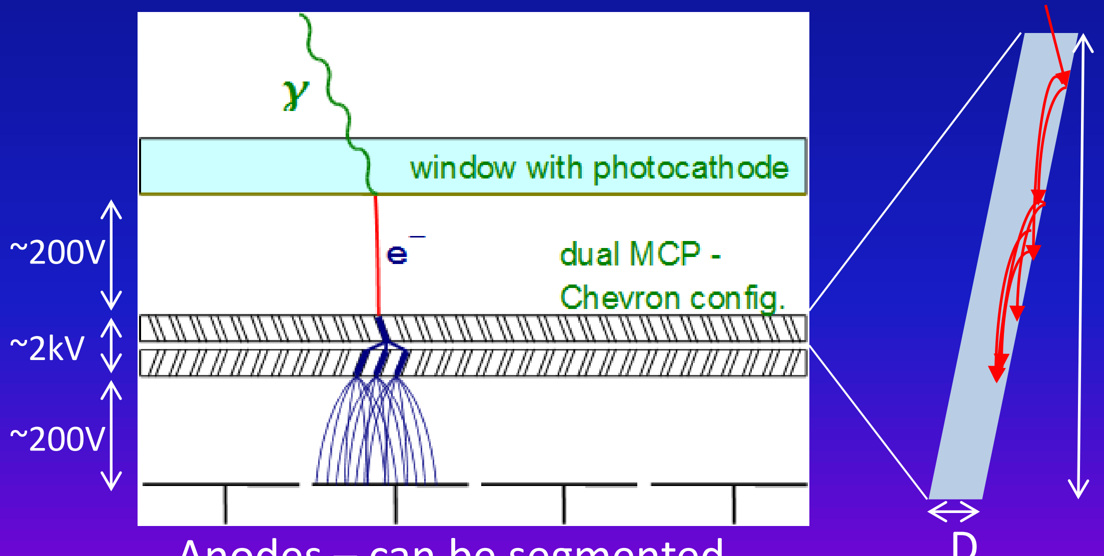

Anodes – can be segmented according to application needs

MCP-PMT: Single photon pulse height and timing

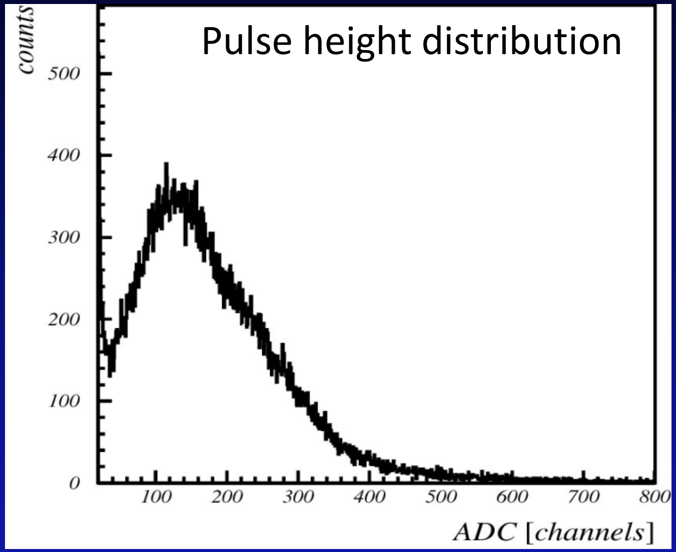

Gain in a single channel saturates at high gains due to space charge effect → peaking distribution for single photoelectron

Typical single photon timing distribution with narrow main peak (σ ~ 40 ps) and contribution from photoelectron back-scattering.

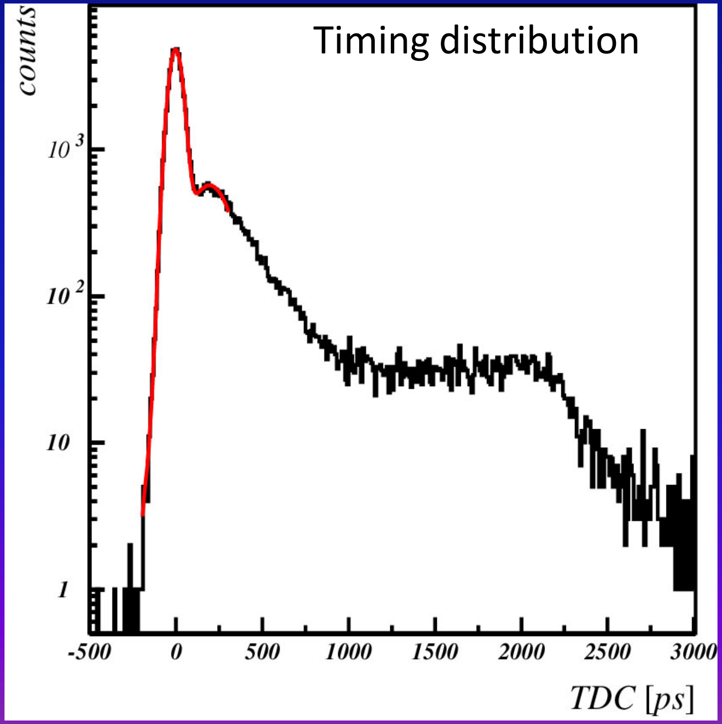

Photoelectron backscattering produces rather long tail in timing distribution and position resolution.

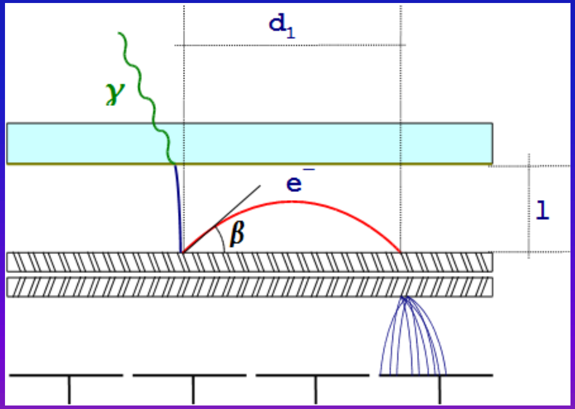

Range equals twice the photocathode-MCP distance (2l).

MCP-PMT: Charge sharing

Secondary electrons spread when traveling from MCP out electrode to anode and can hit more than one anode → Charge sharing
Can be used to improve spatial resolution.

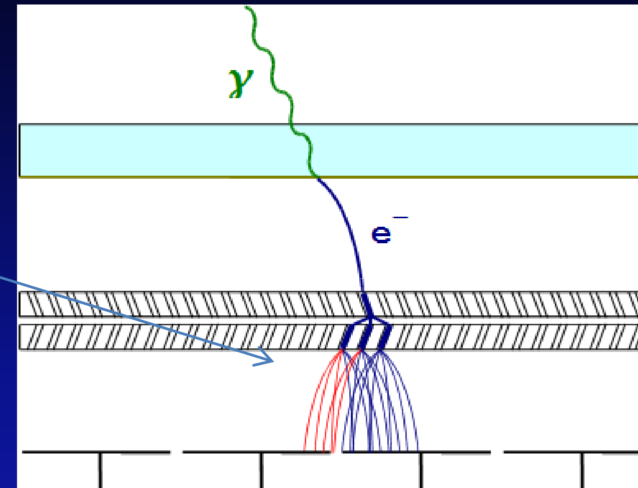

Fraction of the charge detected by left pad as a function of light spot position (red laser)

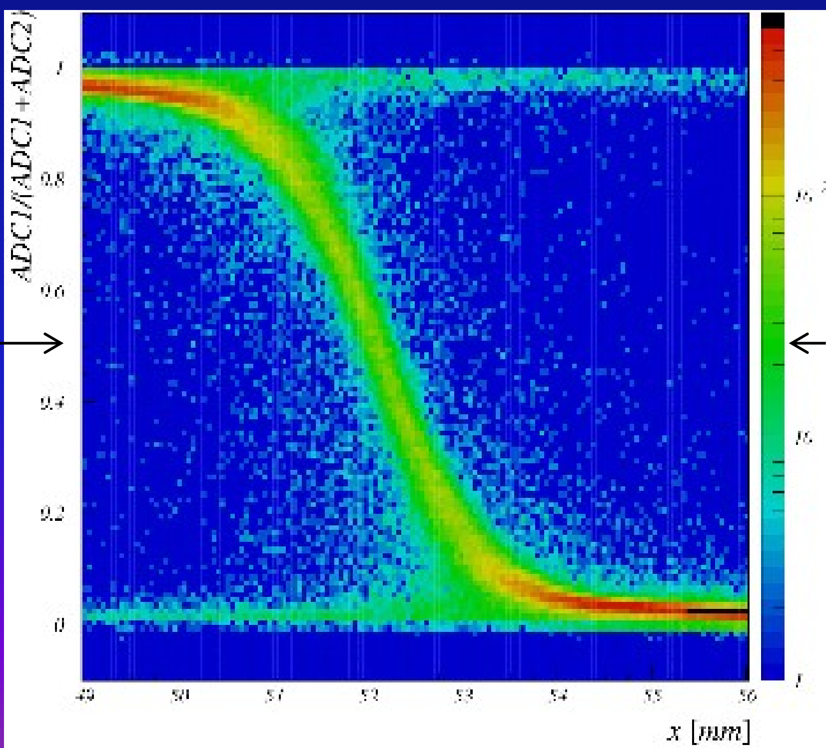

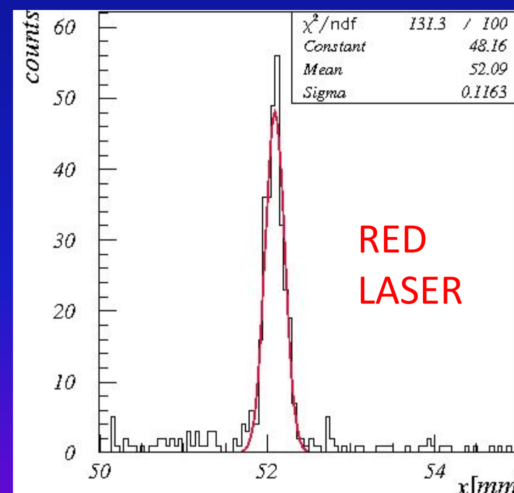

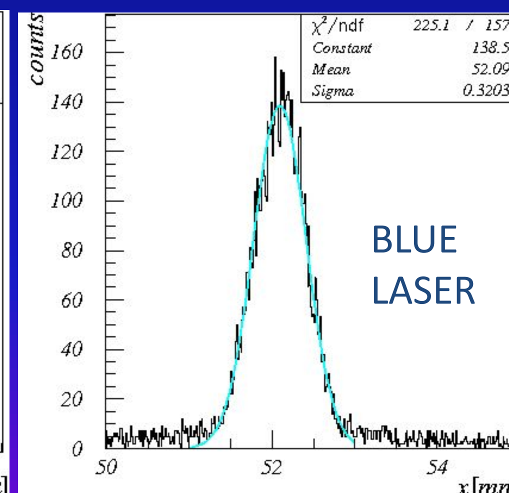

Slices at equal charge sharing for red and blue laser) – pad boundary. Resolution limited by photoelectron energy.

MCP-PMT: Operation in magnetic field

- Narrow amplification channel and proximity focusing electron optics allow operation in magnetic field (~ axial direction).
- Amplification depends on magnetic field strength and direction.
- Effects of charge sharing and photoelectron backscattering on position resolution are strongly reduced while effects on timing remain

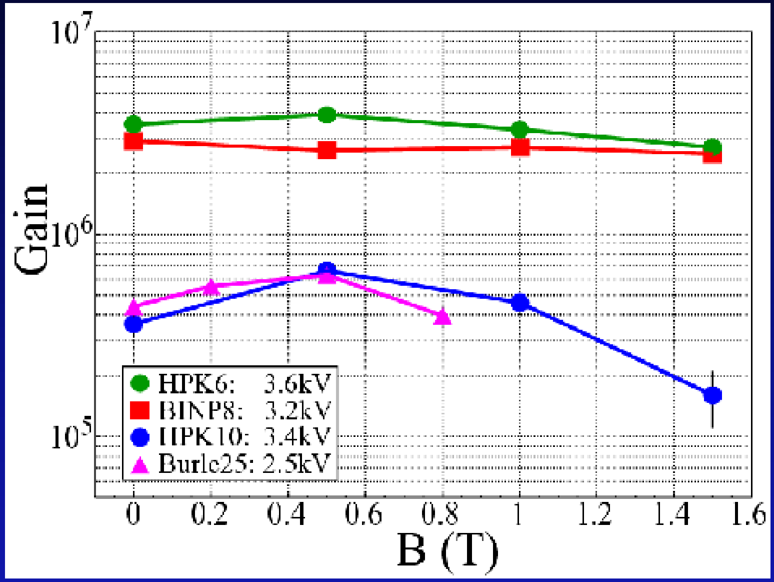

K. Inami @ PD07

Gain vs. Magnetic field for MCP-PMT samples with different pore diameter.

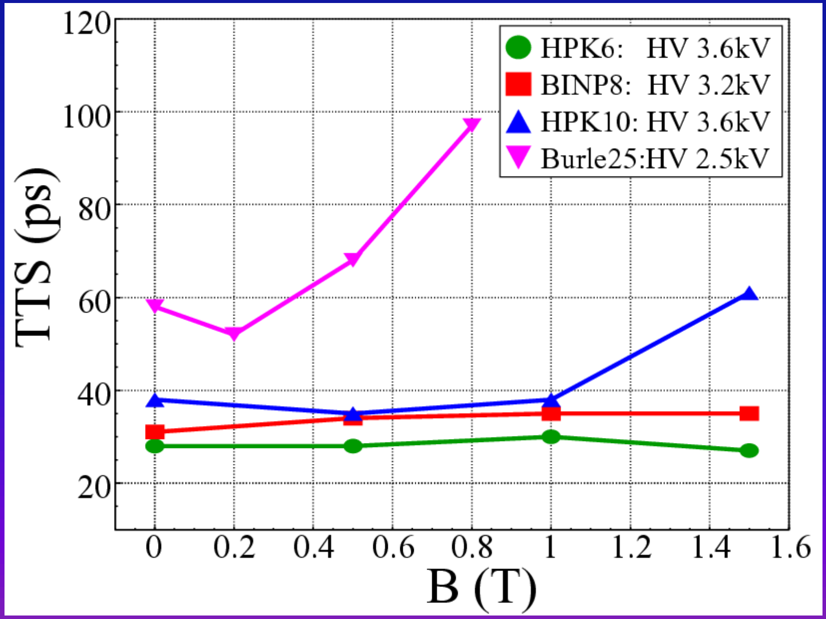

TTS vs. Magnetic field for MCP-PMT samples with different pore diameter.

MCP-PMT: Ion feedback and aging

- During the amplification process atoms of residual gas get ionized → travel back toward the photocathode and produce secondary pulse
- Ion bombardment damages the photocathode reducing QE
- Thin Al foil (few μm) blocks ion feedback but also about half of the electrons → placed between the MCPs

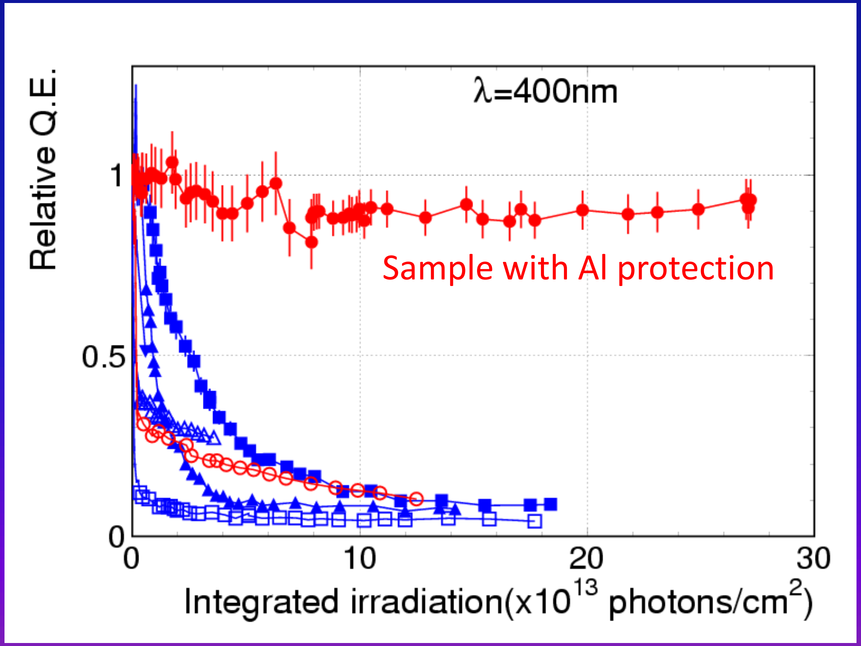

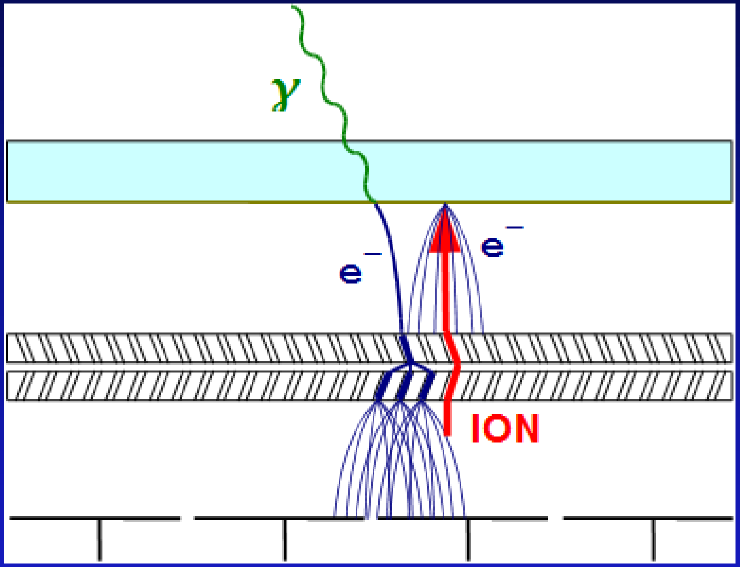

K. Inami @ PD07

Change of relative QE during the typical aging test. MCP-PMTs without Al protection show rapid reduction of QE.

MCP-PMT: TOF applications

- Excellent timing properties require fast light source → Cherenkov radiator directly attached to the MCP-PMT
- Can be used as dedicated TOF (SuperB end-cap PID option) or as part of the proximity focusing RICH (Belle-II end-cap PID option)

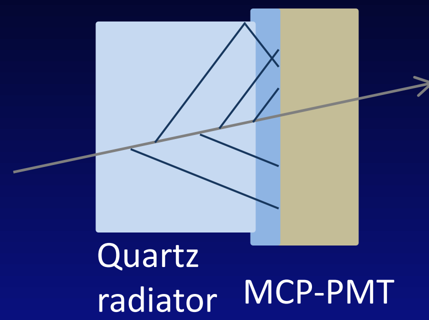

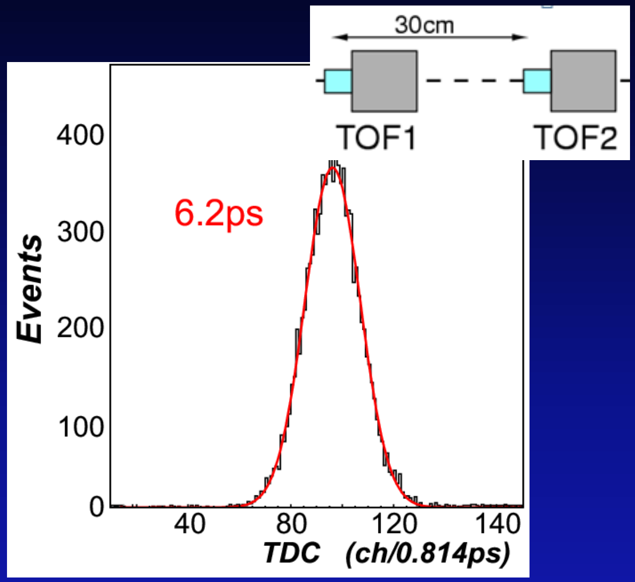

K. Inami @ PD07

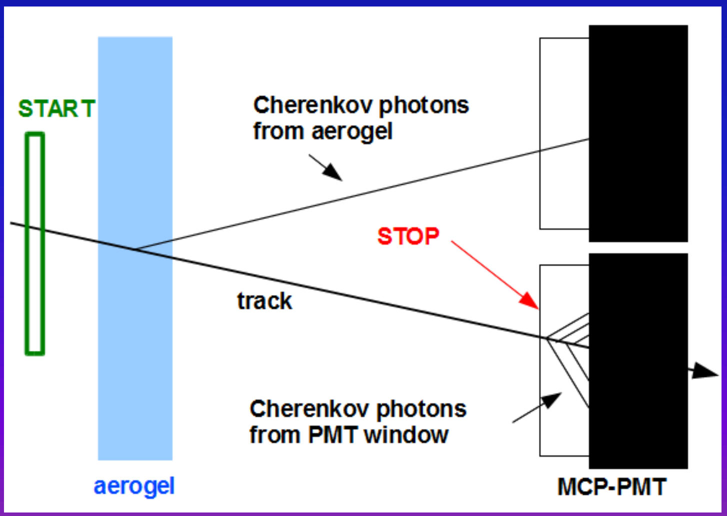

Proximity focusing aerogel RICH with TOF capability

Separation of 2 GeV pions and protons with 0.6 m flight length (start counter σ ~ 15 ps).

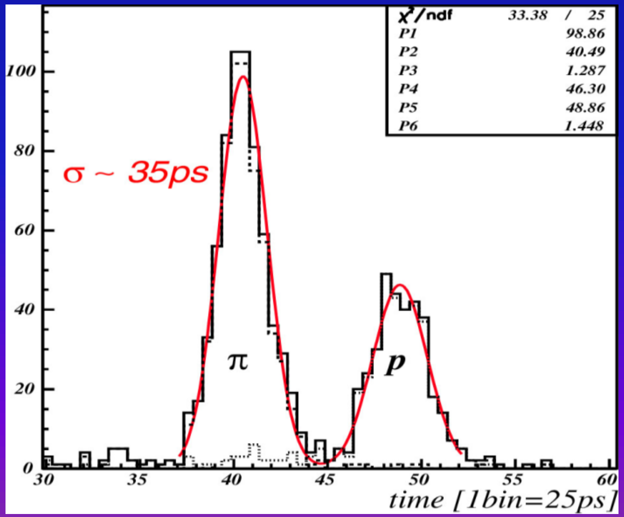

MCP-PMT: RICH with timing information

DIRC concept (BaBar) – 2D imaging

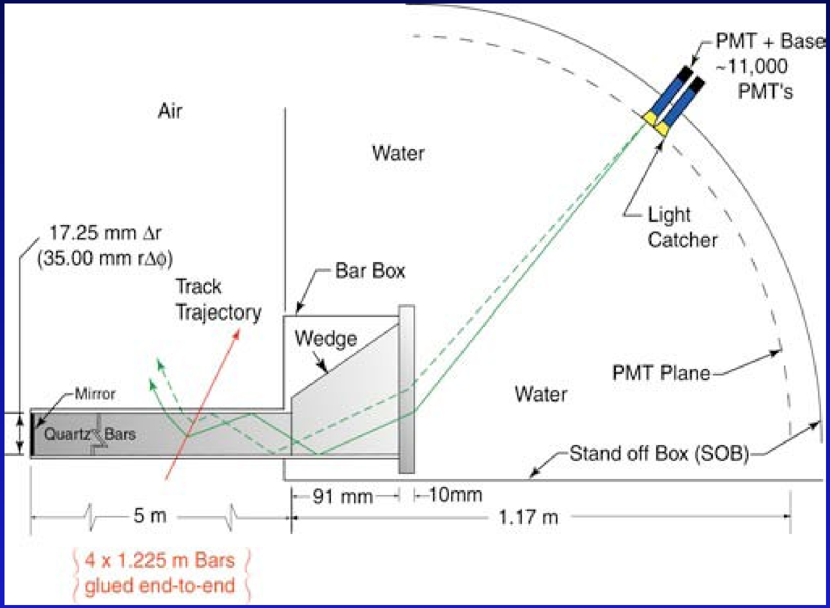

Focusing DIRC with chromatic correction (SuperB) uses measured time of propagation to correct chromatic error.

$$t_p = \frac{L_{path}}{v_g} \qquad v_g = \frac{c}{n(\lambda) - \lambda \frac{dn}{d\lambda}} \quad \text{(group velocity)}$$

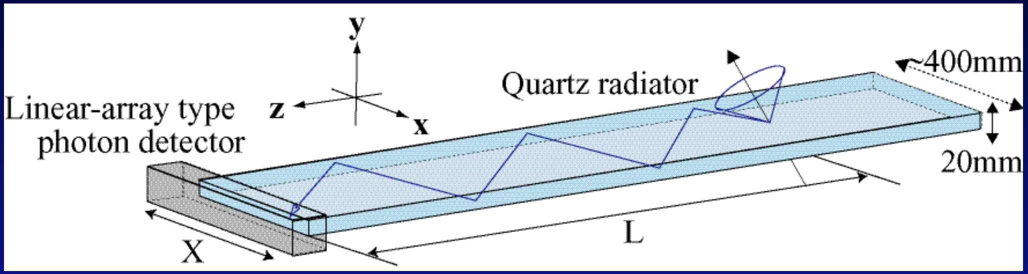

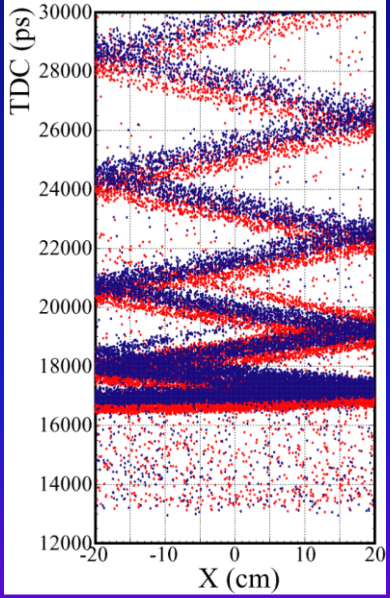

TOP (Time-Of-Propagation) counter based on DIRC concept (Belle-II). Using linear array of MCP-PMTs to measure one coordinate and time of propagation (length of photon path) to obtain 2D image → compact detector.

Hybrid Photon Detectors (HPD's) – Basic Principles

- Combination of vacuum photon detector (image intensifier) and solid-state technologies;
- Input: collection lens, (active) optical window, photo-cathode;
- Gain: achieved *in one step* by energy dissipation of keV pe's in solid-state detector anode; this results in low gain fluctuations;
- Output: direct electronic signal;
- Encapsulation in the tube implies:
  - compatibility with high vacuum technology (low outgassing, high T° bake-out cycles);
  - internal (for speed and fine segmentation) or external connectivity to read-out electronics;
  - heat dissipation issues;

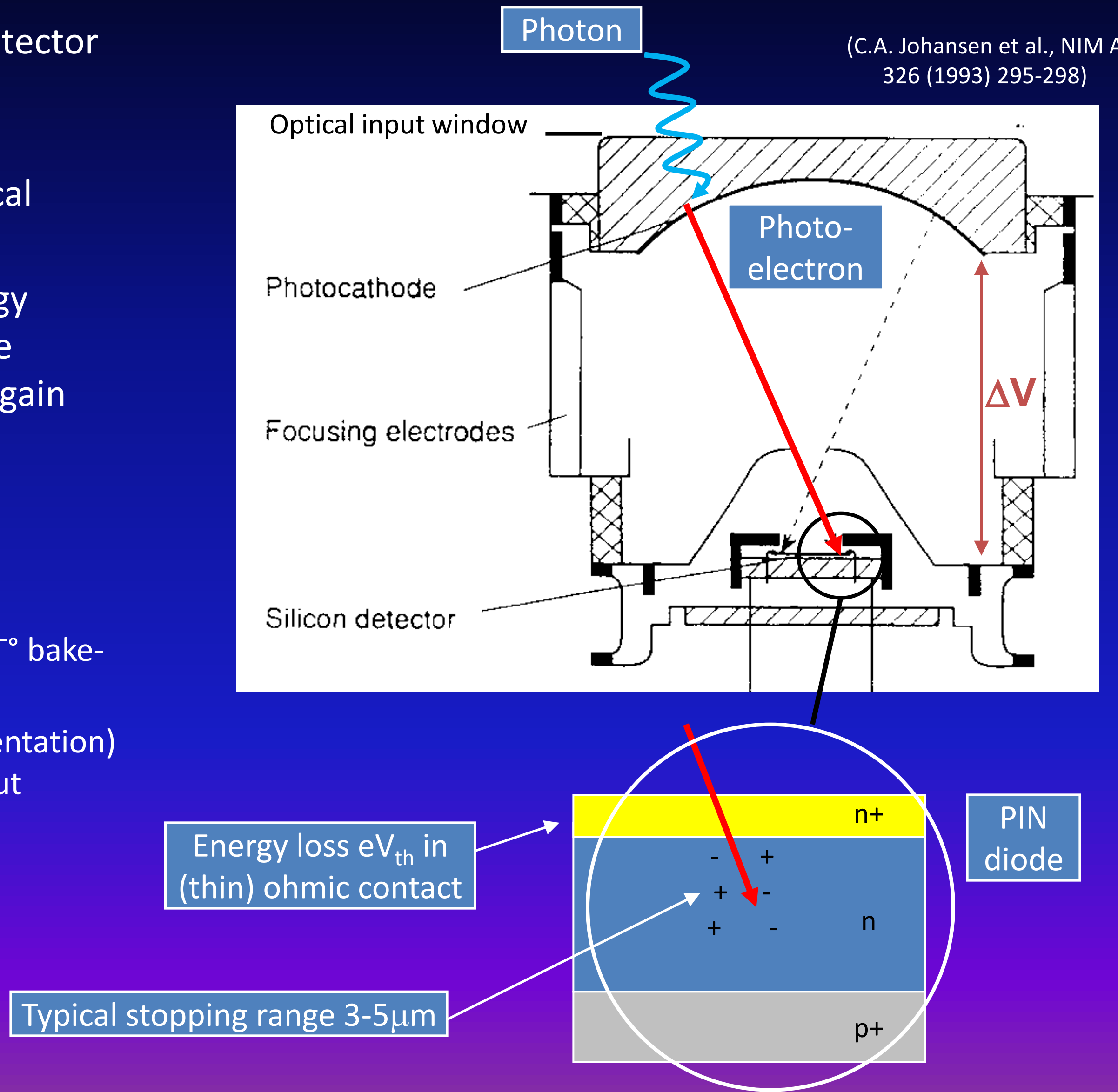

Energy resolution of HPD's - Basic Properties

- Photo-emission from photo-cathode;
- Photo-electron acceleration to $\Delta V \approx$ 10-20kV;
- Energy dissipation through ionization and phonon excitation (W_{Si}=3.6eV to generate 1 e-h pair in Si) with low fluctuations (Fano factor $F \approx$ 0.12 in Si);
- Gain M: $$M = \frac{e(\Delta V - Vth)}{W_{Si}}$$
- Intrinsic gain fluctuations σ_M : $$\sigma_M = \sqrt{F \cdot M}$$

  $\Rightarrow$ overall noise dominated by electronics
- Example: ΔV = 20kV

  $\Rightarrow$ M $\approx$ 5000 and $\sigma_M \approx$ 25
- Suited for single photon detection with high resolution;

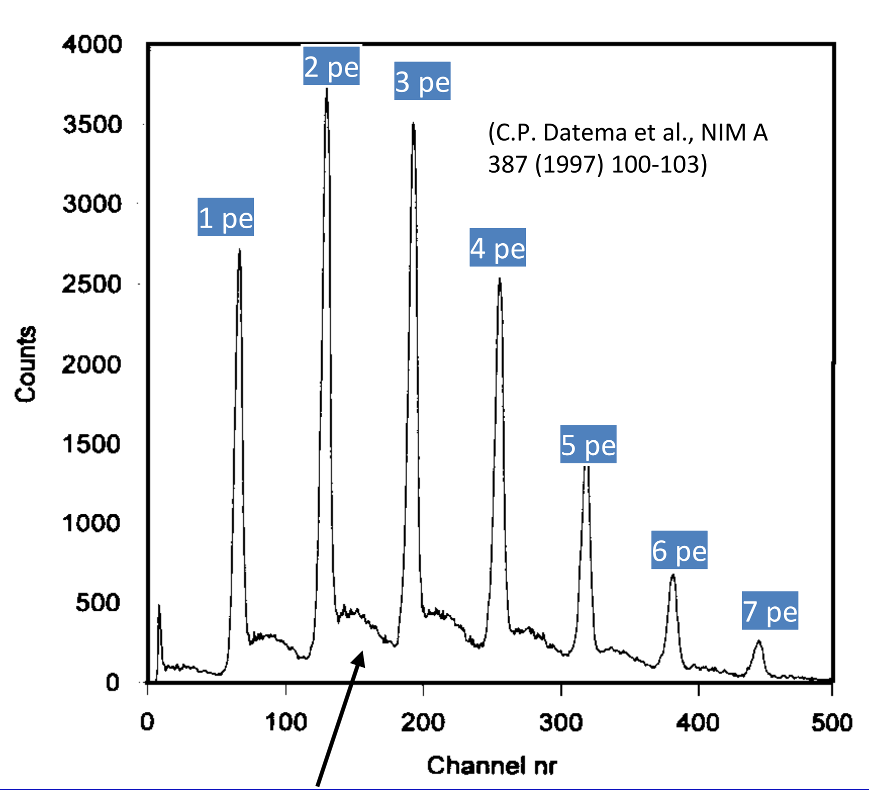

- Continuum from photo-electron back-scattering effects at Si surface
- For proposed models, see eg:
  - C. D'Ambrosio et al., NIM A 338 (1994) 389-397
  - T. Tabarelli de Fatis, NIM A 385 (1997) 366-370

Multi-pixel proximity-focussed HPD – CMS HCAL

- B=4T $\Rightarrow$ proximity-focussing with 3.35mm gap and HV=10kV;
- Minimize cross-talks:
  - photo-electron back-scattering: align with B;
  - capacitive: Al layer coating;
  - internal light reflections: a-Si:H AR coating optimized @ λ = 520nm (WLS fibres);
- Results in linear response over a large dynamic range from minimum ionizing particles (muons) up to 3 TeV hadron showers;

(P. Cushman et al., NIM A 504 (2003) 502)

Possible cross-talks

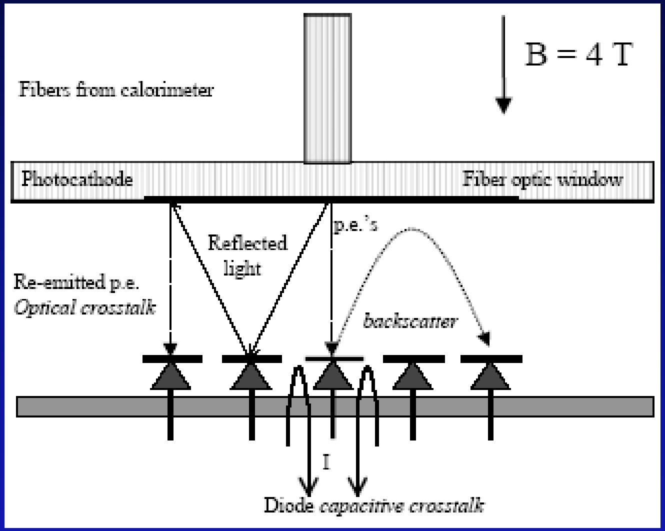

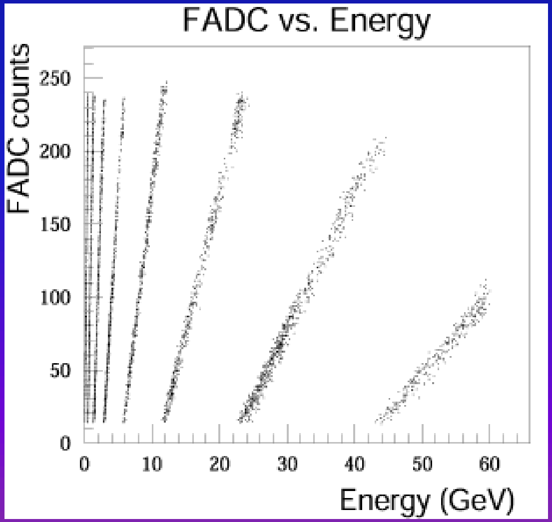

(http://cmsinfo.cern.ch/Welcome.html/CMSdetectorInfo/CMShcal.html)

Various kinds of (semi-) commercial HPD's (1)

Single-diode cross-focussing

(DEP-LAA)

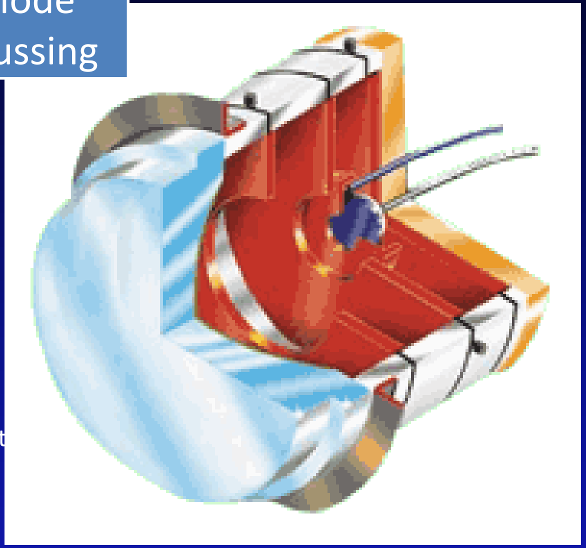

(R. DeSalvo et
NIMA A 315 (1992)

Multi-pixel proximity-focussing

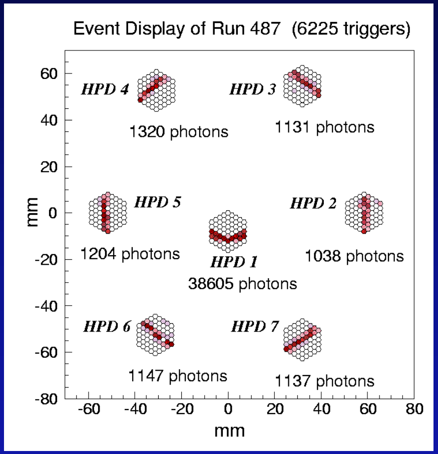

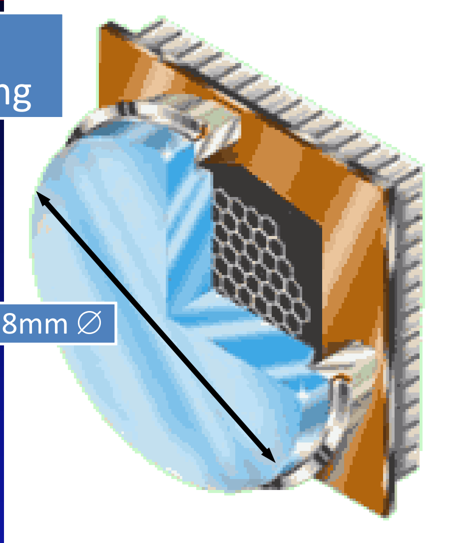

Cb)

(E. Albrecht et al.,
NIMA A 411 (1998) 249-264)

Single avalanche diode HPD

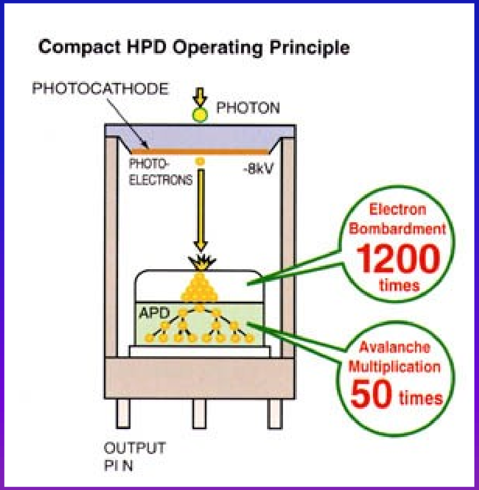

(Hamamatsu)

Hybrid avalanche photodiode array

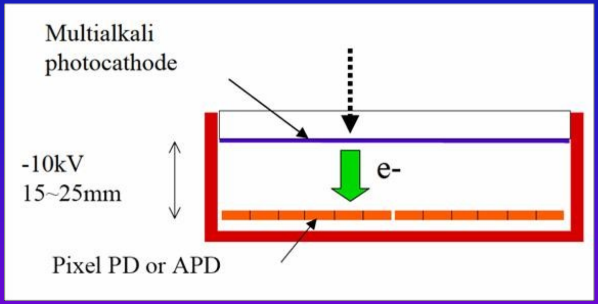

(I. Adachi et al.,
NIM A 623 (2010) 285–287)

(Hamamatsu)

Various kinds of (semi-) commercial HPD's (2)

Multi-pixel, cross-focussing

(DEP-LH

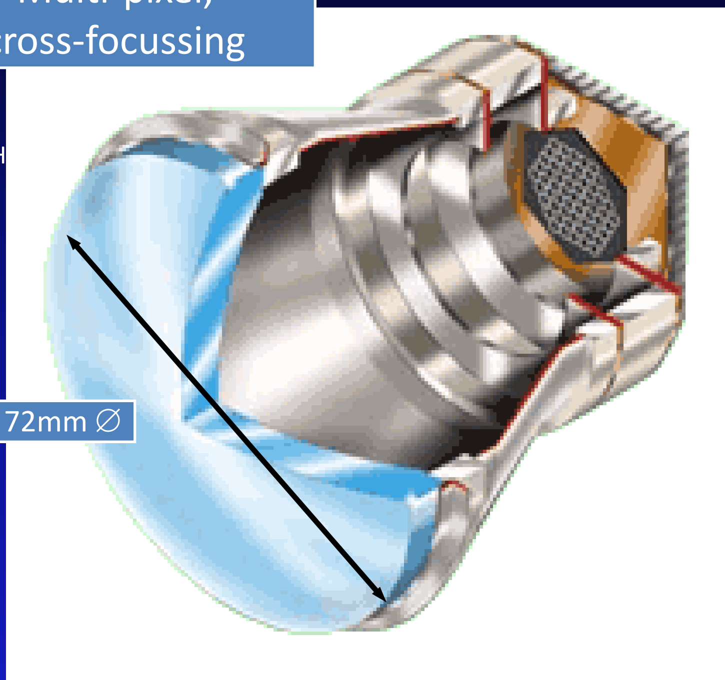

., NIMA A
4-170)

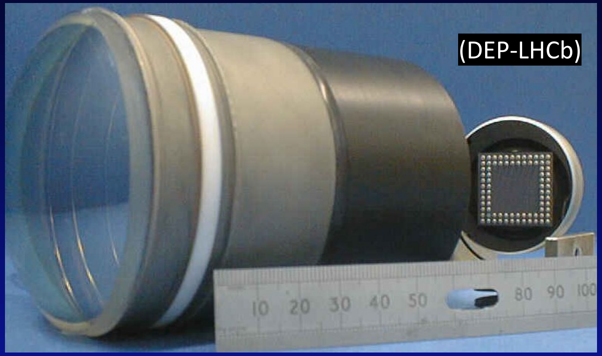

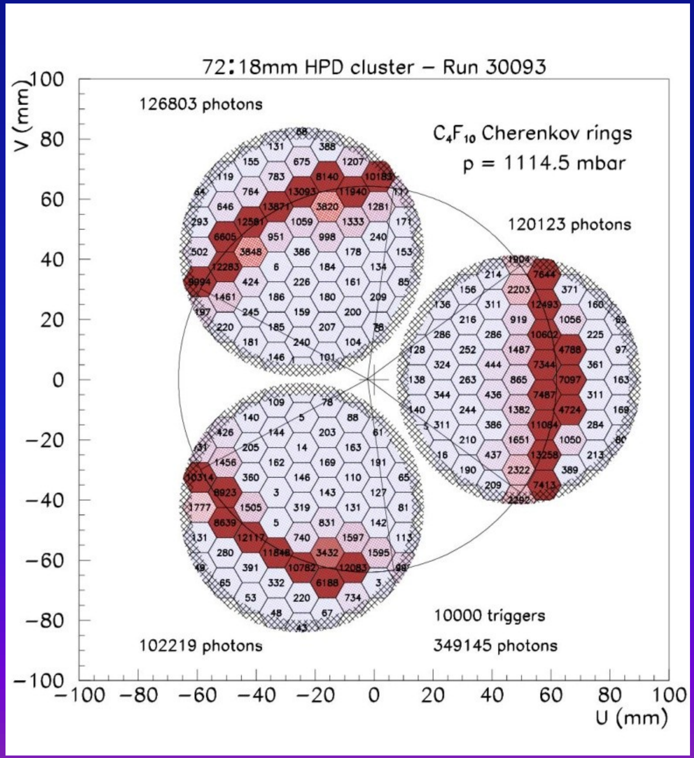

- DEP-LHCb development:
- Commercial anode;
- Cross-focussing electron optics (de-magnification by ~5);
- High intrinsic active area coverage (83%);

Pixel-HPD's for LHCb RICHes: requirements

- Large area (3.3m²) with high overall active area fraction (~65%)
- Fast compared to the 25 ns bunch crossing time
- Have to operate in a small (1-3mT) magnetic field
- Granularity at photocathode 2.5x2.5mm²

$\Rightarrow$ 484 HPDs with 5$\times$ de-magnification and custom anode

72mm ∅

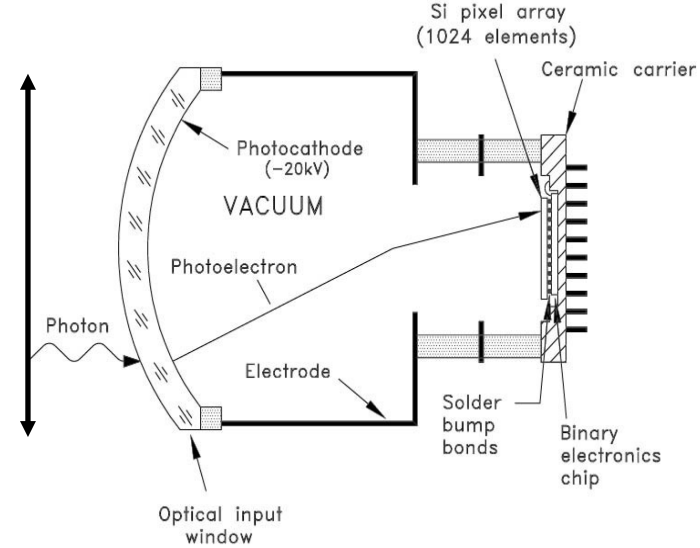

(M. Moritz et al., IEEE TNS Vol. 51, No. 3, June 2004, 1060-1066)

(Photonis-DEP)

~120 mm

50 mm

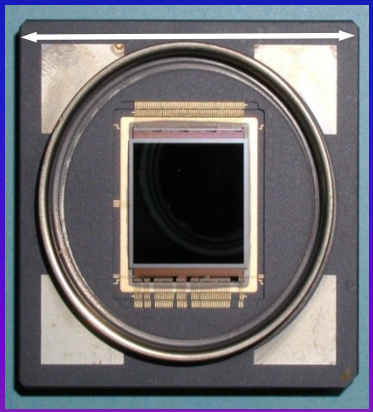

(K. Wyllie et al., NIM A 530 (2004) 82-86)

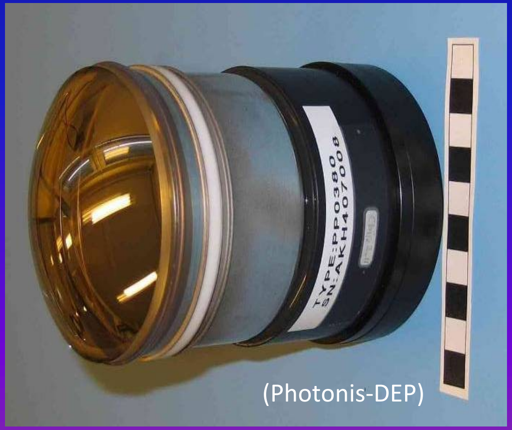

(Photonis-DEP)

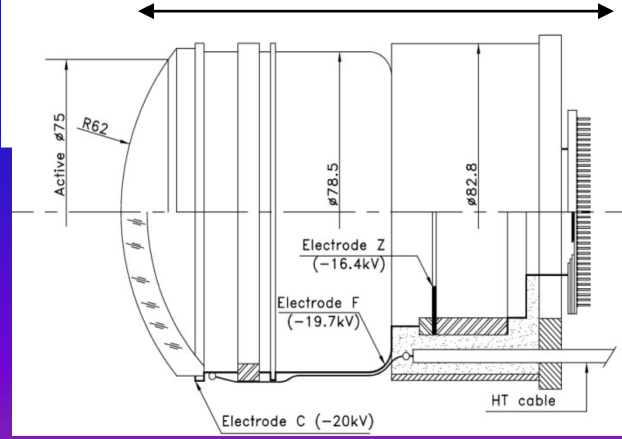

Pixel-HPD's for LHCb RICHes: quantum efficiency

- Must cover 200-600nm wavelength range
- Multi-alkali S20 ($KCsSbNa_2$)
- Improved over production
- Resulted in a ∫QEdE increased by 27% wrt the original specifications

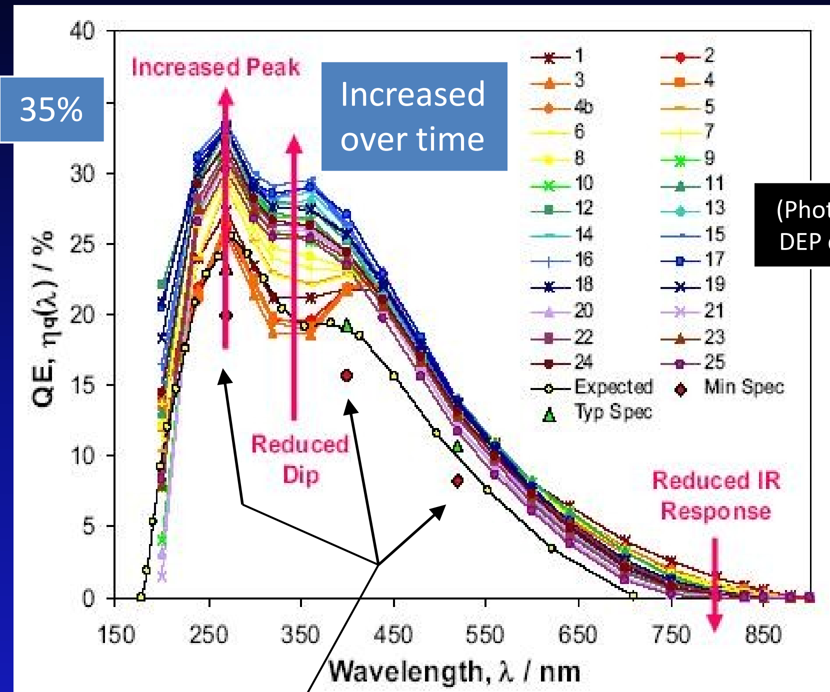

(S. Eisenhardt, NIM A 595 (2008) 142–145)

Typical and minimum QE specs based on prototypes

Cherenkov rings from 80 GeV/c π- through C_4F_{10}

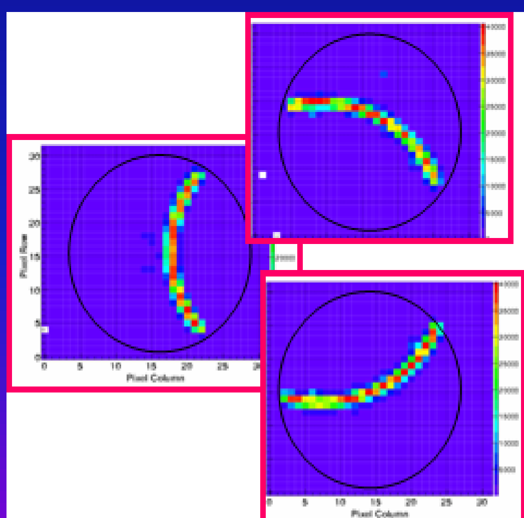

(M Adinolfi et al., NIM A 603 (2009) 287–293)

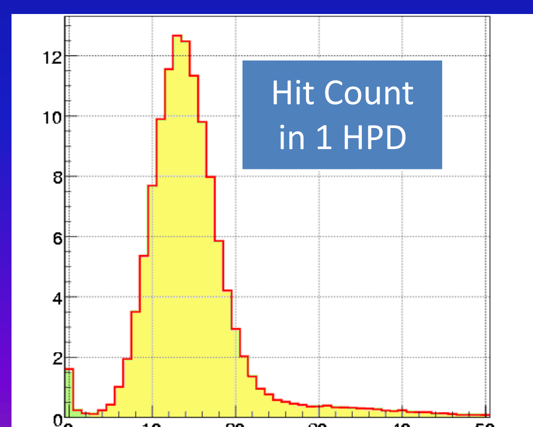

(S. Brisbane, A 595 (2008) 146–149)

Pixel-HPD's for LHCb RICHes: threshold and noise

- The anode is a Si pixel detector with 8192 channels organized in 1024 super-pixels of 500 x 500 μm^2 size, bump-bonded to a custom binary readout chip (lhcbpix1)

  $\Rightarrow$ excellent signal-to-noise ratio achieved by small pixels and optimal sensor-FE coupling

- Very low average threshold and noise

- Typical signal is 5000 e-
  (Si detector dead layer typ. 150nm) with intrinsically low fluctuations (typ. 25 e- rms)

  $\Rightarrow$ ~85% photo-electron detection efficiency for 25ns strobe

- Residual inefficiency is dictated by photo-electron back-scattering (18% probability) and charge-sharing effects

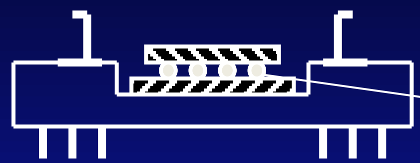

High T solder bumps

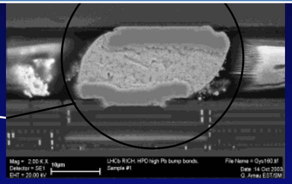

(M. Campbell et al., IEEE TNS **53, 4** (2006), 2296-2302)

Threshold

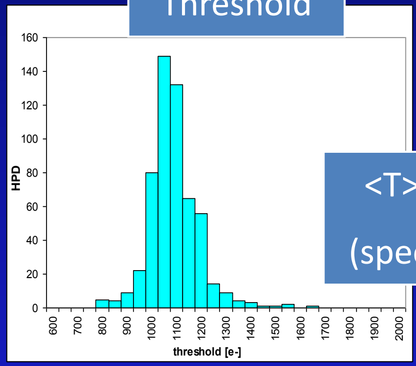

<T>= 1065 e-

(specs 2000 e-)

(S. Eisenhardt, NIM A 595 (2008) 142–145)

Noise

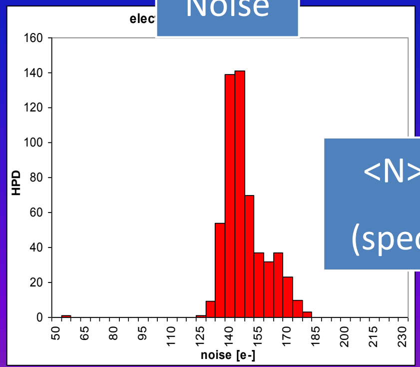

<N>= 145 e-

(specs 250 e-)

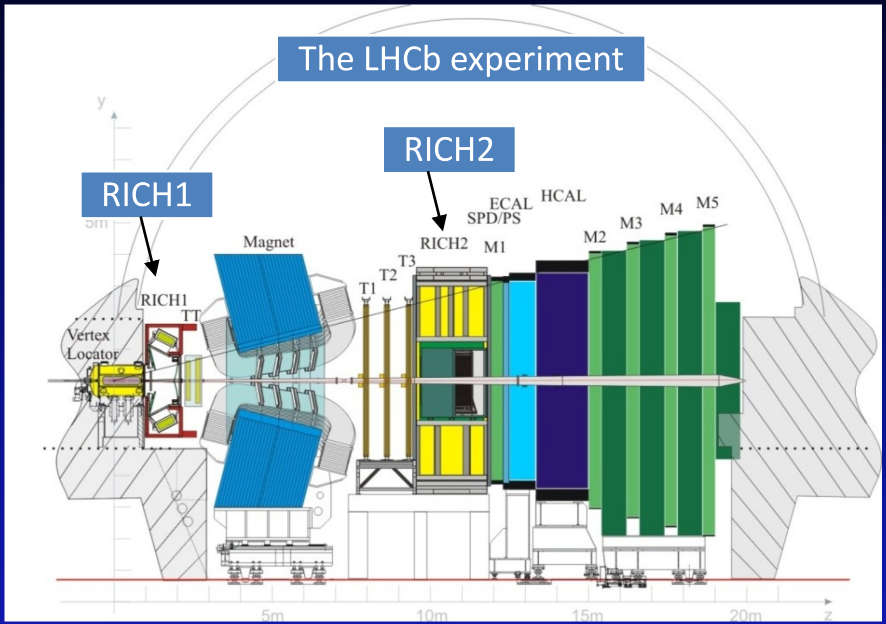

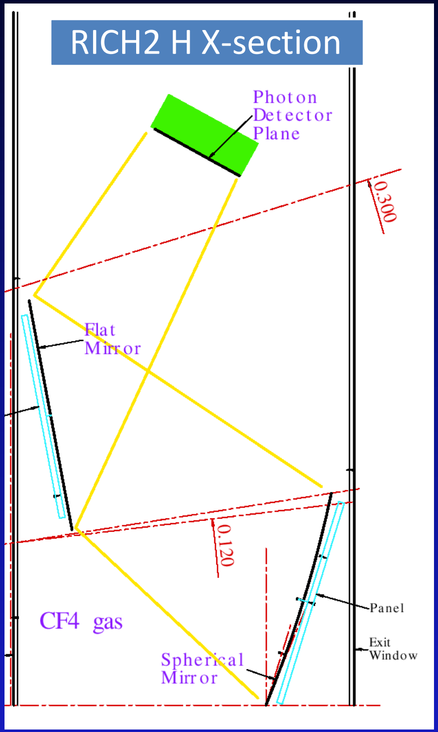

RICH2 HPD plane

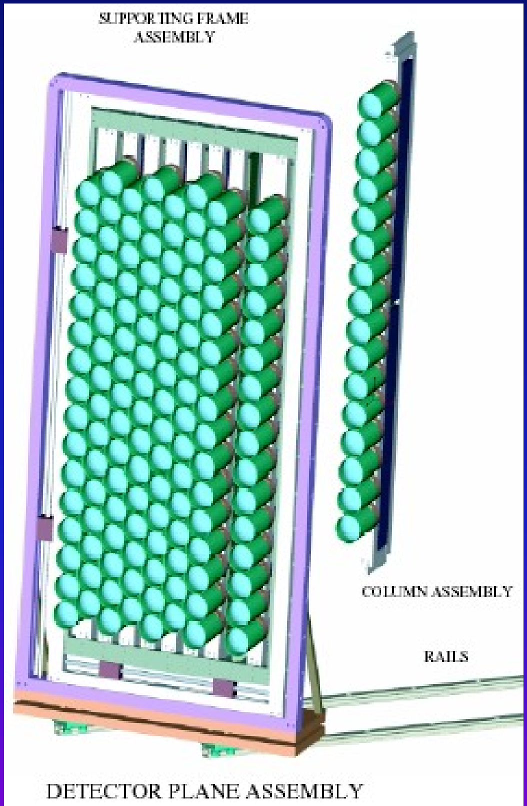

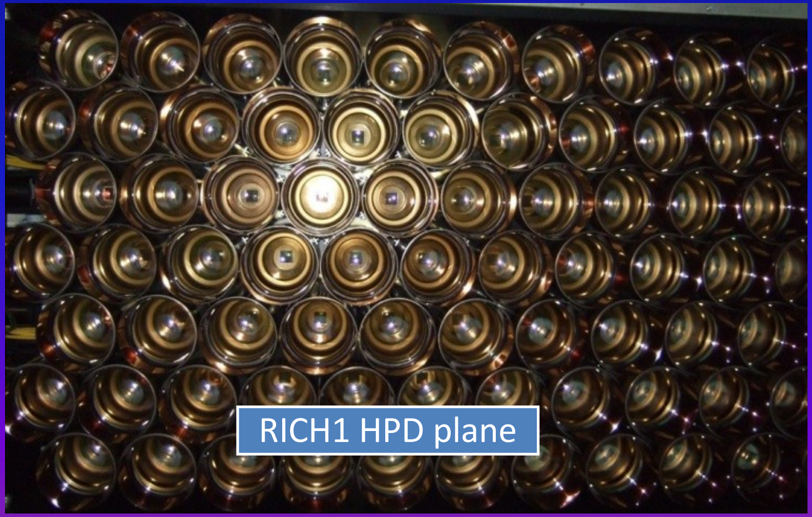

RICH2 EDR
LHCb EDR 2002-009
1 March 2002

Cherenkov photons from p-p collision data at LHC

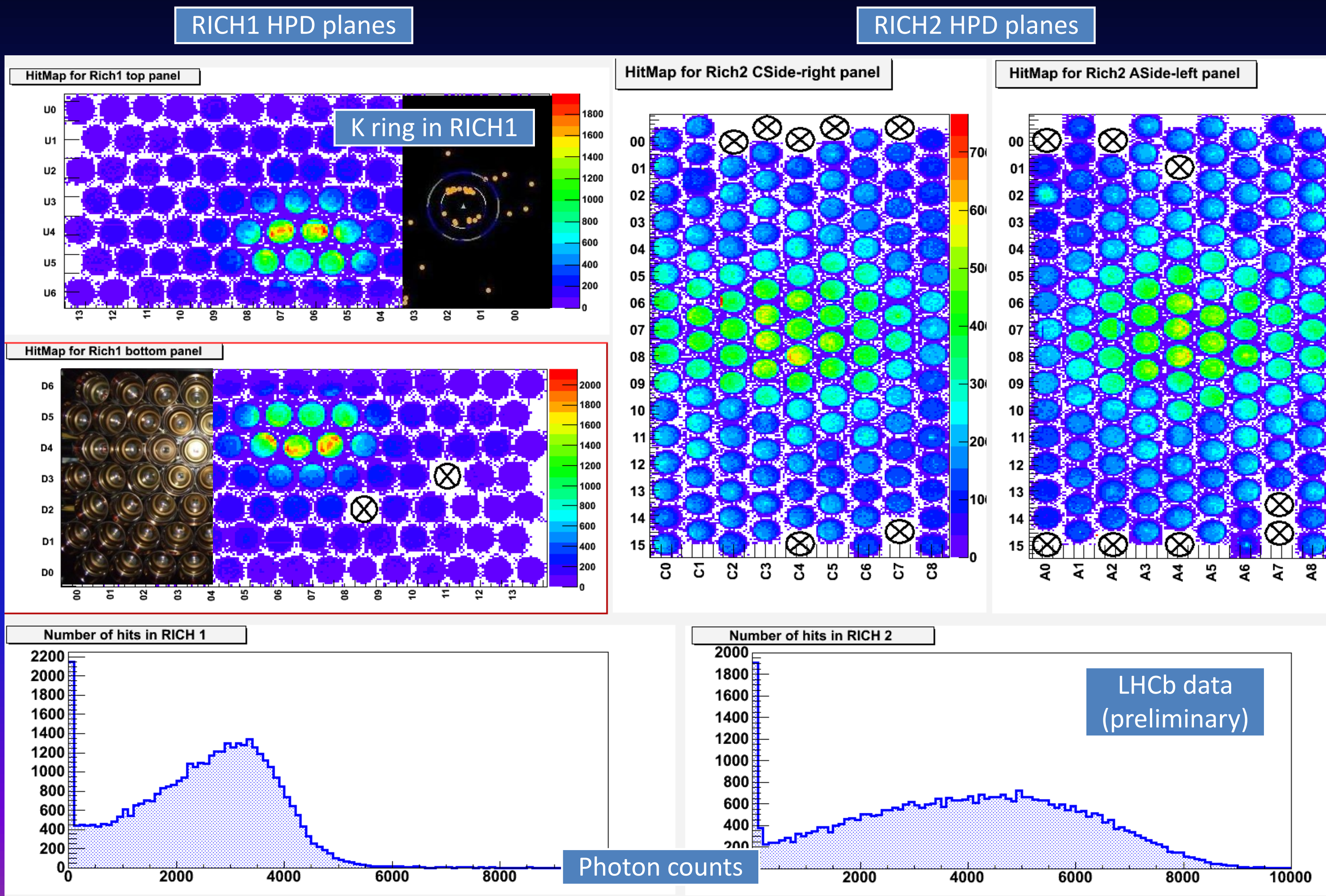

Gaseous photo-detectors

Possible Principles:

A) Ionize photosensitive molecules, admixed to the counter gas (TMAE, TEA);

B) release photoelectron from a solid photocathode (CsI, bialkali...);

Then use free p.e. to trigger a Townsend avalanche → Gain

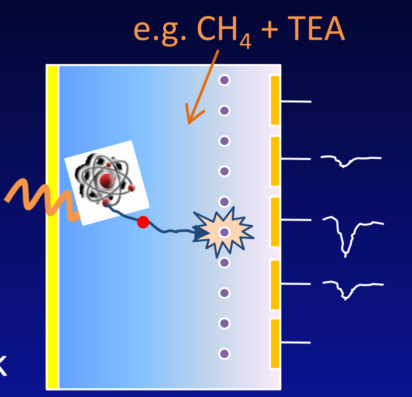

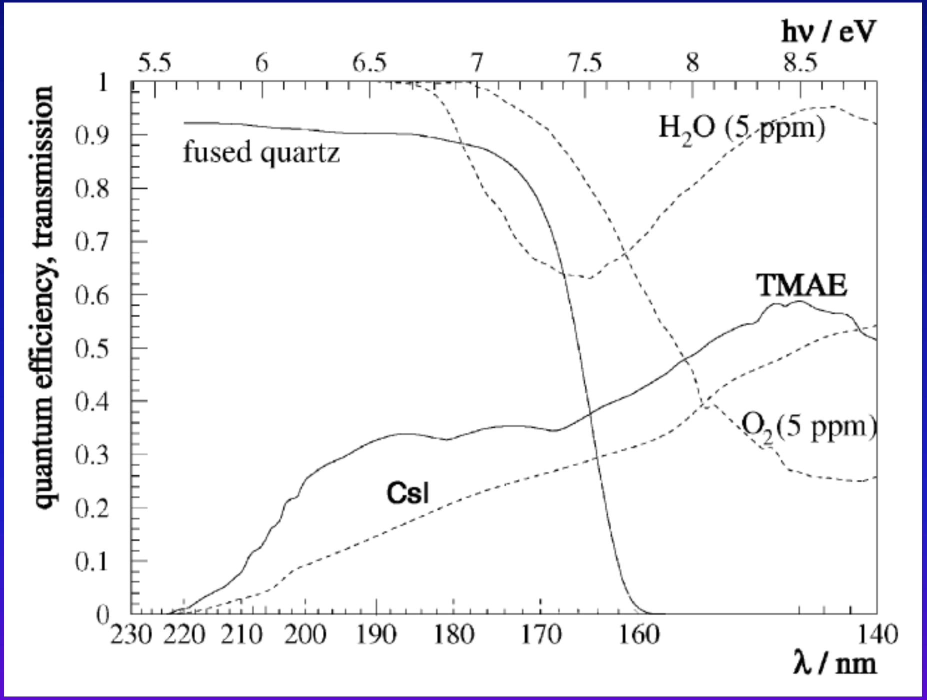

TEA, TMAE, CsI work only in deep UV region.

Bialkali works in visible domain, however requires VERY clean gases. Long term operation in a real detector not yet demonstrated.

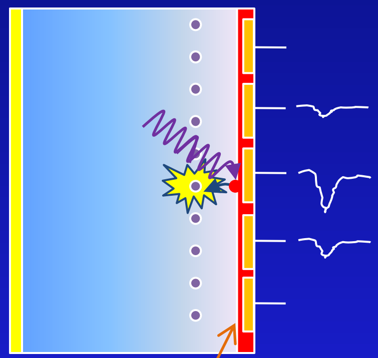

- Usual issues: How to achieve high gain (10^5) ? How to control ion feedback and light emission from avalanche? How to purify gas and keep it clean? How to control aging ?

ous photo-detectors: A few implementations...

Proven technology:

Cherenkov detectors in ALICE, HADES, COMPASS, J-LAB…. Many m[2] of CsI photo-cathodes

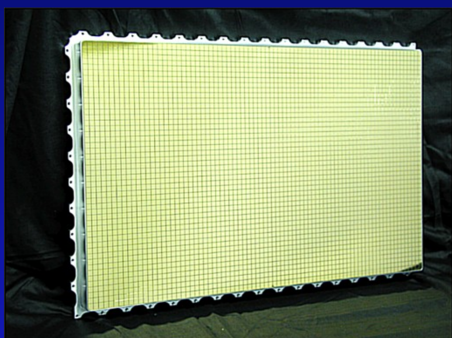

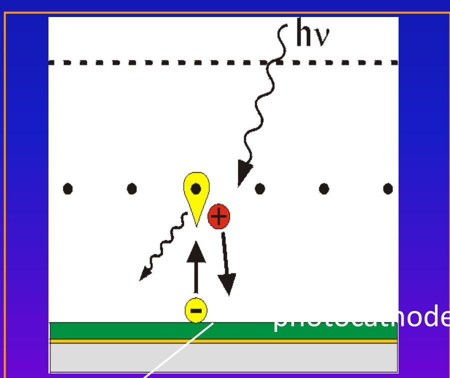

CsI on readout pads

Since recently in use:

HBD (RICH) of PHENIX.

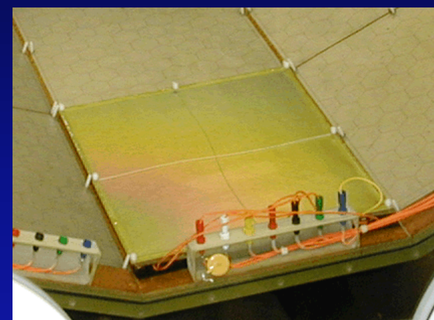

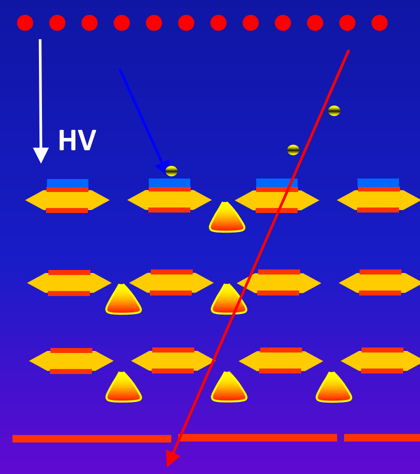

CsI on multi-GEM structure

R&D:

- Thick GEM structures
- Visible PC (bialkali)
- Sealed gaseous devices

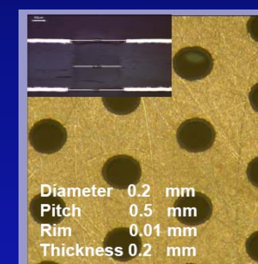

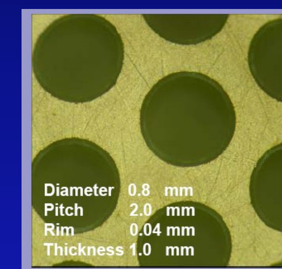

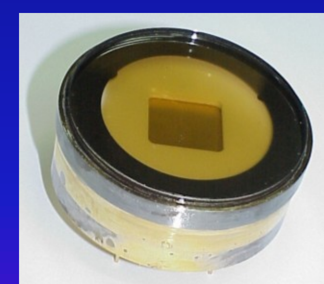

Sealed gaseous photo-detector with bialkali PC. (Weizmann Inst., Israel)

The High Momentum Particle ID (HMPID) Detector of ALICE

Radiator

15 mm liquid C_6F_{14},
n ~ 1.2989 @ 175nm, $\beta_{th} = 0.77$

Photon converter

Reflective layer of CsI
QE ~ 25% @ 175 nm.

Photoelectron detector

- MWPC with CH_4 at atmospheric pressure (4 mm gap) HV = 2050 V.

- Analogue pad readout

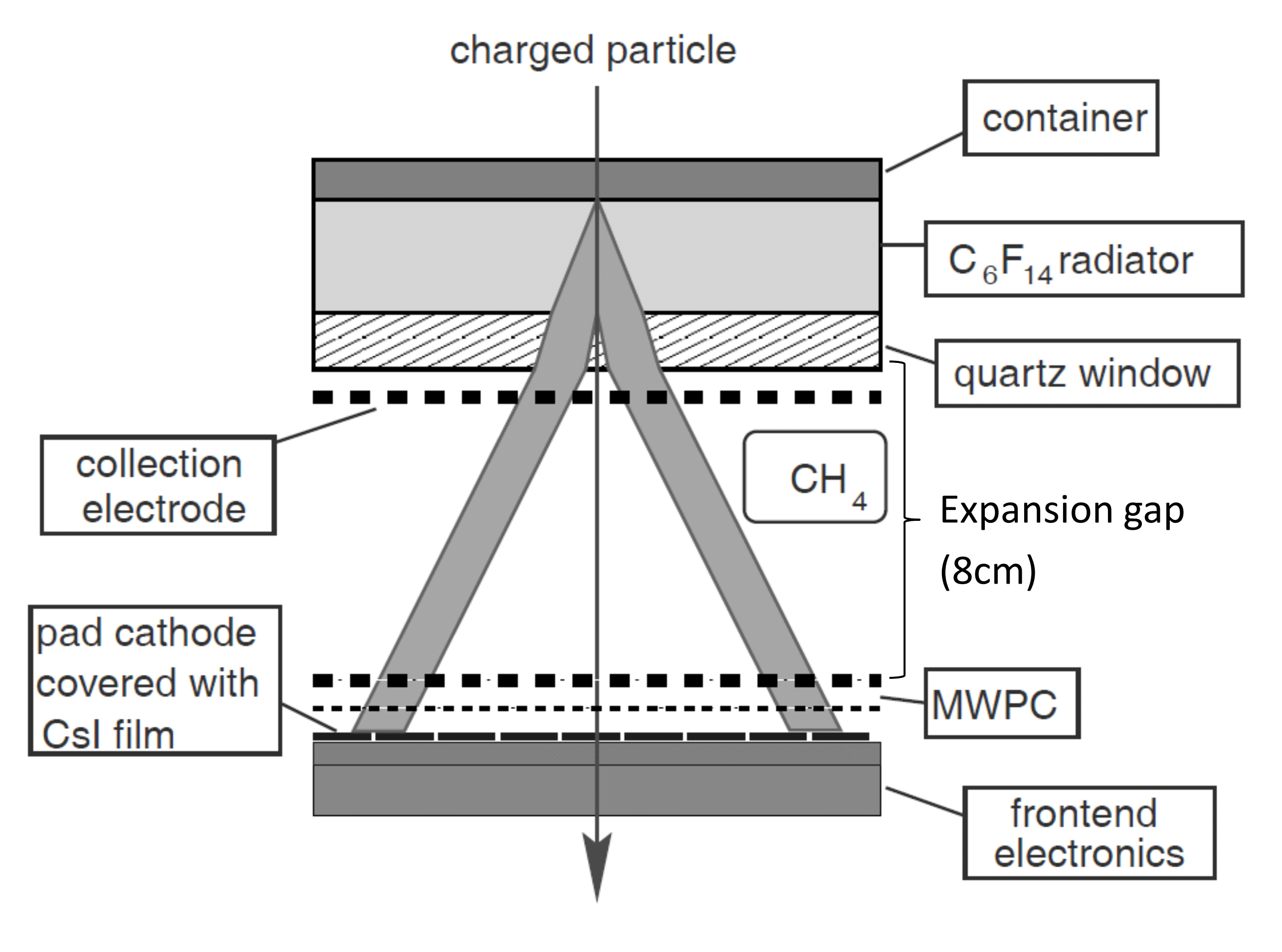

The ALICE Collaboration *et al* 2008 *JINST* **3** S08002

7 modules, each ~1.5x1.5 m^2

3 radiators/module, 8l each

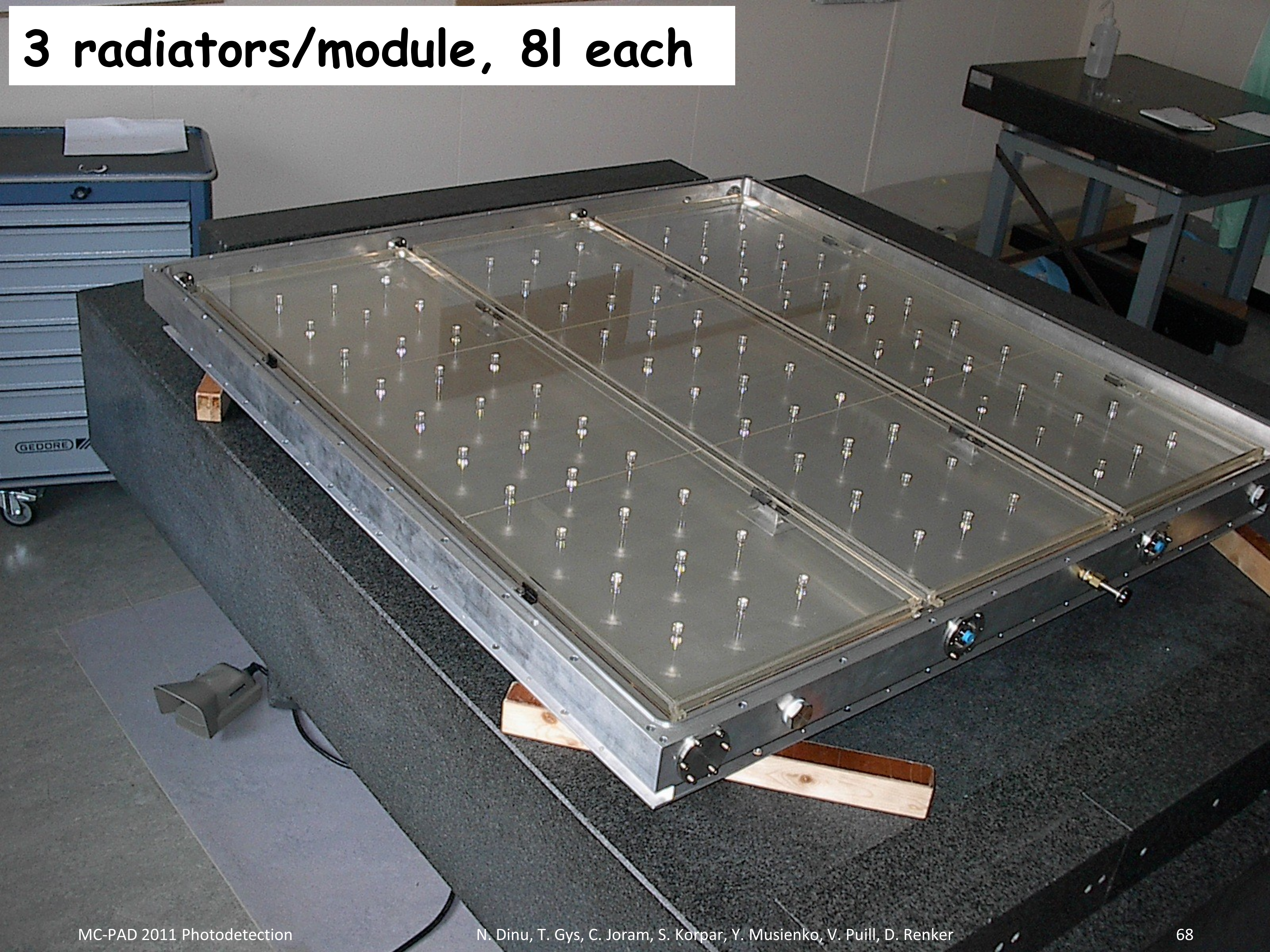

6 CsI photo-cathodes/module, total area > 10 m^2

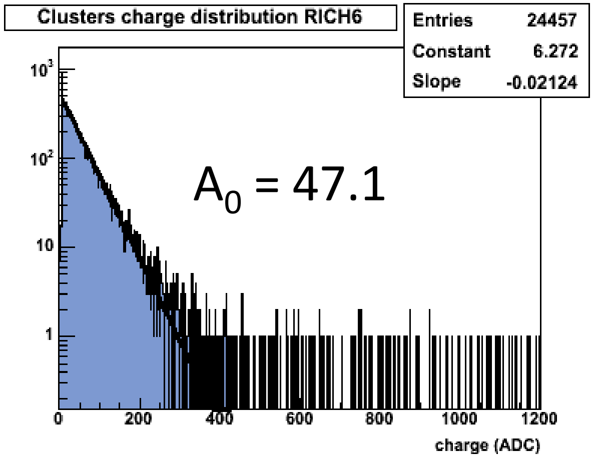

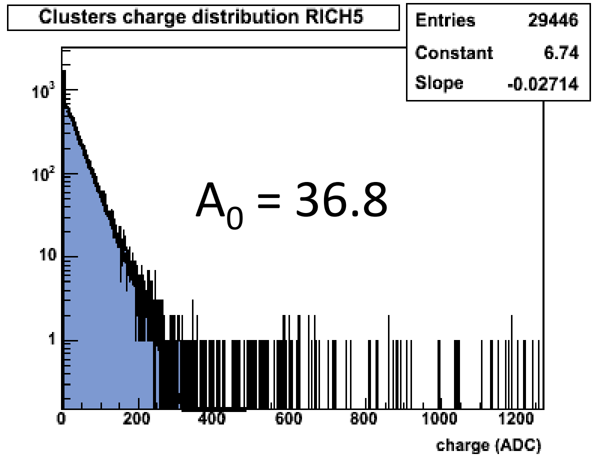

Typical single photo-electron spectra in a MWPC

$$f(z) \propto z^{m-1} e^{-mz}$$

$$z = A/A_0 \quad A = \text{charge}$$

$$m = \text{Polyaparameter}$$

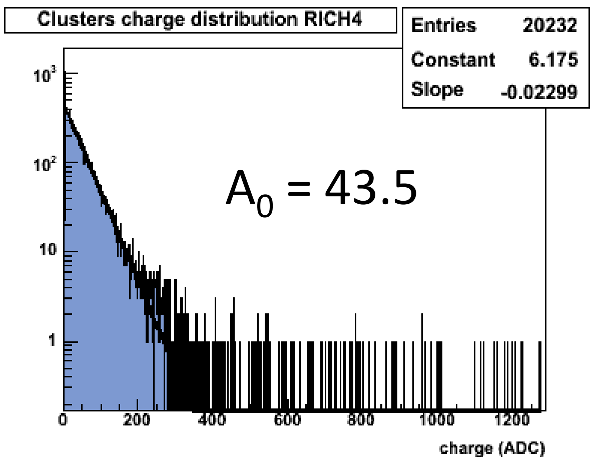

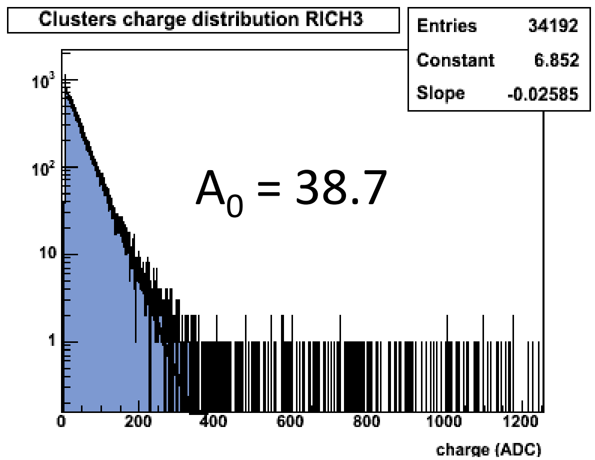

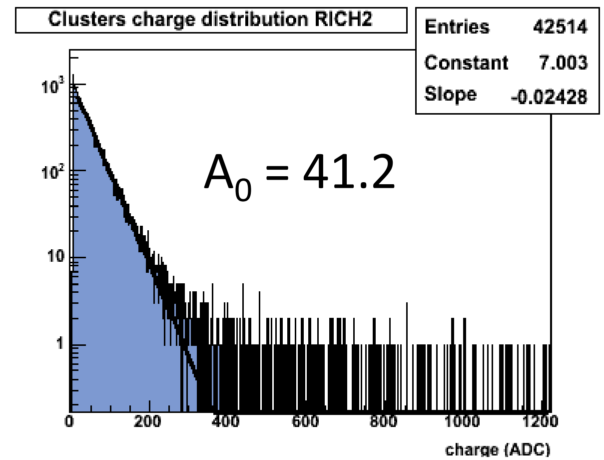

Here: fit with $m = 1$

→ exponential distribution

$$P(A) = \frac{1}{A_0} e^{-\frac{A}{A_0}}$$

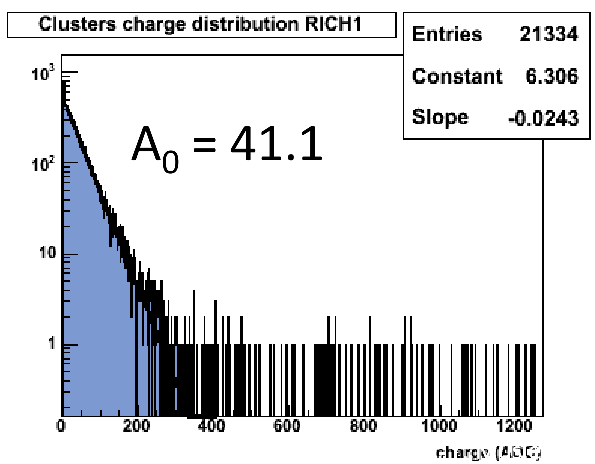

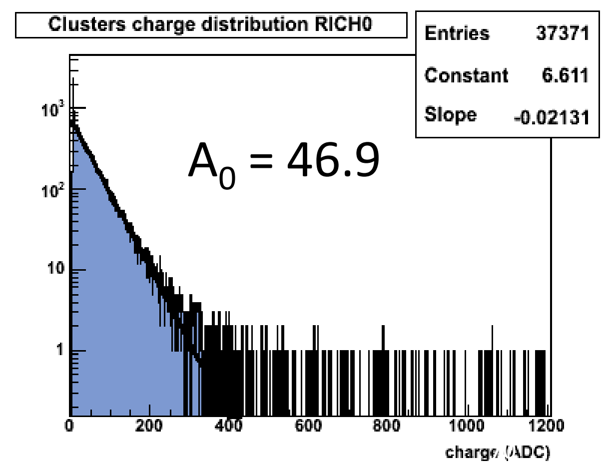

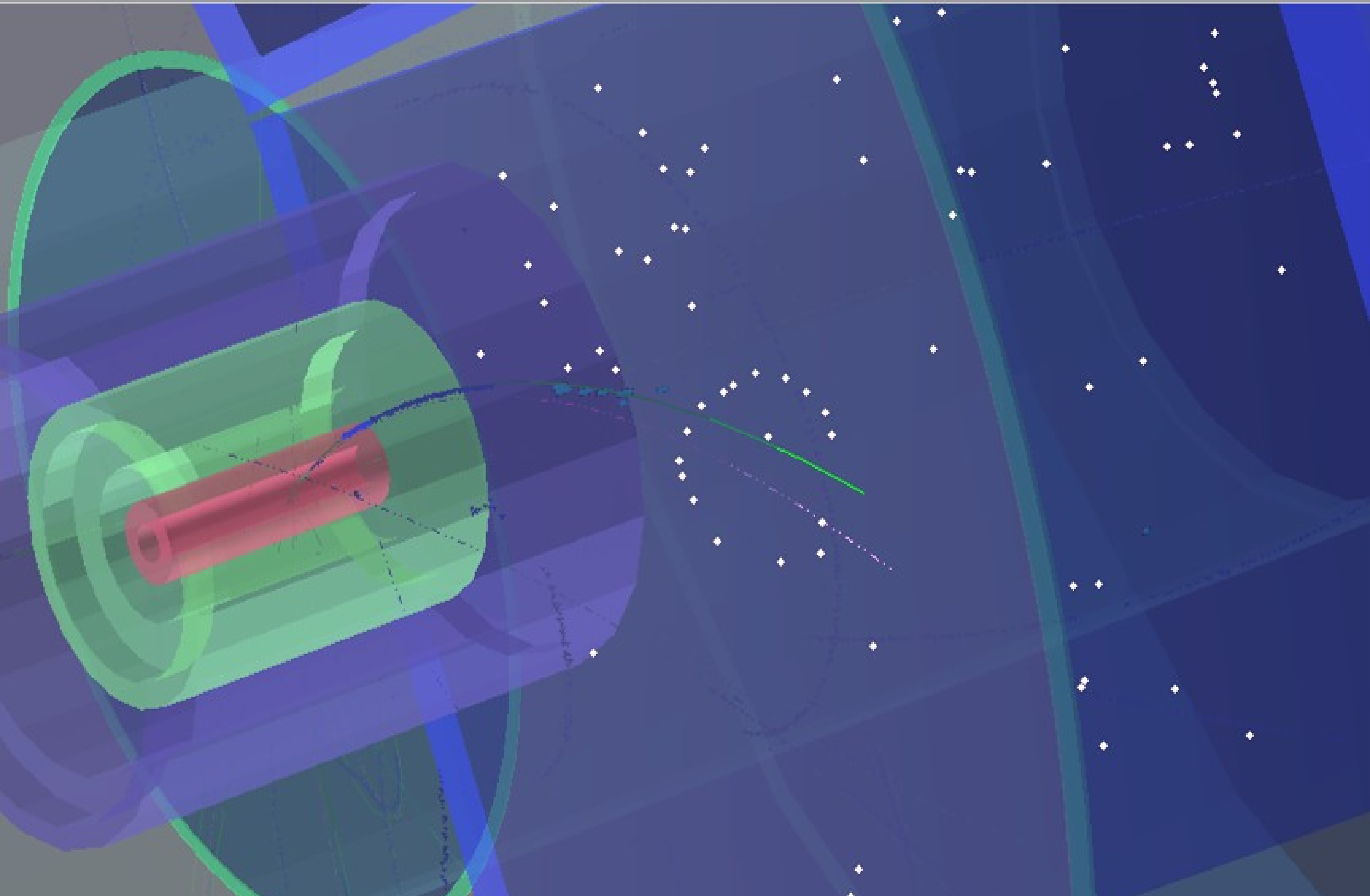

December 2009, typical event

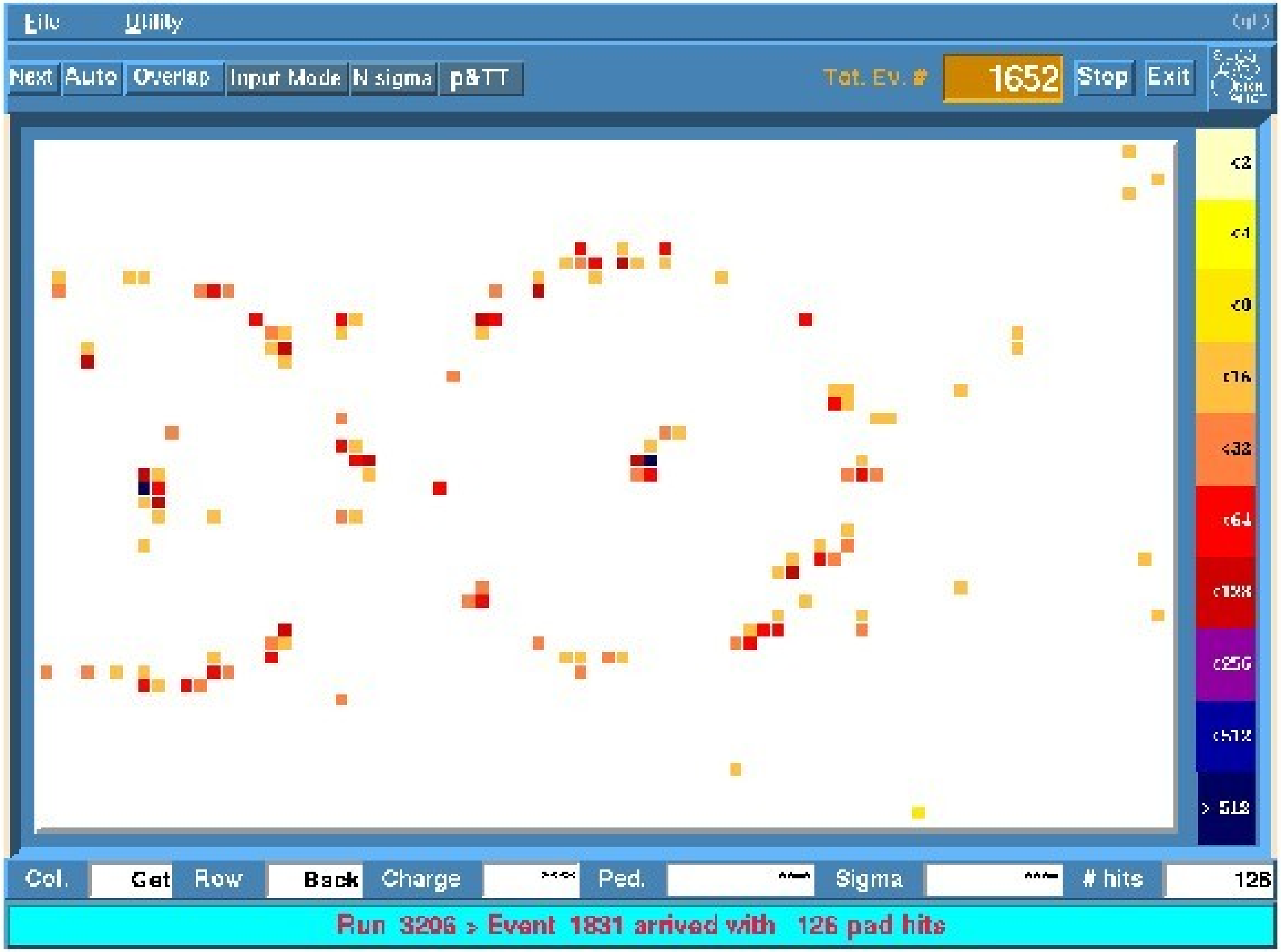
File
Utility
Next
Auto
Overlap
Input Mode
N sigma
p&TT
Tot. Ev. #
1652
Stop
Exit
Col.
Get
Row
Back
Charge
Ped.
Sigma
hits
126
Run 3206 > Event 1831 arrived with 126 pad hits

Internal photoelectric effect in Si

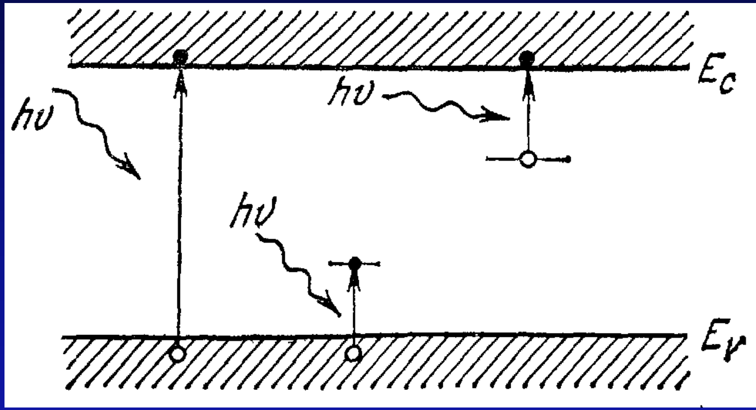

Band gap (T=300K) = 1.12 eV (~1100 nm)

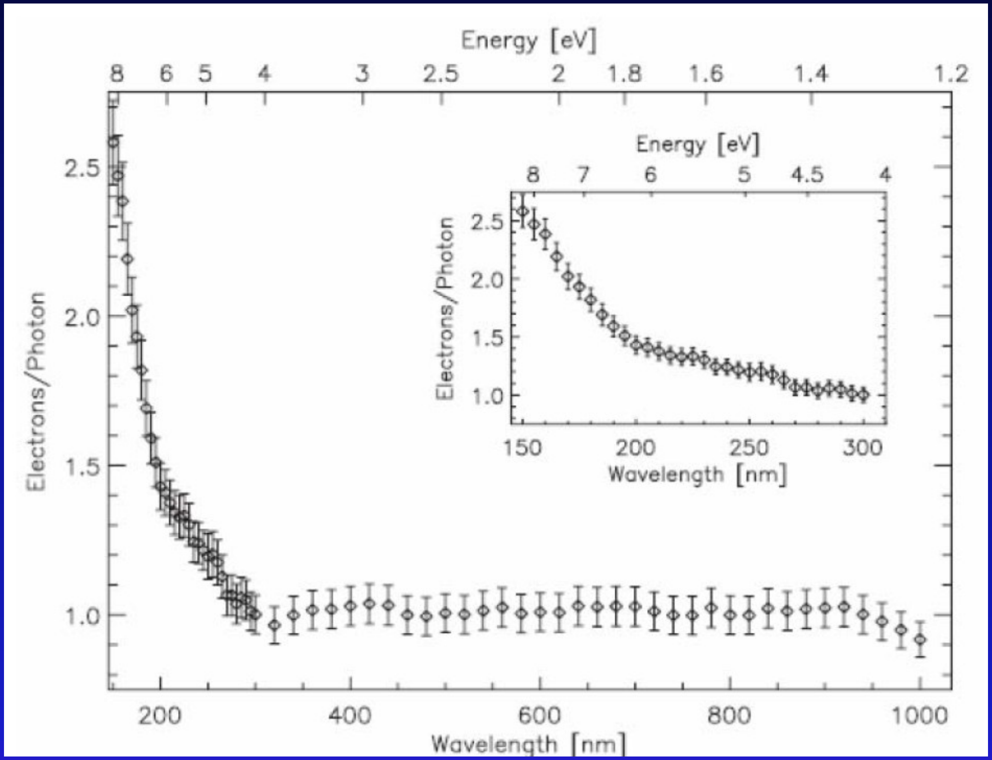

More than 1 photoelectron can be created by light in silicon

PIN photodiode

One of the simplest kind of photodiodes is the p-i-n photodiode in which an intrinsic piece of semiconductor is sandwiched between two heavily (oppositely) doped regions.

The two charge sheets (on the n+ and p+) sides produce a field which, even without an external field supplied, will tend to separate charges produced in the depleted region.

The separated charges will be swept to either terminal and can be detected as a current provided that they did not recombine.

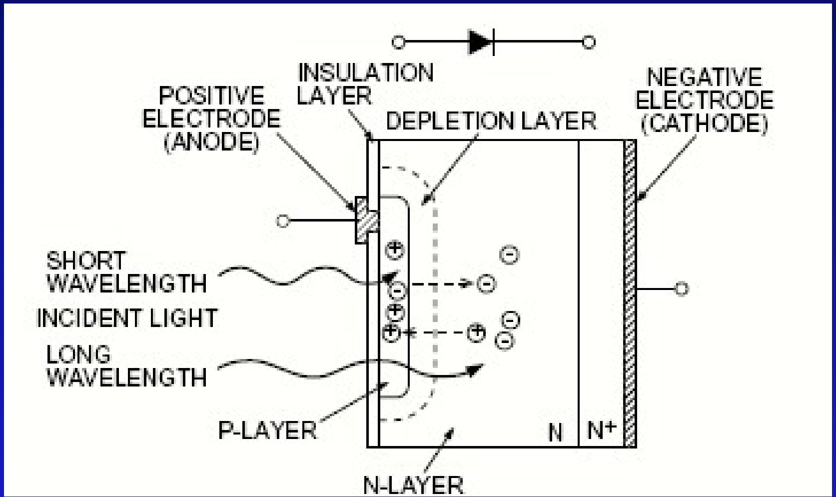

Semiconductor devices: PIN photodiodes

The PIN diode is a very successful device.
It is used in many big calorimeters in high energy physics (Cleo, L3, Crystal Barrel, Barbar, Belle ....)

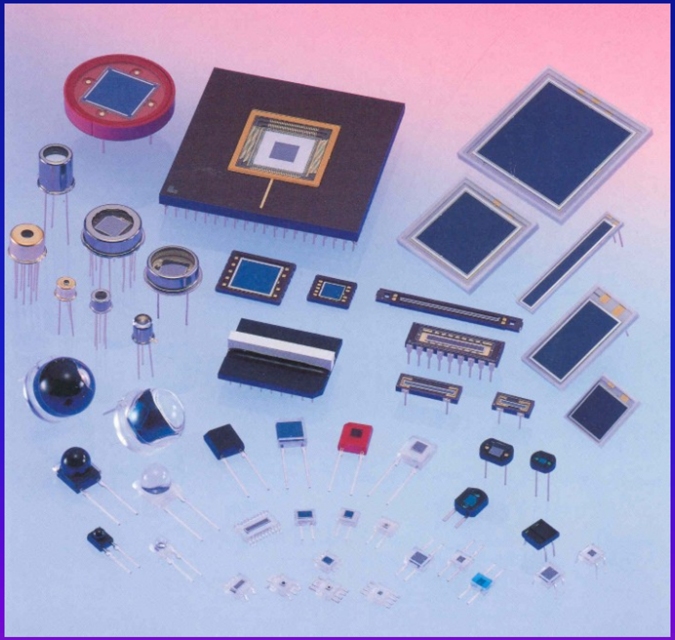

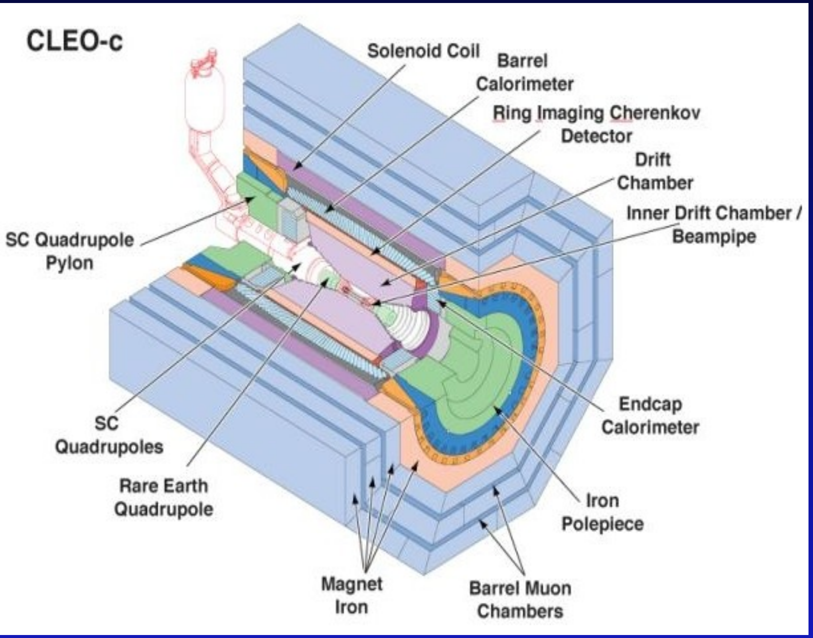

The PIN diode is the simplest, most reliable and cheapest photo sensor.
It has high quantum efficiency (80%), very small volume and is insensitive to magnetic fields

PIN photodiodes – nuclear counter effect

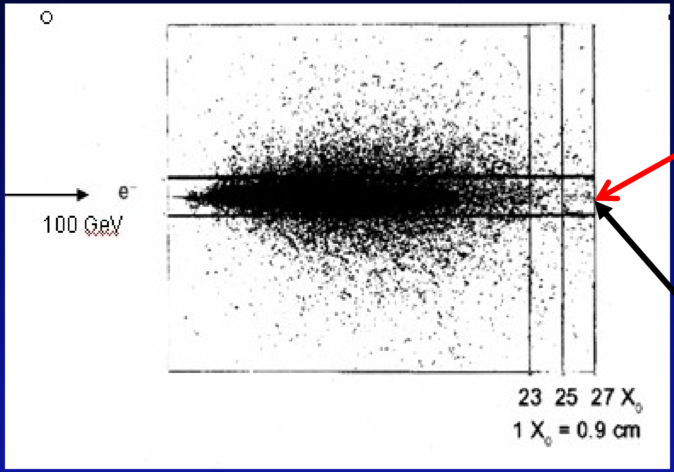

Geant simulation: each dot stands for an energy deposition of more than 10 keV

A MIP in a PIN diode creates ~30,000 e-h pairs (the diode thickness of 300 μ x 100 pairs/μ). A photon with an energy of 7 GeV produces in PbWO4 + PIN diode the same number of e-h pairs.

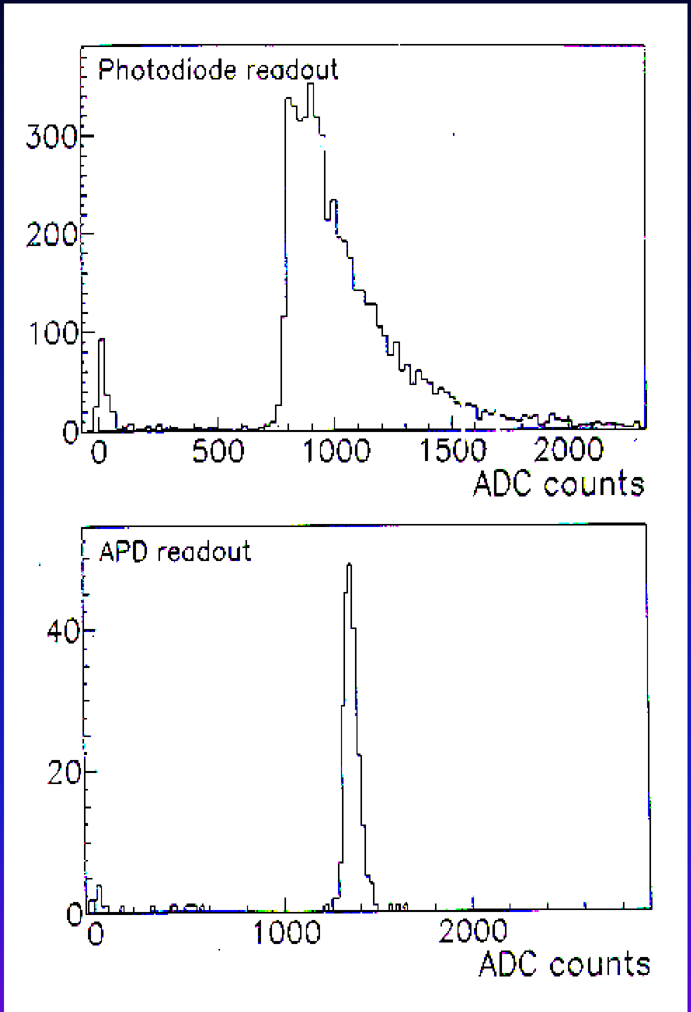

80 GeV e^- beam in a 18 cm long $PbWO_4$ crystal

Basic APD Structure (CMS version)

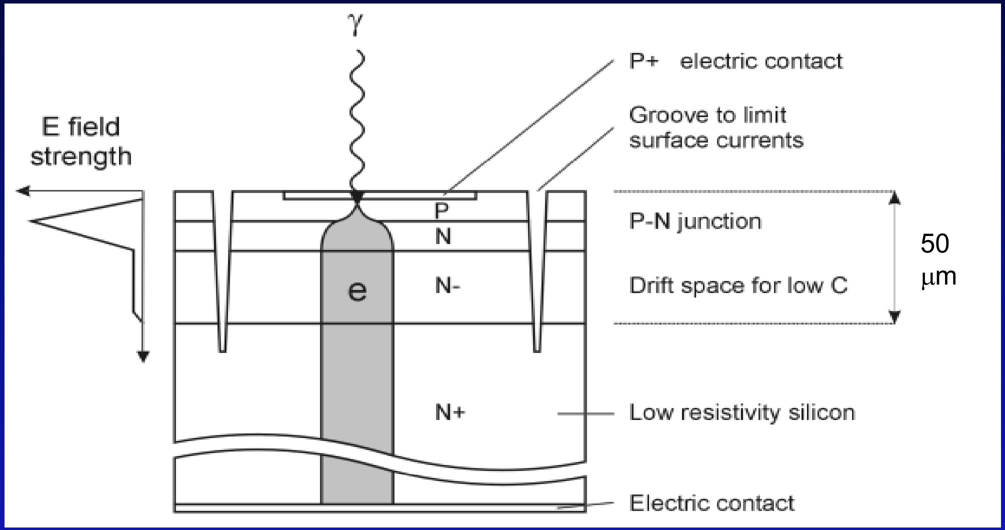

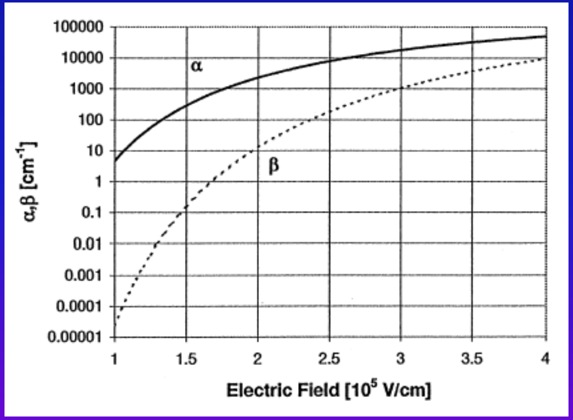

Photons create electron-hole pairs in the thin p-layer on top of the device and the electrons induce avalanche amplification in the high field at the p-n junction.
Holes created behind the junction contribute little because of their much smaller ionization coefficient.

Electrons produced by ionizing particles traversing the bulk are not amplified. The effective thickness for the collection and amplification of electrons which have been created by a MIP is therefore about 6 μm ~(5 x 50 + 45 x 1)/50.

The NCE is 50 times smaller than in a PIN diode.

Ionization coefficients α for electrons and β for holes

APDs in the CMS ECAL

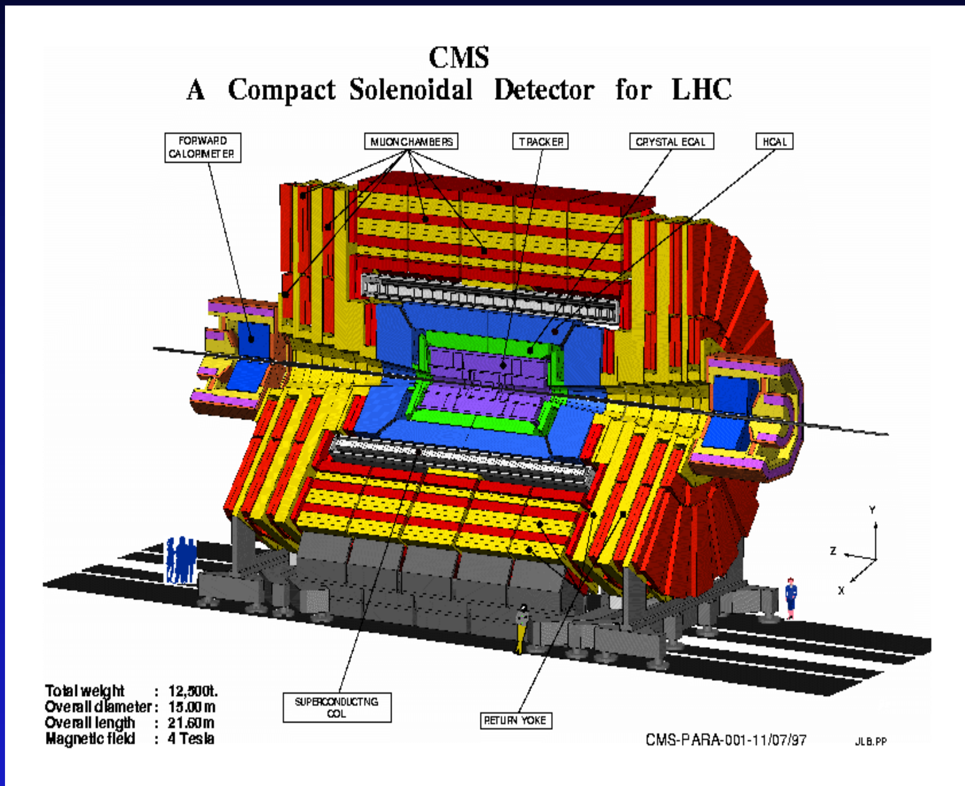

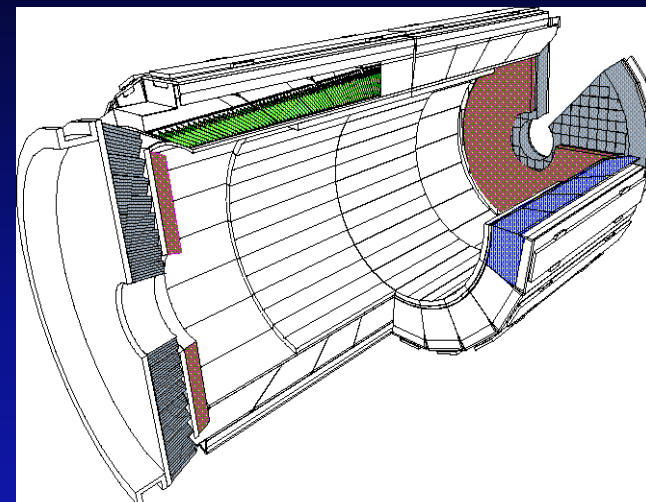

36 supermodules with 1700 crystals each

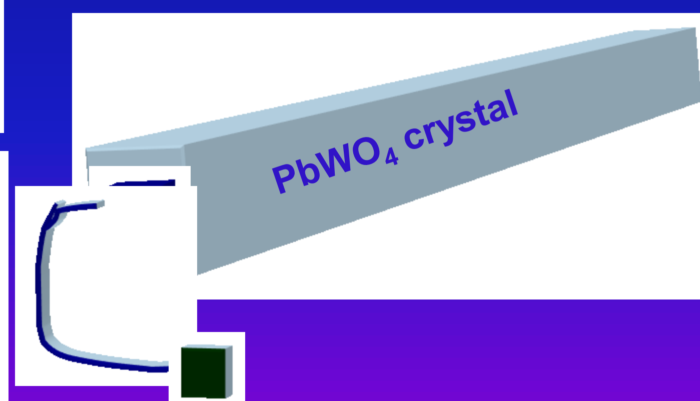

2 APD's/crystal

→ 122.400 APD's

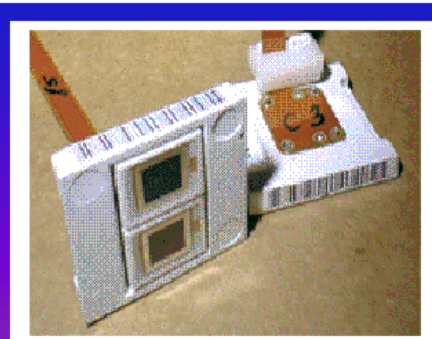

APD Impact on Energy Resolution

$$\frac{\sigma_E}{E} = \frac{a}{\sqrt{E}} \oplus b \oplus \frac{c}{E}$$

ECAL energy resolution:

CMS design goal : *a* ~ 3%, *b* ~ 0.5%, *c* ~ 200 MeV

APD contributions to:

a: photo statistics (area, QE) and avalanche fluctuations (excess noise factor)

b: stability (gain sensitivity to voltage and temperature variation, aging and radiation damage)

c: noise (capacitance, serial resistance and dark current)

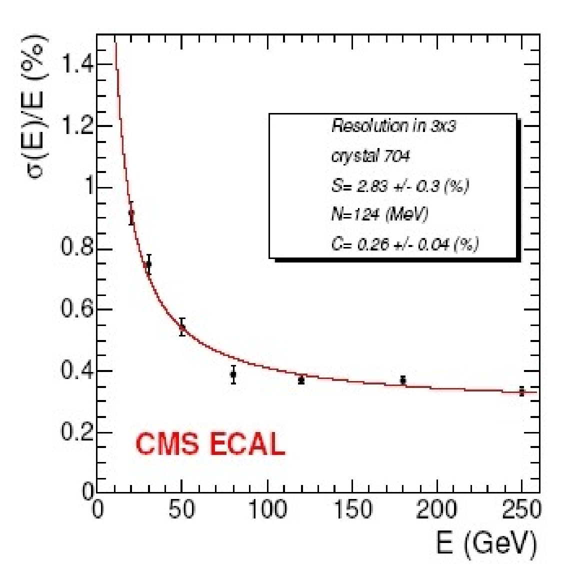

Gain and Dark Current

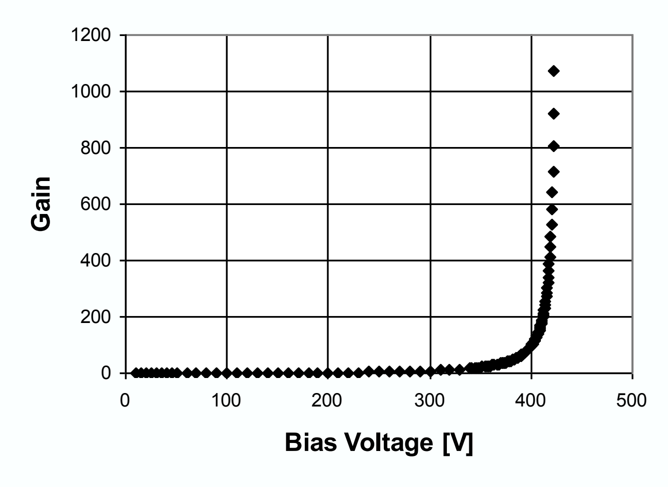

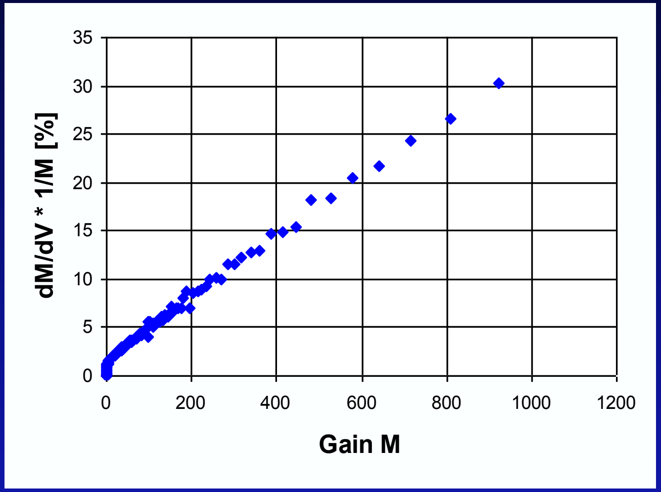

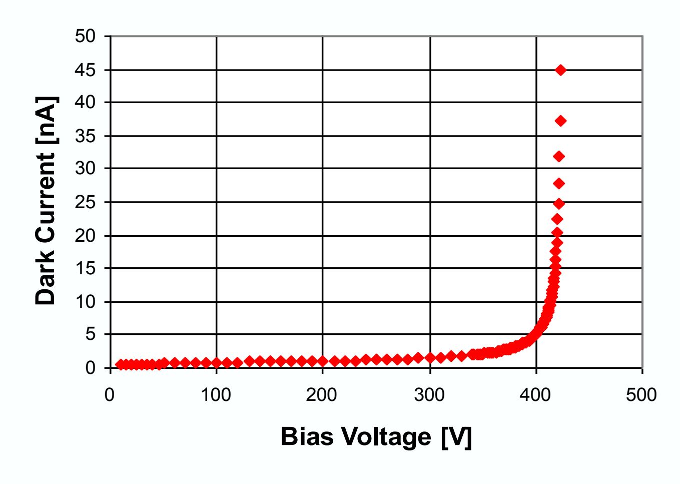

$dM/dV*1/M = const * M$

$\Rightarrow \quad M \sim 1/(V_{breakdown} - V)$

Near the breakdown voltage, where we get noticeable amplification, the gain is a steep function of the bias voltage.

Consequently we need a voltage supply with a stability of few tens of mV.

The gain of an APD is limited

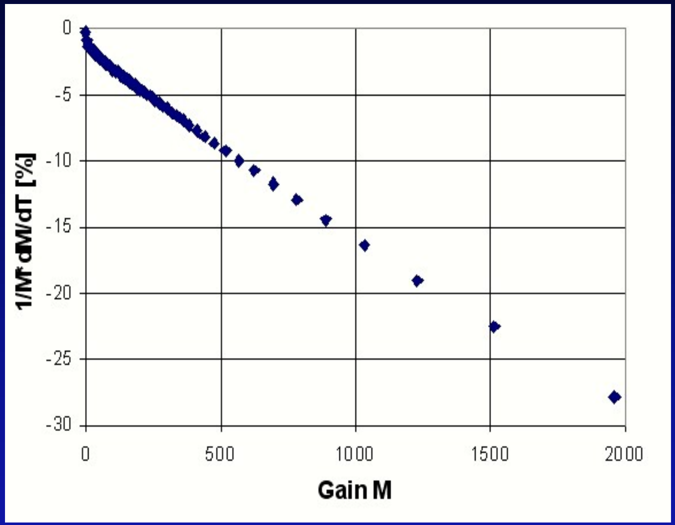

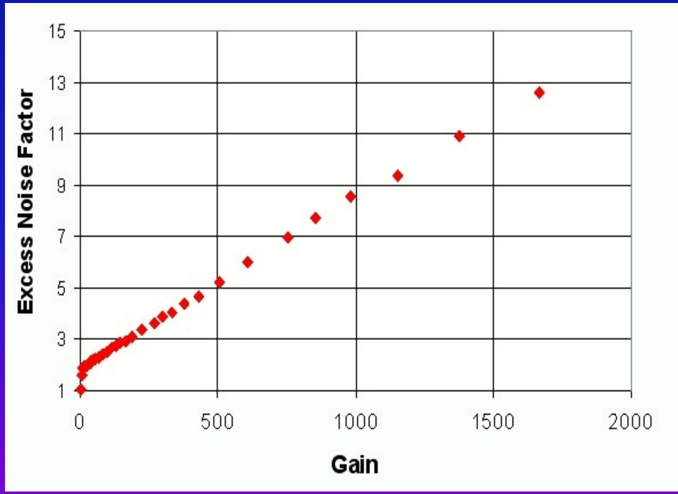

The breakdown voltage depends on the temperature due to energy loss of the electrons in interactions with phonons.
Consequently the gain depends on the temperature and the dependence increases with the gain.

At gain 50 the temperature coefficient is - 2.3% per degree C.

Good energy resolution can only be achieved when the temperature is kept stable (in CMS the temperature is regulated with a 0.1 degree C precision).

At high gain the fluctuations of the gain become large and the excess noise factor ENF increases:

$$\frac{\sigma}{E} = \sqrt{\frac{ENF}{n_{pe}E}}$$

$$ENF = \frac{M^2 + \sigma_M^2}{M^2}$$

$ENF = k_{eff} \cdot M + (2-1/M) \cdot (1-k_{eff})$

for $M > 10$: $ENF \sim 2 + k_{eff} \cdot M$

$k_{eff} \approx k = \beta/\alpha$

α and β are the ionization coefficients for electrons and holes ($\alpha >> \beta$)

Quantum efficiency (QE)

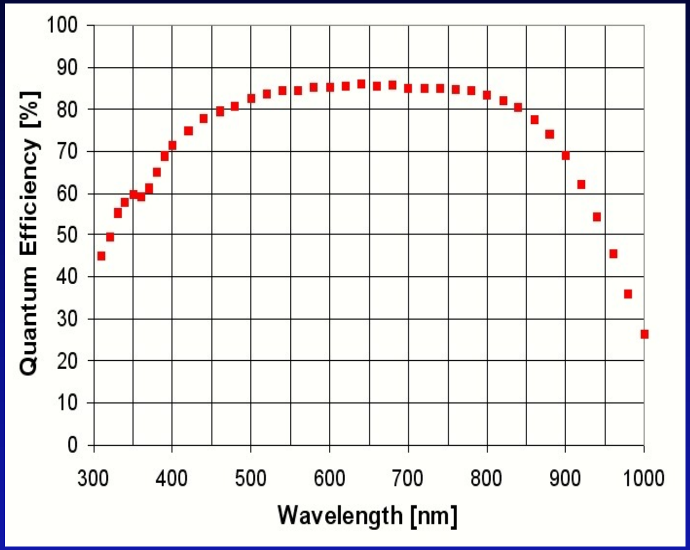

In the APDs selected for CMS (Hamamatsu S8148) the p-n junction is at a depth of about 5 micron. Behind the junction is a 45 micron thick layer of n-doped silicon.

Blue light is absorbed close to the surface. The electrons from the generated e-h pairs drift to the high field of the junction and are amplified

Light with long wavelength penetrates deep into the region behind the p-n junction. Only the generated holes will drift to the junction. They will be much less amplified due to the smaller ionization coefficient.

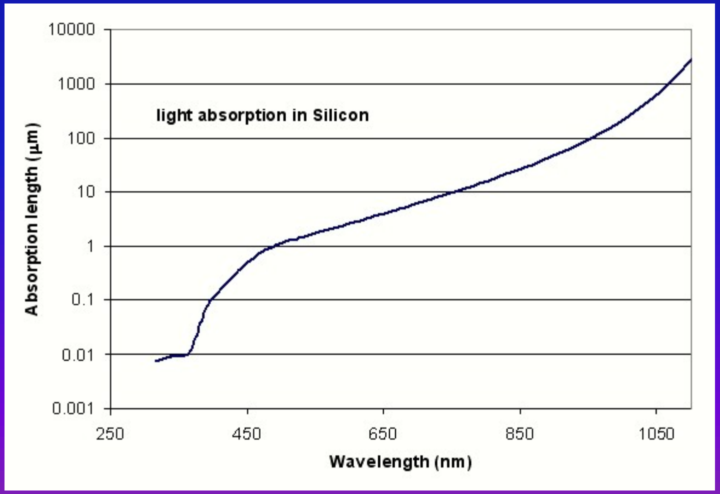

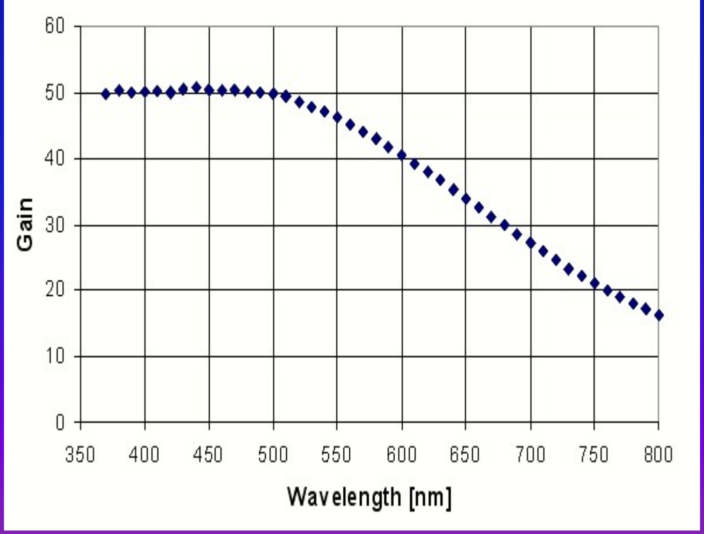

Radiation hardness

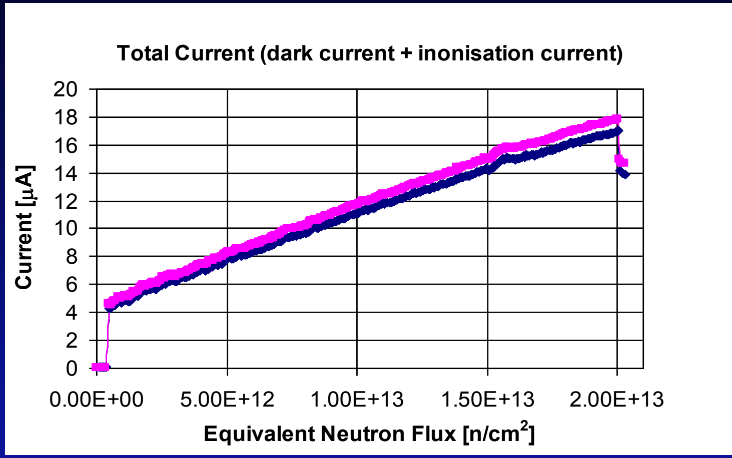

Two APD's have been irradiated at PSI in a 70 MeV proton beam for 105 minutes

$9x10^{12}$ protons/cm^2 corresponds to $2x10^{13}$ neutrons/cm^2 with an energy of 1MeV (10 years fluence expected in CMS barrel)

The mean bulk current after $2x10^{13}$ neutrons/cm^2 is $I_d \approx 280$ nA (non-amplified value).
This corresponds to 14 µA at gain 50 and ~ 80 MeV noise contribution (no recovery considered).

- Neutrons: Displacement of Si atoms => defects in the bulk which generate currents. Slow and never complete recovery at room temperature.
- Ionizing radiation (γ): breakup of the SiO_2 molecules and very little effect in the bulk (10^{-4}) => the surface currents increase. Fast and almost complete recovery for good APD's. There can be a strong reduction of the breakdown voltage if there is a weakness on the surface due to an imperfection in the production process (dust particles, mask misalignment ...).

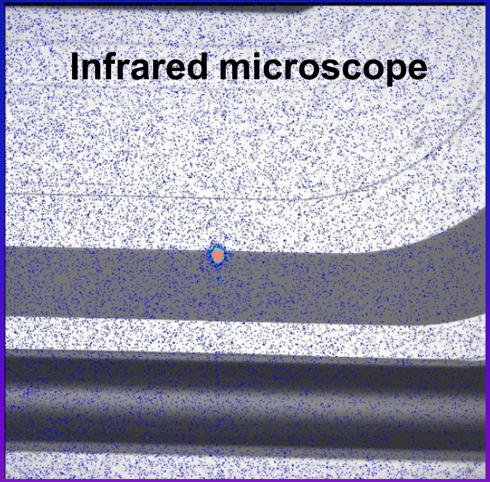

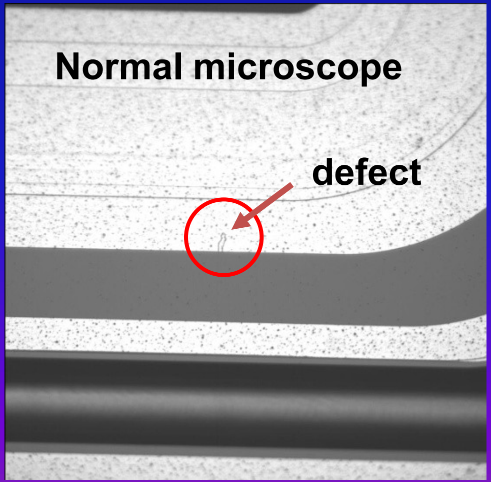

From Photodiode to GM-APD

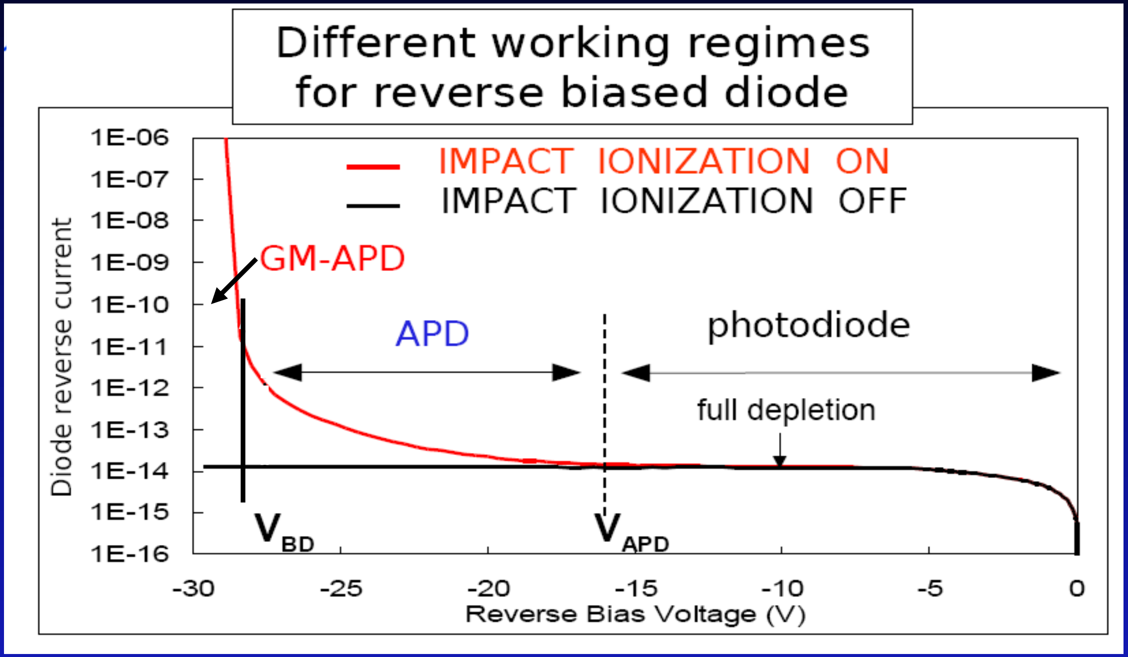

GM-APD

- $V_{bias} > V_{BD}$ (V_{bias}-V_{BD} ~ few volts)
- G ⇨ ∞
- Geiger-mode operation
- Can operate at single photon level

APD

- $V_{APD} < V_{bias} < V_{BD}$
- G = M (50 - 500)
- Linear-mode operation

Photodiode

- $0 < V_{bias} < V_{APD}$ (few volts)
- G = 1
- Operate at high light level (few hundreds of photons)

Geiger Mode – Avalanche Photodiode (GM-APD)

The first single photon detectors operated in Geiger-mode

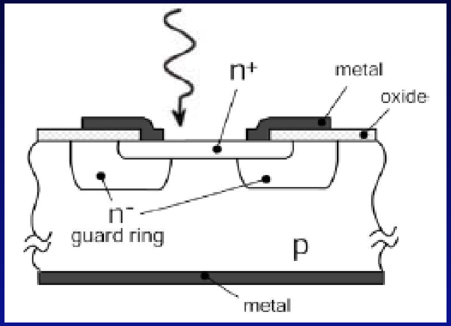

R.H. Haitz
J. Appl. Phys.,
Vol. 36, No. 10 (1965) 3123

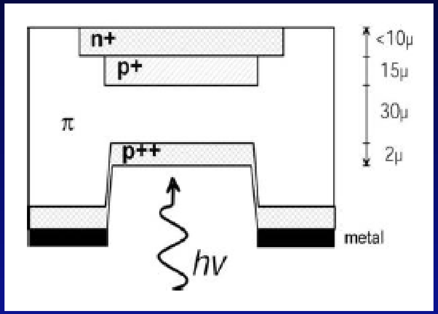

J.R. McIntire
IEEE Trans. Elec. Dev.
ED-13 (1966) 164

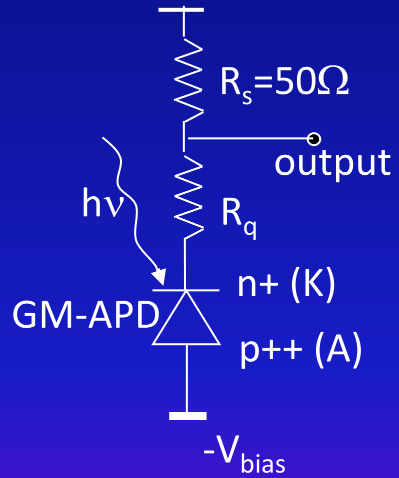

Passive quenching circuit

S. Cova & al.
Appl. Opt., Vol. 35, No 12 (1996) 1956

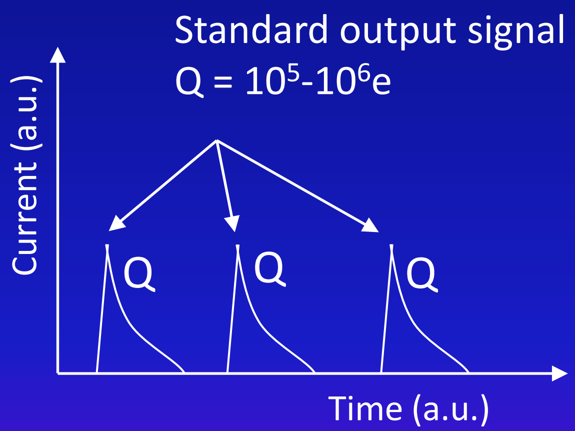

Binary device

- If one or more simultaneous photons fire the GM-APD, the output is anytime a standard signal: $Q \sim C(V_{bias} - V_{BD})$
- GM-APD does not give information on the light intensity

What is a Silicon Photomultiplier (SiPM)?

- matrix of n pixels connected in parallel (e.g. few hundreds /mm^2) on a common Si substrate
- each pixels = GM-APD in series with R_{quench}

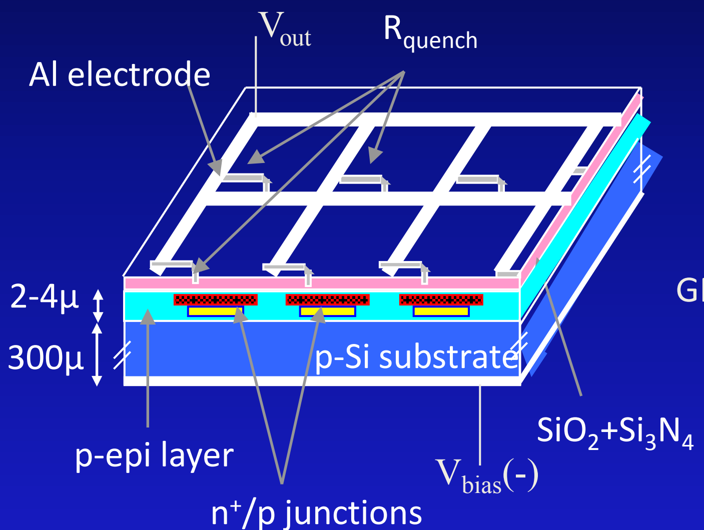

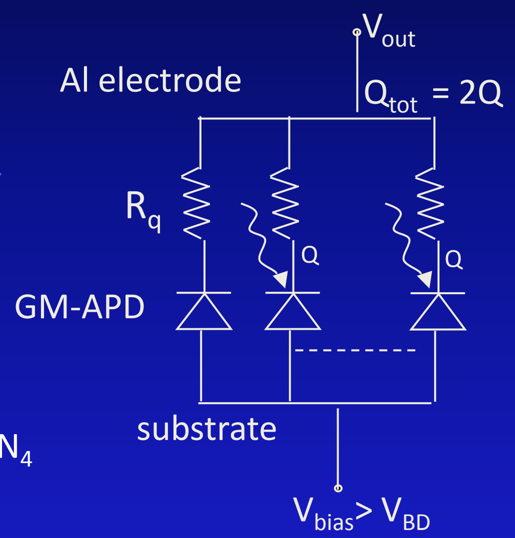

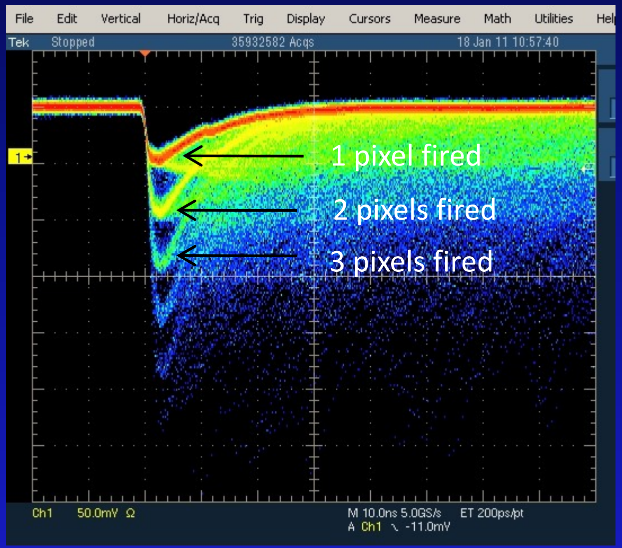

Key personalities in this development:
V. Golovin, Z. Sadygov

Quasi-analog device:

- If simultaneously photons fires different pixels, the output is the sum of the standard signals: $Q \sim \Sigma Q_i$
- SiPM gives information on light intensity

•Different producers give different names: SiPM, MRS-APD, SPM, MPPC…

Silicon Photomultiplier (SiPM)

Advantages

☺ high gain (10^5-10^6) with low voltage (<100V)

☺ low power consumption (<50μW/mm^2)

☺ fast (timing resolution ~ 50 ps RMS for single photons)

☺ insensitive to magnetic field (tested up to 7 T)

☺ high photon detection efficiency (30-40% blue-green)

Possible drawbacks

☹ high dark count rate (DCR) at room temperature

- 100kHz – 1MHz/mm^2
- thermal carriers, cross-talk, after-pulses

☹ temperature dependence

- V_{BD}, G, R_q, DCR

SiPM designs (examples)

Hamamatsu HPK (http://jp.hamamatsu.com/)

25x25µm², 50x50µm², 100x100µm² pixel size

1x1mm²



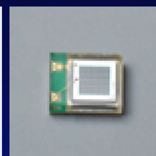

3x3mm²


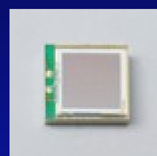

Arrays

1x4mm²
1x4 channels

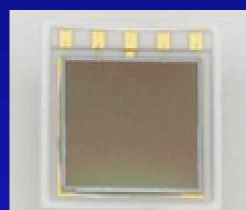

6x6 mm²
2x2 channels

FBK-IRST

50x50µm² pixel size

1x1mm²

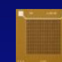

2x2mm²

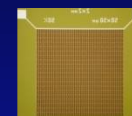

3x3mm²

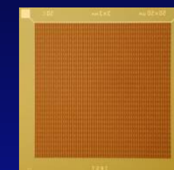

4x4mm²

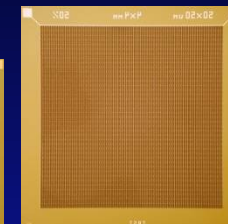

4x4mm²
2x2 channels

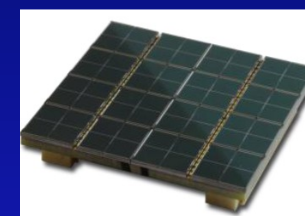

3x3 cm²
8x8 channels

SensL (http://sensl.com/)

20x20µm², 35x35µm², 50x50µm², 100x100µm² pixel size

3.16x3.16mm²
4x4 channels

3.16x3.16mm²
4x4 channels

6 x 6 cm²
16x16 channels

Gain

- Defined as the charge developed in one pixel by a primary charge carrier:

$$Gain = \frac{Q_{pixel}}{e} = \frac{C_{pixel} \times (V_{BIAS} - V_{BD})}{e} = \frac{C_{pixel} \times \Delta V}{e}$$

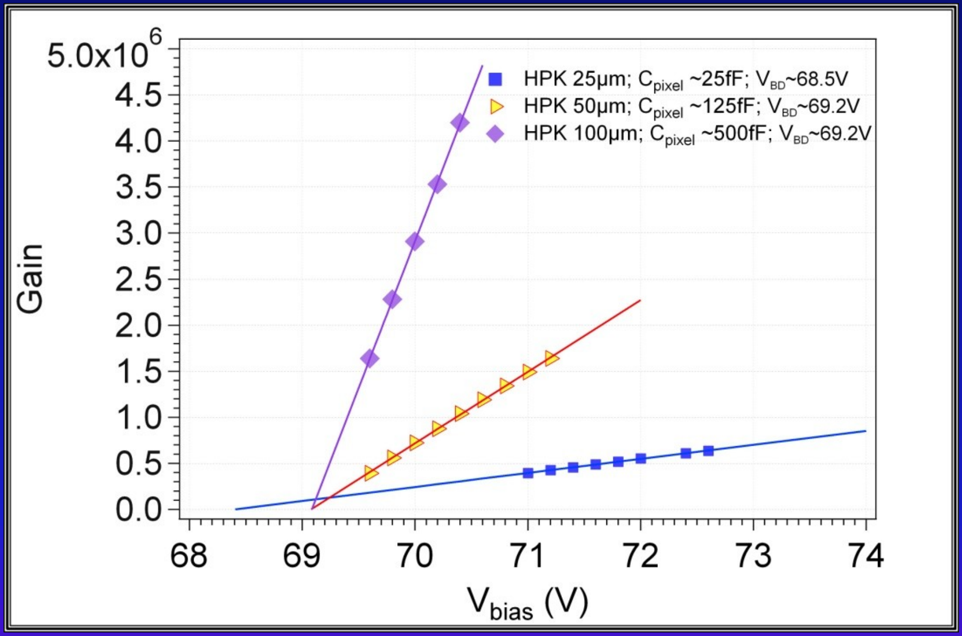

N. Dinu & al, NIM A 610 (2009) 423–426

- G increases linearly with the V_{bias}
  - G: $5x10^5 – 5x10^6 \Rightarrow$ simple or no amplifier required

- The slope of the linear fit of G v.s. V_{bias} $\Rightarrow$ pixel capacitance
  - C_{pixel} : tens to hundreds of fF

- The G and C_{pixel} increase with the pixel geometrical dimensions
  - $C_{pixel} \sim \varepsilon_0 \varepsilon_r S/d$
    - S - pixel junction surface
    - d - pixel depletion thickness

Photon detection efficiency (1)

$$PDE = N_{pulses} / N_{photons} = QE \cdot P_{01} \cdot \varepsilon_{geom}$$

QE = Quantum Efficiency

• probability for a photon to generate a carrier in the high field region

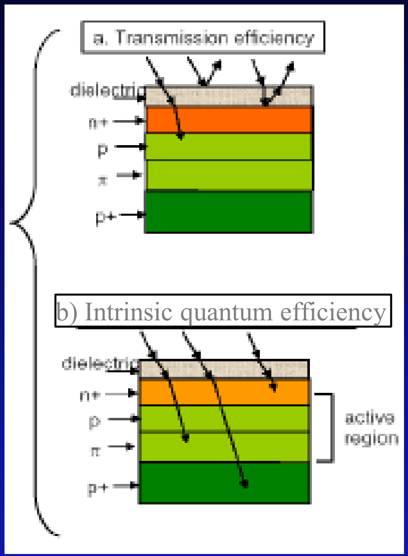

P_{01} = Triggering probability

• probability for a carrier traversing the high field to generate an avalanche

ε_{geom} = Geometrical fill factor

• fraction of dead area due to structures between the pixels e.g. guard rings, trenches, R_{quench}

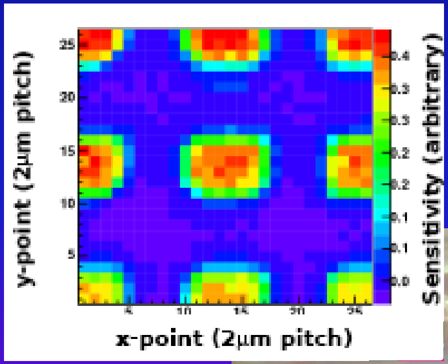

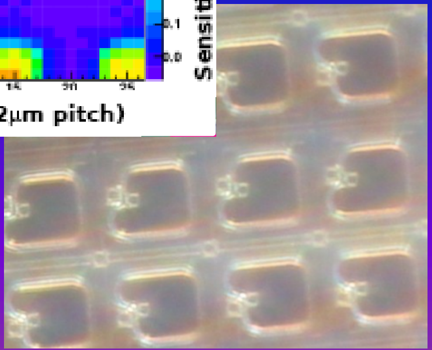

Photon detection efficiency (2)

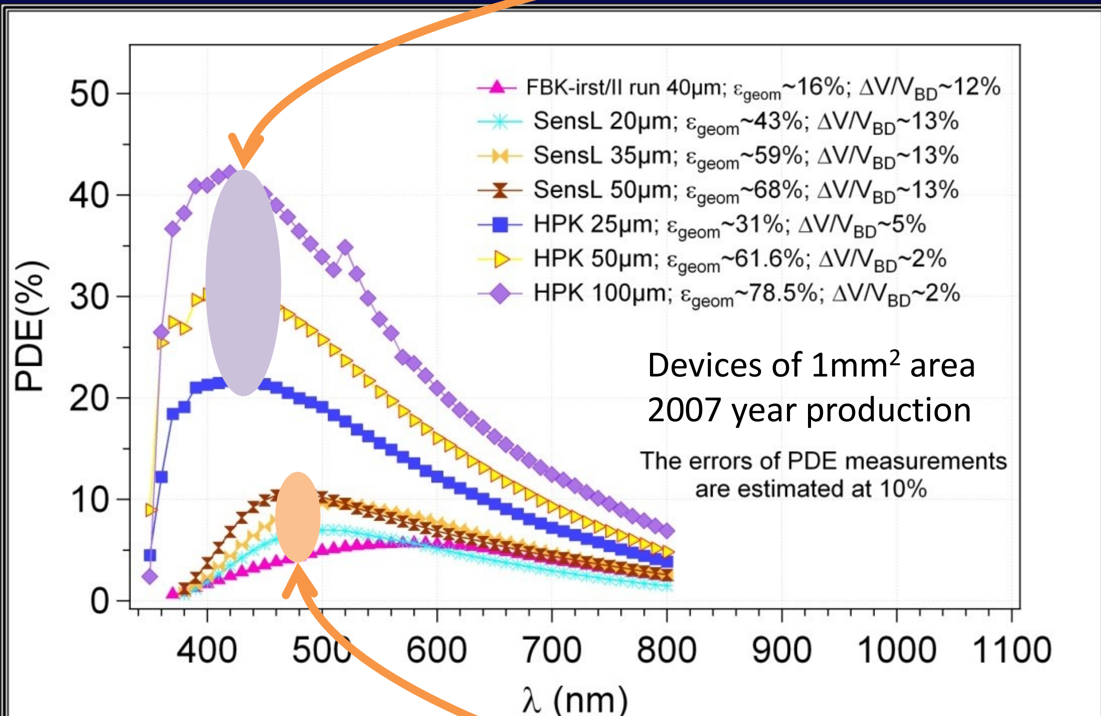

N. Dinu & al, NIM A 610 (2009) 423–426

- **PDE of HPK devices**
  - p+/n pixels on n-type substrate
  - PDE_{max} ~ 20-40% optimized for blue light (420nm)

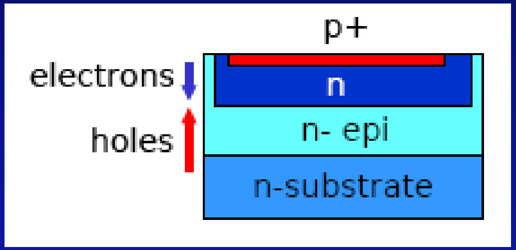

- **PDE of FBK, SensL**
  - n+/p pixels on p-type substrate
  - PDE_{max} ~ 6-10% for green light (500-600nm)

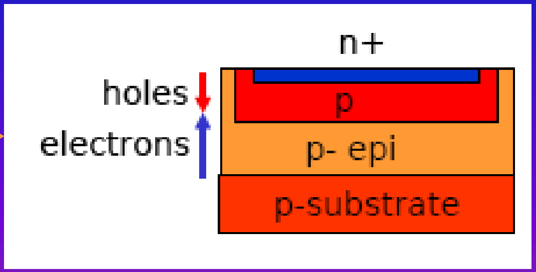

- PDE is depending on the SiPM structure
  - p+/n is more blue sensitive than n+/p
  - electron triggering probability is higher than hole triggering

SiPM timing resolution

Two components :

- fast component of gaussian shape with σ O(100ps)
  - due to photons absorbed in the depletion region
  - its width depends on the statistical fluctuations of the avalanche build-up time (e.g. photon impact position → cell size)
- slow component: minor non gaussian tail with time scale of O(ns)
  - due to minority carriers, photo-generated in the neutral regions beneath the depletion layer that reach the junction by diffusion

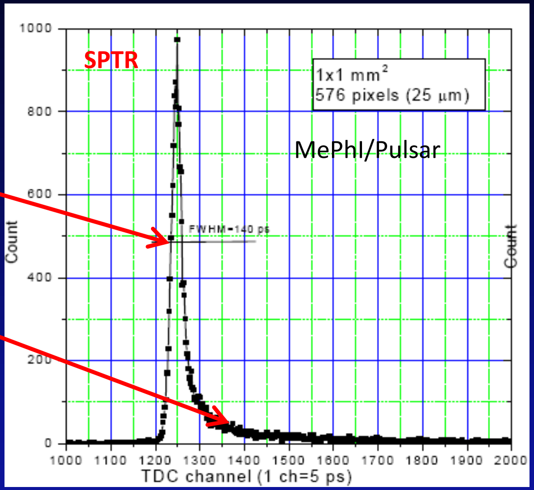

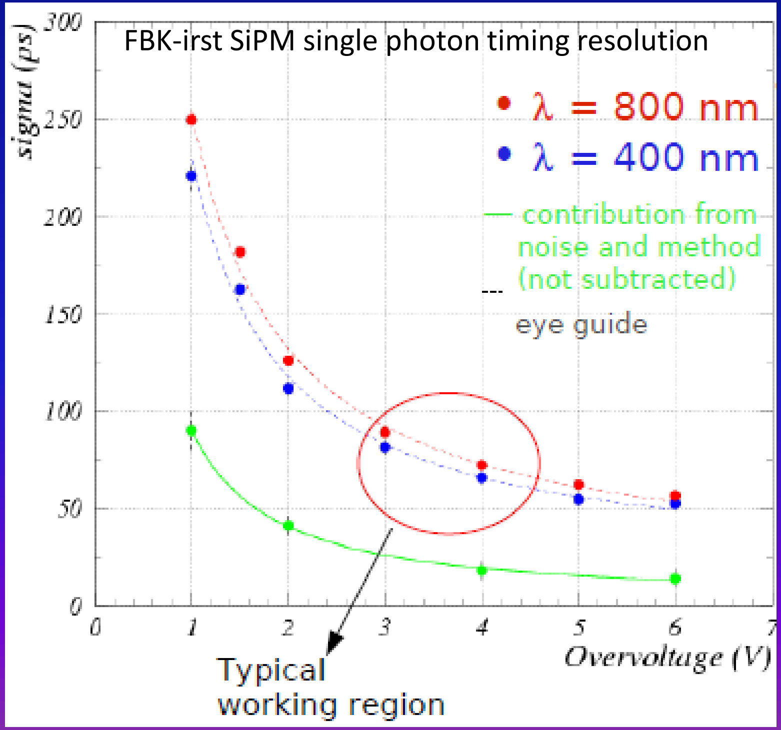

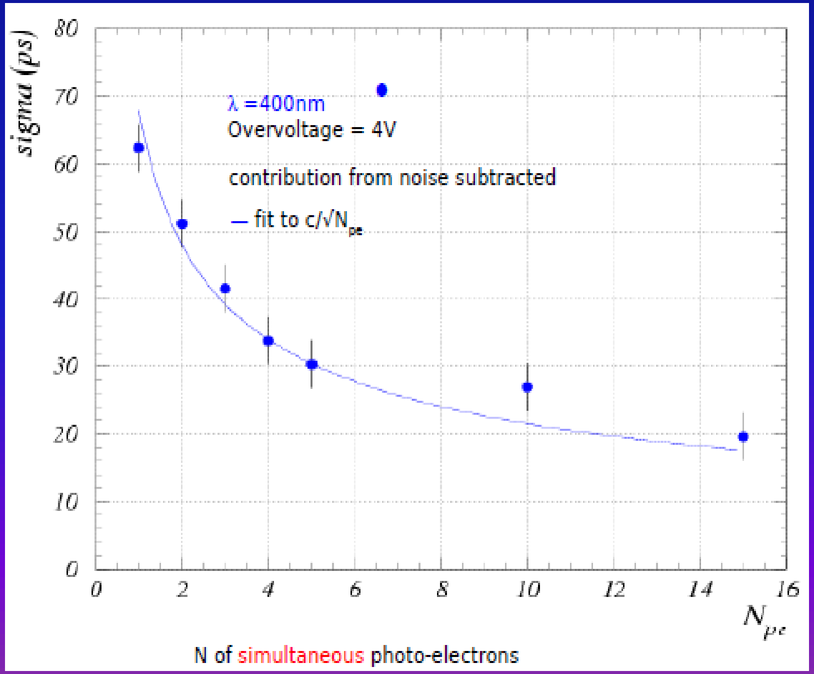

Poisson statistics:
$\sigma \propto 1/\sqrt{N_{pe}}$

Dynamic range

The output signal is proportional to the number of fired pixels as long as the number of photons on a very short laser pulse (N_{photon}) times the photon detection efficiency PDE is significantly smaller than the number of the pixels N_{total}

$$A \approx N_{firedpixel} = N_{total} \cdot \left(1 - e^{-\frac{N_{photon} \cdot PDE}{N_{total}}}\right)$$

Two or more photons in one pixel look like a 1 single photon

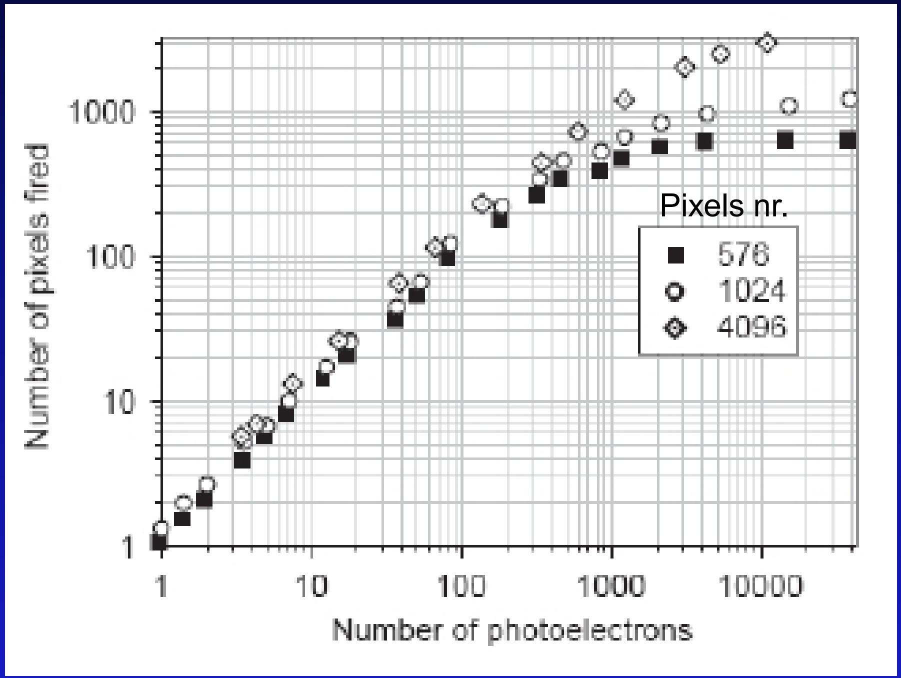

NIM A 540 (2005) 368

When 50% of the pixels are fired, the deviation from linearity is 20%

SiPM noise

- The number of counts/s registered by the SiPM in the absence of the light
- It limits the SiPM performances (e.g. single photon detection)
- Three main contributions:
  - **Thermal/tunneling** – thermal/ tunneling carrier generation in the bulk or in the surface depleted region around the junction ⇔ ***looks the same as a photon pulse***
  - **After-pulses** – carriers trapped during the avalanche discharging and then released triggering a new avalanche during a period of several 100 ns after the breakdown
  - **Optical cross-talk** – 10^5 carriers in an avalanche breakdown emit in average 3 photons with an energy higher than 1.14 eV (A. Lacaita et al. IEEE TED 1993)
    – these photons can trigger an avalanche in an adjacent µcell

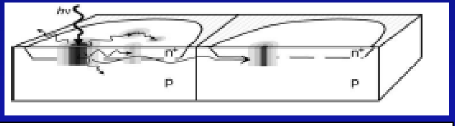

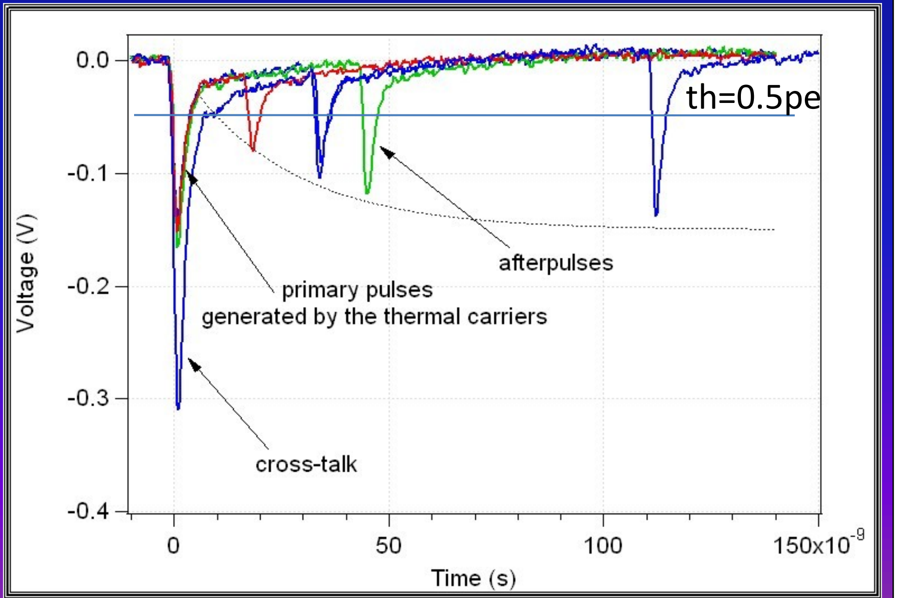

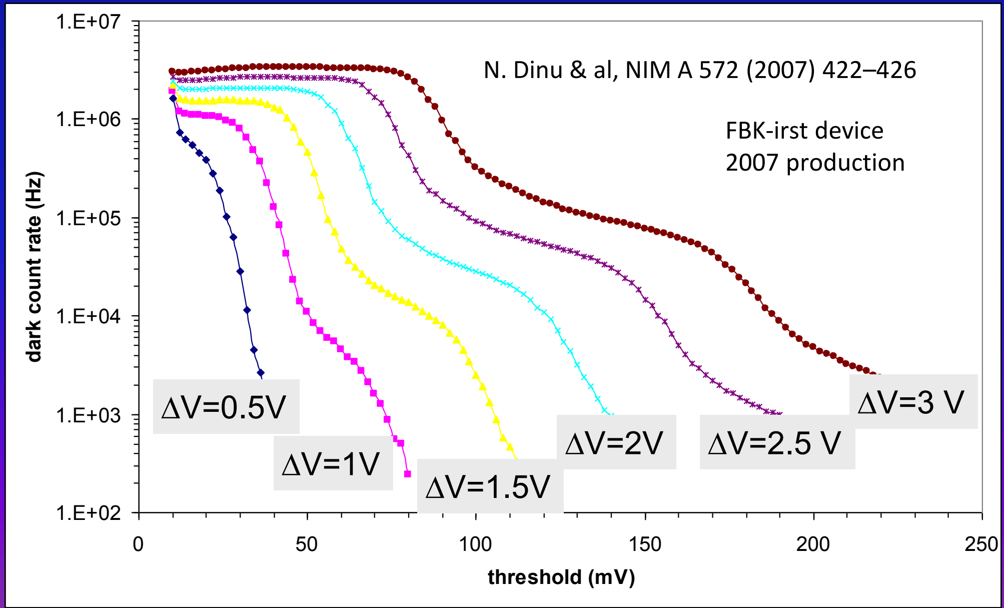

Temperature dependence

- Some SiPM parameters exhibits temperature variations:
  - V_{BD} increases with T (S. M. Sze and Kwok K. Ng, *Physics of semiconductor devices*, 2007)
    - $(dV_{BD}/dT)_{MPPC\ Hamamatsu}$ ~ 59 mV/°C
    - $(dV_{BD}/dT)_{SiPM\ FBK-IRST}$ ~ 80 mV/°C
  - G shows small variations with T if the overvoltage $\Delta V = V_{bias} - V_{BD}$ is kept constant
  - DCR decreases with decreasing T over many orders of magnitude
    - DCR @ ΔV=1.5V @ 30°$C_{MPPC\ Hamamatsu}$ ≅ 500 kcounts/s
    - DCR @ ΔV=1.5V @ -100°$C_{MPPC\ Hamamatsu}$ ≅ few counts/s

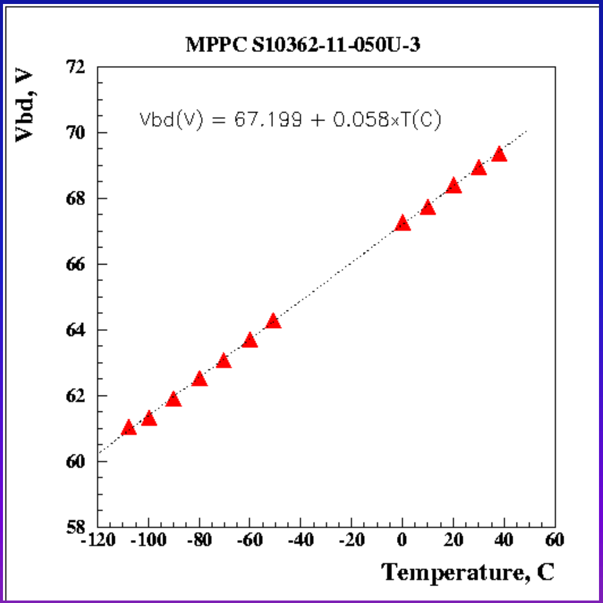

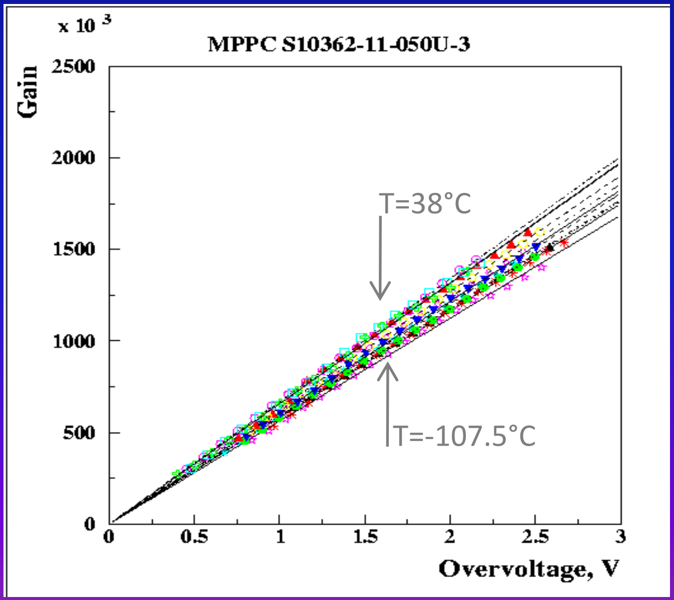

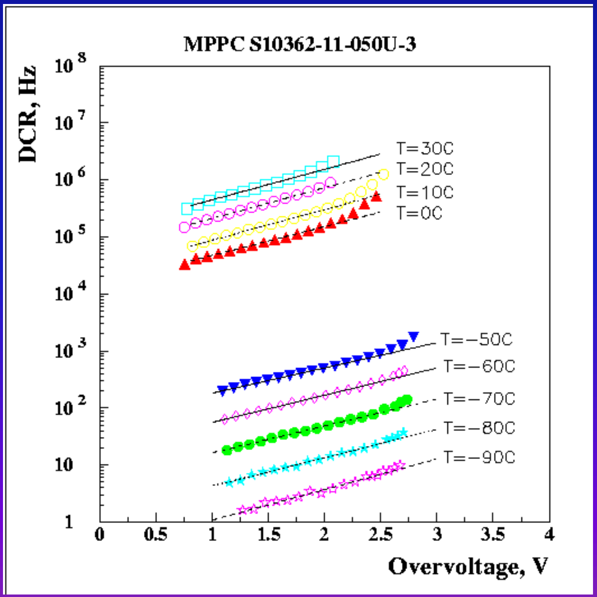

N. Dinu & al, IEEE NSS 2010 Proceedings

Radiation damage

- Radiation damage effects on SiPM:
  - increase of dark count rate due to introduction of generation centers
  - increase of after-pulse rate due to introduction of trapping centers
  - may change V_{BD}, leakage current, noise, PDE….

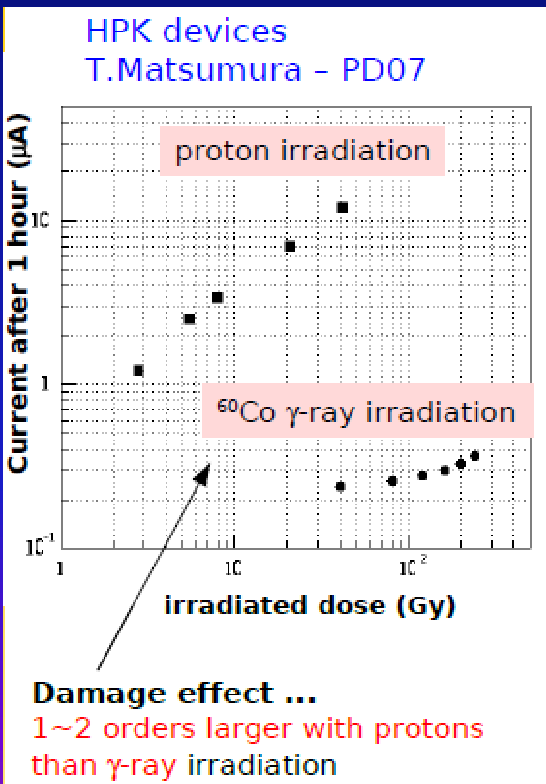

Damage effect …
almost the same for protons and neutrons

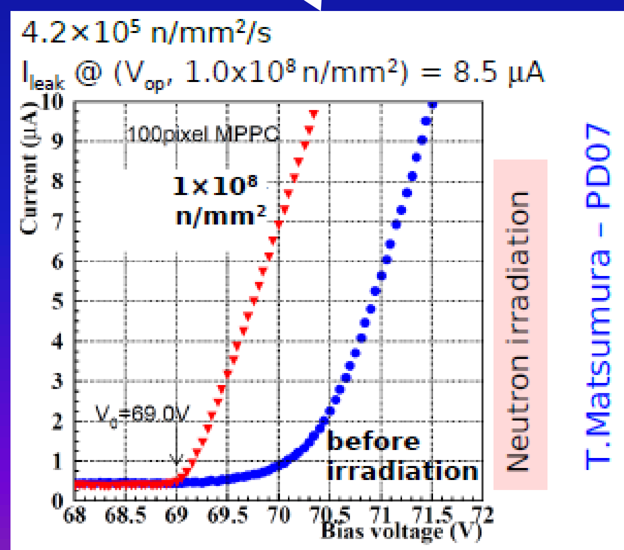

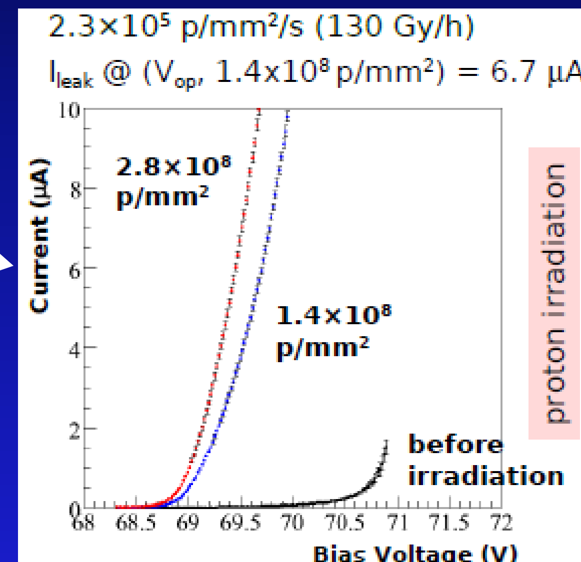

SiPM in the ILC HCAL

HCAL: steel/scintillator sandwich calorimeter

e+ e- collider (1 TeV)

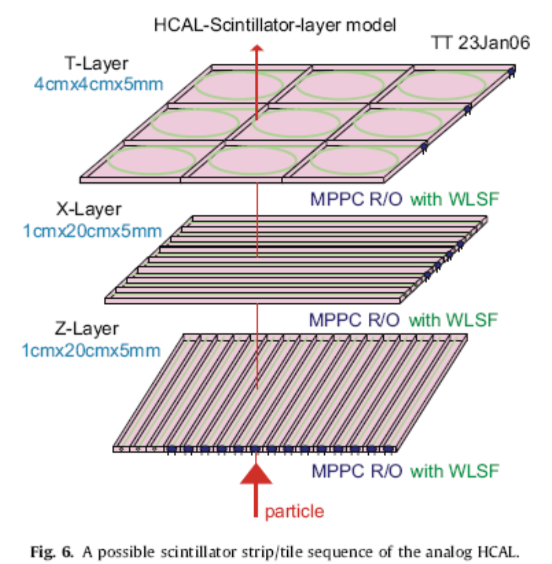

Fig. 6. A possible scintillator strip/tile sequence of the analog HCAL.

High granularity hadronic calorimeter optimised for the Particle Flow measurement of multi-jets final state at the ILC

photo-detector requirements:

- insensitive to magnetic field (~ 5T)
- coupling with a scintillator (blue emission)

photo-detectors: tests with MePHI/PULSAR SiPM , HAMAMATSU MPPC

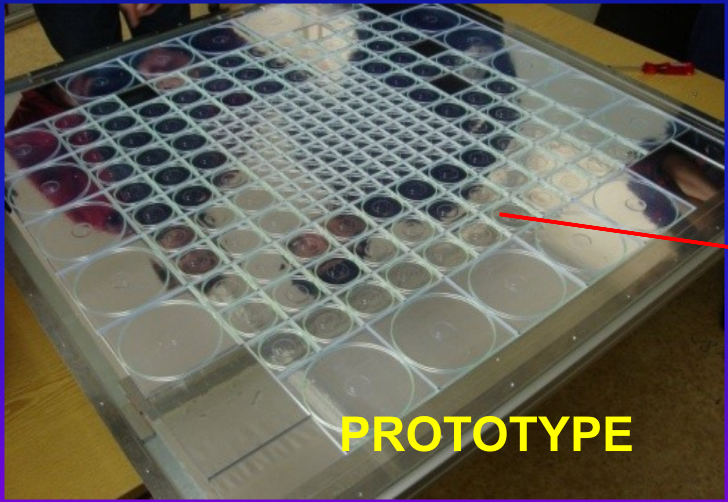

216 tiles/layer (38 layers in total) ~8000 channels

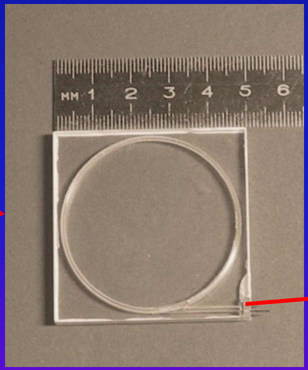

5 x 5 cm² plastic scintillator tile with embedded WLS fiber + SiPM

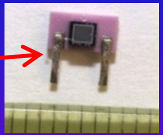

SiPM 1 mm²

Readout of SiPMs by the SPIROC ASIC (LAL)

SiPM in the ILC HCAL

On-going R&D

Different SiPM couplings to scintillator tile

with WLS fiber (for MEPHI SiPM)

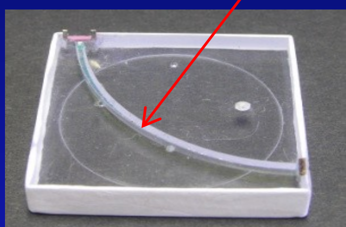

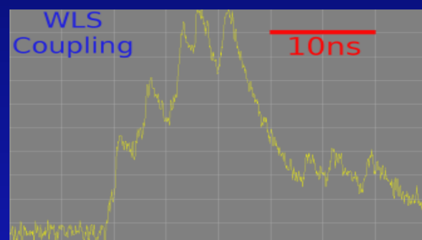

direct coupling (for MPPC)

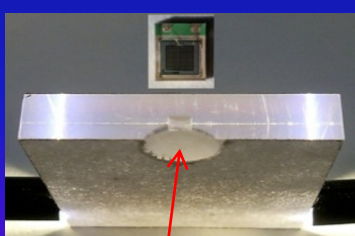

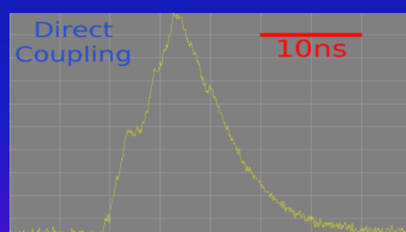

hole to integrate the SiPM

Calibration

2 ways:

- LED monitoring system
- test beam

DESY 3 GeV electron testbeam

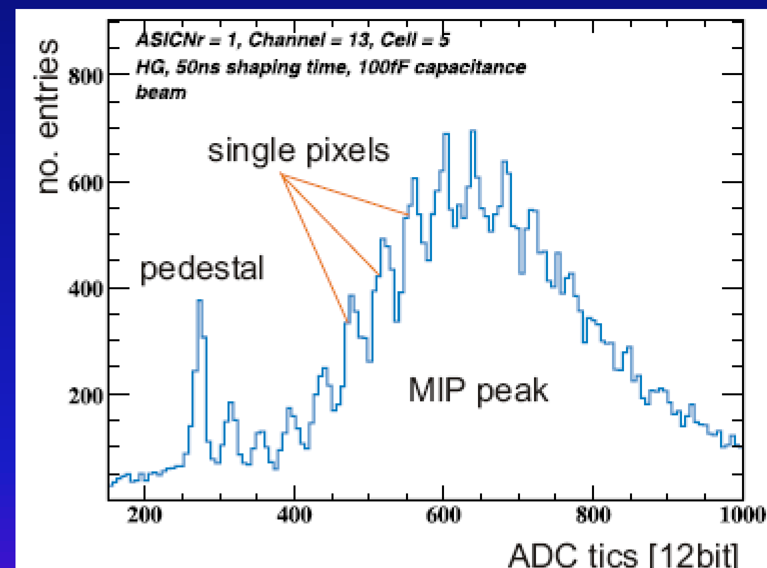

- Channel energy calibration by ~3 GeV electrons, which are minimum ionizing particles (MIPs).

- Crosstalk determination.

IEEE Nuclear Science Symposium, Oct. 30th - Nov. 6th, 2010, Knoxville, TN, USA

Example: Tokai to Kamioka (T2K)

study of ν oscillations

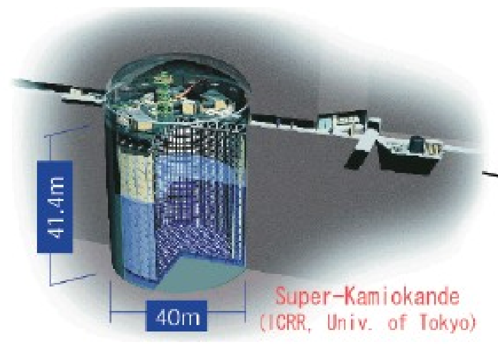

Far detector : Super Kamiokande

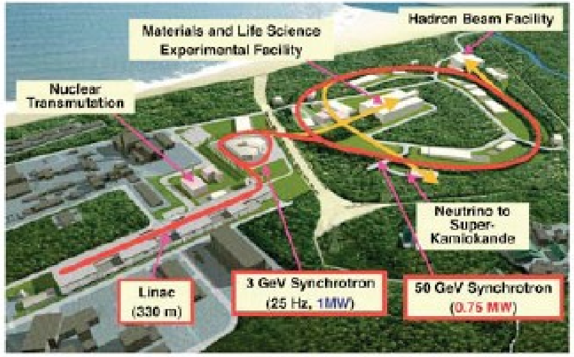

ν beam : J-PARC facility

ND280 : off axis neutrino beam flux and SuperK backgrounds measurements

Two Fine Grain Detectors (FGDs):

- X,Y planes of fine segmented scintillator bars
- wavelength shifting fibers collect the light from scintillators
- MPPC's detectors read-out the light from fibers

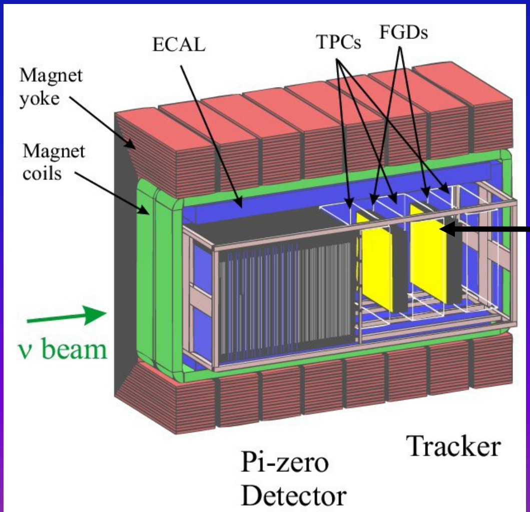

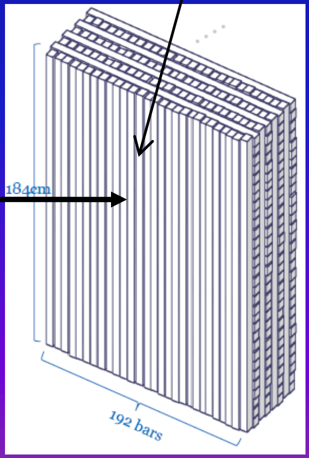

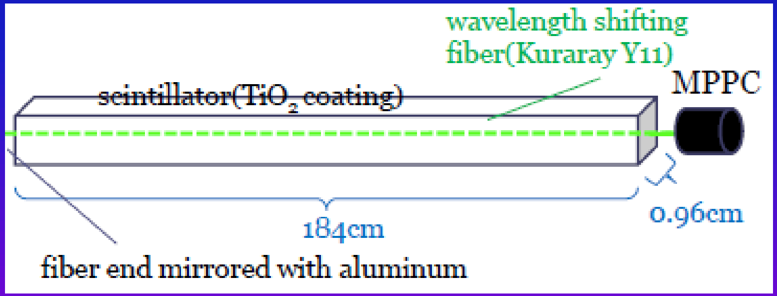

8448ch of MPPC were installed

ECAL : Light produced in scintillator bar is readout using a Y11 WaveLength Shifting (WLS) fibre coupled to a SiPM.

Scintillator bar readout cut view (ECAL)

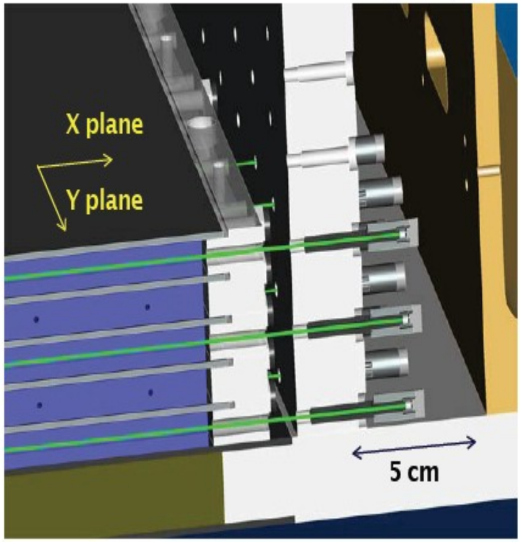

Connector design for P0D/ECAL

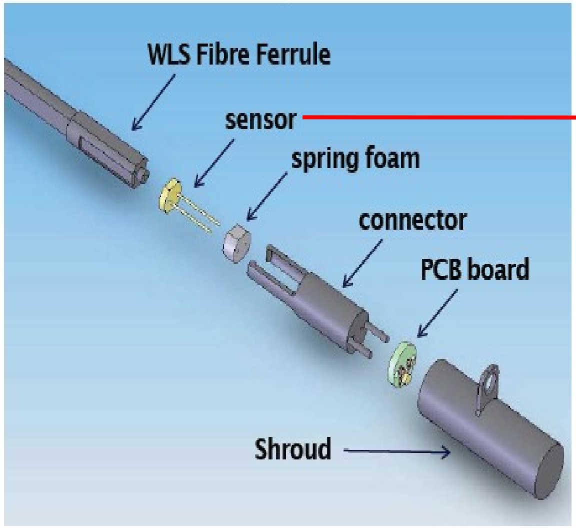

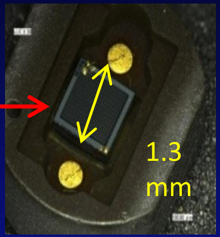

Total number of SiPMs in T2K = 56000 →first large experiment to use this type of sensor.

Electromagnetic calorimeter
Side muon range detector
Pi zero detector
Fine grain detector
On-axis detector

System	Channels	Bad channels	Fraction
ECAL (DSECAL)	22336 (3400)	35 (11)	0.16% (0.32%)
SMRD	4016	7	0.17%
P0D	10400	7	0.07%
FGD	8448	20	0.24 %
INGRID	10796	18	0.17 %
Total	**55996**	**87**	**0.16 %**